Synthesis and biological evaluation of thiazole and metergoline derivatives as antimycobacterial and antiplasmodial agents

Faith Riziki Mjambili

August 2013

Synthesis and biological evaluation of thiazole and metergoline derivatives as antimycobacterial and antiplasmodial agents

A dissertation submitted to the University of Cape Town in fulfillment of the requirements for the degree

Masters in Chemistry

by

Faith Riziki Mjambili

Supervisor: Professor Kelly Chibale

Department of Chemistry

University of Cape Town

Rondebosch, 7701

Cape Town

South Africa

August 2013

Declaration

I declare that ***Synthesis and biological evaluation of thiazole and metergoline derivatives as antimycobacterial and antiplasmodial agents*** is my original work and has not been presented for the award of any degree at any university. I know the meaning of plagiarism and declare that all of the work in the document, save for that which is properly acknowledged, is my own.

_____

Faith Riziki Mjambili

August 2013

Acknowledgements

I would like to sincerely thank my supervisor, Professor Kelly Chibale for his support, guidance, advice, correction, encouragement and patience throughout this project. I also thank Dr. Aloysius Nchinda and Ms. Elaine Rutherfoord-Jones for ensuring a good working environment and taking care of all the administrative issues.

Special thanks to all the Department of Chemistry administrative and technical staff, specifically Ms. Deirdre Brooks (administration), Mr. Gianpiero Benincasa (MS analysis), and Mr. Pete Roberts (NMR analysis).I appreciate Prof. Pete Smith, Dr. Carmen Lategan (UCT Pharmacology), Dr. Helene Boshoff (NIH) and Dr. Digby Warner and Ms. Krupa Naran (UCT/IIDMM) for the *in vitro* testing of all my compounds, and Mr. Mathew Njoroge for the *in vitro* metabolic stability work.

Many thanks to KCs' medicinal chemistry research group, especially Dr. Richard Klaus Gessner, Dr. Jamy Feng, Dr. Candice Soares De Melo- for taking me under their wings and teaching me the nitty gritty of organic chemistry synthesis and writting, and Dr. Yassir Younis for his sound advice. To my Kenyan family in Cape Town; Anto (Nina), Dennis, Gladdy, Liz (& Jude), Mathew, Nick, and Peggy-Thank you all for your great friendship and company (and the many sumptuous meals), you made it feel like home. To my friends Chris, Dorothy, and Mike, I am glad I met you guys, thanks for being there for me.

To my parents Norman and Mary Mjambili, your unconditional love, support and continuous prayers have kept me going even in the toughest of times, my siblings Andrew, Chirry, Nduva, Dzame, and Noel-you guys are the best, thank you for your love and support. My nephew and nieces Joy, Gift, Joann, Jean, and baby Ariela-I love you to bits, thank you for bringing joy into my life.

To my fiancé Marcus-I can't put it in words love; you have been my greatest motivation and I forever thank God for you.

And finally to the one who holds my life in His hands-Lord you have been good and faithful to me, and all this is for you.

Conferences

July 2013 – Poster Presentation:

Synthesis of 2-amino-4-(2-pyridyl) thiazoles for evaluation as antimycobacterial agents presented at the **Gordon research conference on tuberculosis drug development**, 21 – 26 July 2013, Renaissance Tuscany Il Ciocco Resort in Lucca (Barga) Italy.

ABSTRACT

TB patients show poor compliance to available drugs due to the costs, adverse side effects, and prolonged treatment, leading to multi-drug resistant (MDR), extensively drug resistant (XDR), and most recently totally drug resistant TB. Shared drug toxicities and drug interactions with antiretrovirals compound the problem. The rapid development of resistance to known antimalarials compared to the rate at which new agents are coming into the market still remains a big challenge is combating malaria. Currently, with resistance to ACTs having been documented in South-East Asia, the situation is dire as there is no ready alternative to these drugs. There is thus a heightened need for research towards the development of new anti-TB and anti-malarial drugs based on novel chemotypes. Towards addressing this need, SAR studies were conducted on the 2-amino-4-aryl thiazole scaffold by synthesizing a series of derivatives with different motifs at the various positions of the scaffold. These derivatives exhibited moderate antiplasmodial activity in the CQS strain of *P. falciparum*, and good antimycobacterial activity on the H37Rv strain of *M.tb*. A 2-pyridyl group at position 4 of the thiazole ring as well as a substituted phenyl at position 2 was found to be essential for antimycobacterial activity. However, the 2-pyridyl group was not essential for antiplasmodial activity while the substituted phenyl at position 2 was essential for antiplasmodial activity. The linker between these two groups affected antimycobacterial activity with little influence on the antiplasmodial activity. In addition structural modifications were performed on the ergoline backbone of metergoline, and a number of derivatives synthesized with different *para* substituted phenyls. These compounds exhibited moderate antiplasmodial activity in the CQS strain of *P. falciparum*, and moderate antimycobacterial activity on the H37Rv strain of *M.tb*. The presence of a substituted phenyl group attached to the nitrogen atom of the amine was found to be essential for antimycobacterial activity, however, this substituted phenyl group didn't confer optimum antimycobacterial activity as the compounds were less active than metergoline. The antiplasmodial activity of these compounds was better than that of metergoline and was enhanced by the hydrophobicity of the substituent on the phenyl ring. Changing the linker

between the ergoline backbone and the substituted phenyl ring didn't have any significant effect on either the antimycobacterial or the antiplasmodial activity.

Abbreviations

°C	degree celsius
µg/Ml	microgram per milliliter
µM	micro molar
ACTs	Artemisinin Combination Therapies
ADME	Absorption, Distribution, Metabolism, Excretion
AIDS	Acquired Immuno Deficiency Syndrome
Br_2	bromine
CDC	Centre for Disease Control
$CDCl_3$	deuterated chloroform
CHO	Chinese Hamster Ovarian
CQ	Chloroquine
CQS	Chloroqiune Sensitive
DAD	Diode Array Detector
DCM	dichloromethane
DMF	*N, N*-dimethylformamide
DMSO	dimethyl sulfoxide
DMSO-d_6	deuterated dimethyl sulfoxide
DOT	Directly Observed Therapy
EDCI	1-Ethyl-3-(3-dimethylaminopropyl) carbodiimide
EMB	Ethambutol
EtOAc	ethyl acetate
EtOH	ethanol
HBr	hydrobromic acid
HIV	Human Immunodeficiency Virus
HLM	Human Liver Microsomes
HOBt	*N*-hydroxybenzotriazole
HPLC	High Performance Liquid Chromatography
Hr	hour
HTS	High Through-put Screen
IC_{50}/IC_{90}	inhibitory concentration required to inhibit the growth of 50%/90% of organisms
IM	intramuscular
INH	Isoniazid
IV	intravenous
KCl	potassium chloride
LRMS	Low Resolution Mass Spectroscopy
LTBI	Latent Tuberculosis Infection
M.tb	*Mycobacterium tuberculosis*
M/Z	mass to charge ratio
MDR	Multi-Drug Resistant
MeOH	methanol
Mg/kg	milligram per kilogram

MH_Z	Megahertz
MIC_{90}/MIC_{99}	minimum inhibitory concentration which inhibits growth of 90%/99% organisms
MLM	Mouse Liver Microsomes
MS	Mass Spectroscopy
MTT	3-(4, 5-dimethylthiazol-2-yl)-2, 5- diphenyltetrazoliumbromide
Na_2SO_4	sodium sulphate
NaCl	sodium chloride
NADPH	Nicotinamide Adenine Dinucleotide Phosphate
$NaHCO_3$	sodium hydrogen carbonate
NaOH	sodium chloride
NIH	National Institute of Health
nM	nano molar
NMR	Nuclear Magnetic Resonance
PBS	Phosphate Buffered Saline
Pd/C	palladium on carbon
ppm	parts per million
PZA	Pyrazinamide
QSAR	Quantitative Structure Activity Relationship
RIF	Rifampicin
RLM	Rat Liver Microsomes
RT	Room Temperature
SAR	Structure Activity Relationship
SI	Selectivity Index
TAACF	Tuberculosis Antimicrobial Acquisition and Coordinating Facility
TB	Tuberculosis
TDR	Total-Drug Resistance
THF	tetrahydrofuran
TLC	Thin Layer Chromatography
TMS	Tetramethylsilane
t_r	retention time
WHO	World Health Organization
XDR	Extensive-Drug Resistance
δ	NMR chemical shift

TABLE OF CONTENT

CHAPTER 1: Introduction and literature review

1.1 TUBERCULOSIS (TB)

1.1.1 Etiology and history

Tuberculosis (TB) is a prevalent, and often fatal, infectious disease caused by different strains of mycobacterium, mainly *Mycobacterium tuberculosis* (*M.tb*).[1] *M.tb* is a small obligate aerobic nonmotile bacillum,[1] which was identified by Robert Koch in 1882.[2] It is the second highest cause of mortality from infectious disease globally after Human Immunodeficiency Virus (HIV) infection, and was declared a global public health emergency by the World Health Organization (WHO) in 1993.[3]

TB predominantly affects the lungs (pulmonary TB), but in some cases, the bacteria can enter the blood stream and spread to other parts of the body (extra pulmonary TB) especially in immunocompromised persons like those co-infected with HIV and young children.[1] The tubercle bacillus replicates slower than most bacteria[1] and can adopt a persistent nonreplicating state,[4] which is unresponsive to treatment. The complex structure and composition of its cell wall, which contains peptidoglycans and complex lipids, predominantly mycolic acids, contributes to its virulence.[1]

Other disease causing strains include *Mycobacterium bovis*, which is transmitted through contaminated milk, or beef, and causes a nonpulmonary form of TB,[2] and *Mycobacterium africanum* which is spread by aerosol transmission and causes a disease similar to that of *M.tb*.[1,5]

TB had all but disappeared from public view of developed nations by the late-nineteenth centuary,[6] largely due to the emergence of effective therapeutic agents and public health systems, but it never left the scene in less developed countries.[2] This status changed in the mid 1980s with cases of the disease re-emerging, and occurrences increasing in the developed world.[2]

The emergence of multi-drug resistance (MDR) and extensive-drug resistant (XDR) strains of *M.tb*, and the acceleration of disease spread and progression by HIV infection further compounded the problem.[6] This resistance is either intrinsic, due to the mycobacterium structural and functional characteristics that give it the ability to resist the activity of certain drugs, or acquired by spontaneous mutations that arise when the mycobacterium is exposed to suboptimal drug concentrations.[7] The global TB epidemic seems unabated,[8] as the pathogen uses a number of adaptations to survive in a different host lesions and to hide from immune surveillance.[1]

TB has a gender and age component as it is more common in men than women,[3] except in childhood,[9] and mostly affects economically productive adults between the ages of 15-59.[10]

1.1.2 Epidemiology

WHO recorded 8.7 million incident cases of TB in 2011.[3] Approximately 1 million deaths occurred due to TB infection among HIV negative people and an additional 0.4 million deaths resulted from HIV associated TB.[3] The TB prevalence in 2011 was estimated to be about 12 million cases worldwide, with 80% TB cases among people infected with HIV in Africa.[3] In addition there were 3.7% new cases of MDR-TB and 20% of re-occurrences from previously treated TB.[3]

The TB burden is highest in Asia and Africa, respectively accounting for 40% and 24% of TB cases globally.[3] Among the top five countries with the highest incidence of TB, South Africa ranks third, with an average of 0.5 million cases in 2011.[3] These findings indicate that there are shortcomings in the current treatment strategies and the effectiveness of public health systems in resource poor countries where the main TB burden lies.[8]

An epidemiologic synergy exists between TB and HIV, co-infections represent 13% of the global TB incidence, and account for approximately a quarter of HIV/AIDS-associated deaths.[3] In this synergistic interaction each disease increases the pathogenicity of the other. *M.tb* causes disease at any stage of HIV infection, exacerbates the course of HIV infection by effectively increasing replication of HIV,[4] and is the leading cause of HIV-related morbidity and mortality in

less-developed countries.[11] In turn, HIV affects the course of tuberculosis in several ways; first it promotes progression to active tuberculosis in people with either recently acquired or latent tuberculosis infection.[11] Secondly it increases the rate of recurrence of tuberculosis following treatment completion or cure, mainly due to an increased risk of disease following reinfection.[12]

Without treatment, TB mortality rates are high. This is further complicated by the emergence of resistant strains of *M.tb* which gives rise to MDR-TB, and XDR-TB, which is almost incurable,[13] accounting for about 5.4% of MDR-TB cases.[8]

1.1.3 Transmission and Pathogenesis

TB is airborne.[14] The main mode of transmission is therefore aerosol. When a person with active TB coughs or sneezes, tiny particles containing *M.tb* are expelled into the air. These particles, called droplet nuclei, can remain suspended in the air for several hours depending on the environment.[15] If another person inhales air that contains these droplet nuclei, transmission occurs and the droplet nuclei are deposited in the lungs, triggering an immune response. [14]

In the lungs, droplet nuclei containing *tubercle bacilli* travel to the alveoli where they are ingested by alveolar macrophages, which destroy or inhibit the majority of them. A small number may, however, survive and multiply intracellularly and will be released when the macrophages die. Upon release, the bacilli can spread by way of lymphatic channels or through the bloodstream to more distant tissues and organs. This systemic dissemination sensitizes the immune system for a systemic response. Within two to ten weeks, the immune system produces macrophages that surround the *tubercle bacilli*, forming a hard shell (granuloma) that keeps the bacilli contained and under control, a state known as latent TB infection (LTBI).[8,14,15] Although persons with LTBI have *M.tb*, they do not have the active disease form and are therefore unable to spread the infection.

The unique structure of the *M.tb* cell wall allows it to lie dormant for many years as a latent asymptomatic infection, particularly as it can grow readily inside the macrophages, thus

effectively hiding it from the host's immune system.[1,16] If the immune system cannot keep the bacilli under control, the bacilli begin to multiply rapidly leading to TB disease.[15]

M.tb requires oxygen to grow, and hypoxia has been shown to induce a non replicative metabolic state of bacterial phenotypes, leading to tolerance towards certain drugs.[8] Lack of potent drug activity on these bacterial phenotypes may be responsible for the prolonged TB treatment duration.[8] Both the latent asymptomatic state of the disease and the non-replicative metabolic state of the bacilli are referred to as the dormant state of the disease.[8] It is estimated that one-third of the world's population harbor the latent form of *M.tb* with a 5% risk (higher in immunocompromised persons) of reactivation. The bacilli remain non-pathogenic in healthy individuals, and are mostly reactivated in immune compromised persons such as those infected with HIV, or those on anti-tumor therapy.[8]

1.1.4 Treatment

TB can be cured,[6] with antibiotics being the most effective agents for treatment of actively growing *M.tb.*[4] Treatment using combinations of anti-TB drugs developed in the 1940s and 1950s can dramatically reduce mortality rates.[10] **Table 1.0** shows some of the drugs currently in use.[13]

Table 1.0: Drugs currently in use for treatment of tuberculosis[13]

First line	**Second line**			**Third line**
	Fluoroquinolones	**Injectable agents**	**Oral agents**	
Isoniazid	Moxiflaxacin	Kanamycin	Prothionamide	Clofazimine
Ethambutol	Levofloxacin	Amikacin	Ethionamide	Thioacetazone
Pyrazinamide	Ciprofloxacin	Streptomycin	Cycloserine	Linezolide
Rifampicin	Ofloxacin	Capreomycin	Terizidone	Amoxicillin/Clavulonate
Rifabutin	Gatifloxacin		*p*-amino salicylic acid	Imepenem/Silastatin
Rifapentine				Clarithromycin

Drugs used in the treatment of TB generally have either bactericidal or sterilizing activity.[17,18] Bactericidal activity is the ability of a drug to kill rapidly replicating *M.tb*, while sterilizing activity is the ability of a drug to kill the slowly replicating or the non replicating forms of *M.tb*[17], hence eliminating latent bacilli in persons with LTBI. The sterilizing activity of drugs in any given TB regimen determine the duration of treatment as to ensure a reduction of the viable bacterial population to levels that will not allow relapses to occur.[7,17]

The WHO recommended standard chemotherapeutic treatment for latent tuberculosis is six to nine months of **isoniazid** (INH).[19,20] For active TB treatment, the WHO recommends a treatment regimen consisting of two phases, lasting a total of six months, during which four drugs are used (Figure 1.0). The initial intensive phase lasts 2 months and consists of treatment with **rifampicin** (RIF), (INH), **ethambutol** (EMB), and **pyrazinamide** (PZA). This is followed by a continuation phase lasting four months using RIF and INH.[20]

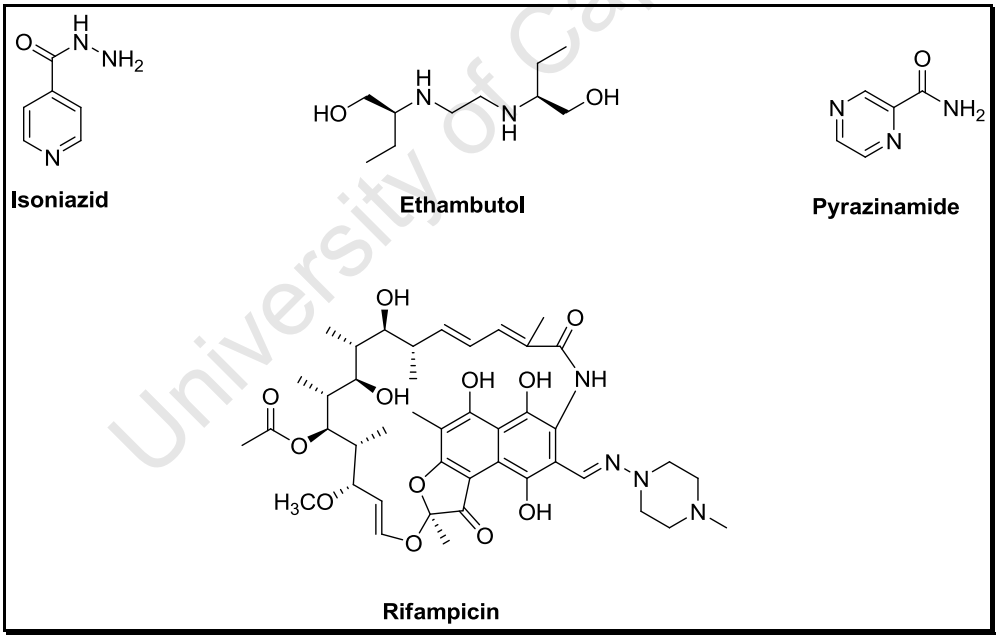

Figure 1.0: Chemical structures of first line drugs for treatment of active drug-sensitive TB.[1]

This regimen is effective and can cure up to 95% of people with non resistant forms of the disease if administered under direct observed therapy (DOT) as recommended by WHO to

ensure patients compliance.[1,4,8,14,21] Patient non-compliance due to the prolonged duration of treatment and poor management of chemotherapy, however, has led to the emergence of drug resistance, signified by the global appearance of MDR, and XDR-TB strains.[1,4]

MDR and XDR TB can either be primary or secondary.[15] Primary resistance is caused by person-to-person transmission of drug-resistant strains of the organisms while secondary resistance develops during TB treatment, either because the patient was treated with an inappropriate treatment regimen or because of patient non compliance to the prescribed treatment regimen.[8,15]

MDR-TB is resistant to the two most significant first line antituberculosis drugs INH and RIF.[7] Second line drugs, like **fluoroquinolones** (Figure 1.1) are used in the treatment of MDR-TB although there is no standard regimen[14,21] Treatment is individually designed depending on the susceptibility of the *M.tb* strain in question to currently available drugs.[14,22] If drug susceptibility testing is not available, which is the case in many developing nations, the choice of drugs is dependent on the pattern of drug resistance in the local geographical region, drugs the patient has been exposed to previously, any patient underlying medical conditions, and the adverse effects associated with the drug.[21] In the management of MDR-TB the duration of treatment is prolonged and varies between 18-24 months and may include a combination of eight to ten different drugs, most of which were not originally developed to treat TB.[8,21] These drugs are often more toxic and less effective than the first line drugs, with low cure rates, ranging from 50% to 70%.[8]

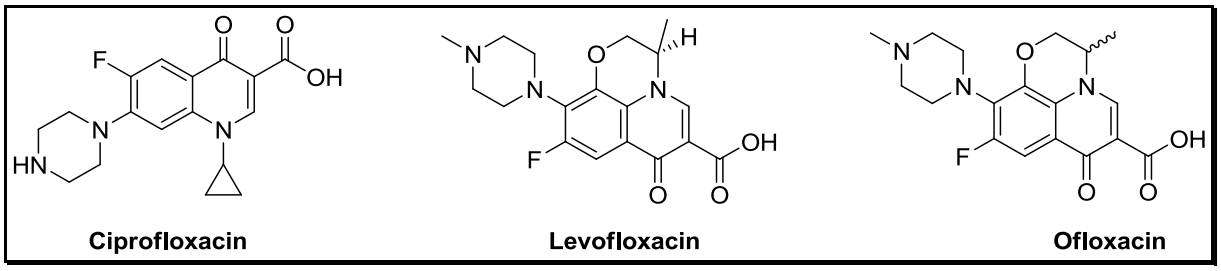

Figure 1.1: Chemical structures of fluoroquinolines used in the treatment of MDR-TB.[23]

XDR-TB is resistant to INH and RIF, as well as any fluoroquinolone and at least one of the second line injectable anti-TB drugs **amikacin**, **kanamycin** or **capreomycin** (Figure 1.2).[4,14] XDR-TB is virtually incurable,[4] due to very limited treatment options, and it takes much longer to treat using third-line anti-TB drugs which are costly and have more side effects.[21] It is associated with very high mortality rates, especially for patients co-infected with HIV.[8,21] Recently, the term totally drug-resistant TB (TDR-TB) has been used to describe TB caused by *M.tb strains* that are resistant to all available TB drugs[8,14,21]

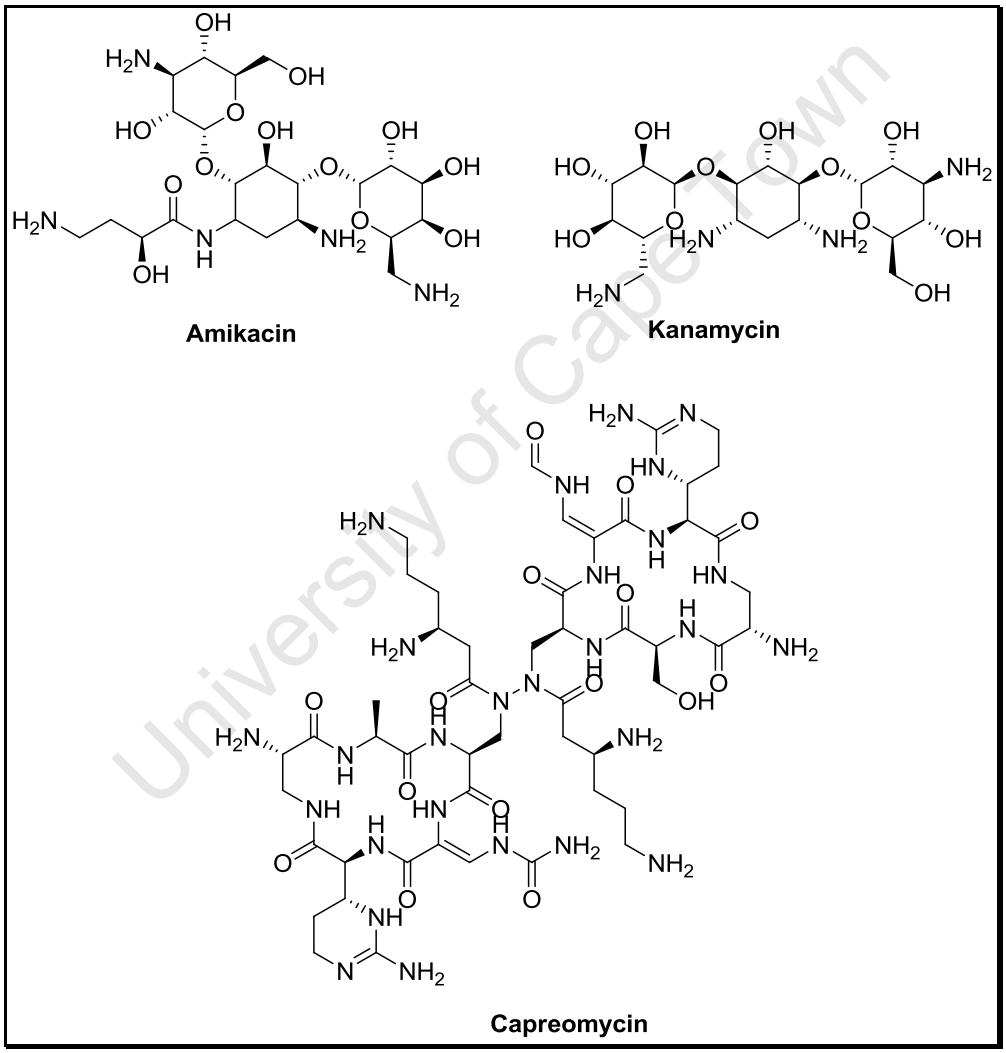

Figure 1.2: Chemical structures of injectable second line anti TB drugs.[23]

1.1.4.1 Treatment challenges

Treatment of TB presents many a challenge and, in as much as TB is curable, it takes a minimum of six months on a cocktail of various antibiotics to achieve cure. This prolonged duration of treatment and the high pill burden has led to poor patient compliance to the recommended treatment regimen, which resulted in the emergence of MDR and XDR TB.[1,24] The first-line treatment regimen has remained essentially unchanged for decades and there have been no breakthroughs to decrease either the treatment duration or the pills burden.[1,4,8,21,24]

The high pill burden is compounded if the patient is co-infected with HIV, furthermore, common antiretroviral drugs are also not compatible with the current TB treatment regimen due to shared drug toxicities and drug-drug interactions.[1,21] The most significant of these being rifampicin-induced cytochrome P450 activation that increases metabolism of protease inhibitors, resulting in decreased plasma levels of this class of antiretrovirals, which renders them less effective.[1,4,25] There has also been reports of incompatibility of the antituberculosis agents with drugs used for other chronic diseases such as diabetes.[8]

Current anti-TB drugs also have side effects that compound morbidity, leading to poor patient compliance, and results in failed treatments or relapses.[8,21,24] In addition, the management of pediatric TB is difficult since, despite the availability of antibiotics to treat TB, there are no suitable drug formulations for children.[4] Beyond the medical limitations, the cost of treatment is also high in the context of developing nations where the disease is most prevalent.[1,4]

To address these challenges, there needs to be efforts to discover new antituberculosis agents that will

i. shorten the duration of treatment
ii. reduce the pill burden and lower dosing frequency
iii. be effective in treating latent, MDR and XDR TB
iv. be suitably formulated to manage pediatric TB
v. be affordable for developing nations

vi. be effectively co-administered with other drugs for chronic illnesses especially HIV. [1,4,8,19]

Although there is an existing pipeline of drugs under development that will bring new antituberculosis agents into clinical use in the near future,[1,26,27] it is still not sufficient to address the alarming rate at which the current drugs are becoming ineffective due to resistance, which stresses the need for a completely novel TB treatment regimen.[8]

1.2 MALARIA

1.2.1. Etiology and history

Malaria is a parasitic infectious disease caused by parasites of the genus *Plasmodium*.[28] The name malaria originates from the Italian terms "mal" or bad and "aria" or air. It means foul or bad air as people initially noted that malaria was common in areas surrounding marshes and swamps, and pegged the disease on rot and decay that passed out through the foul air.[29–31]

Malaria is an ancient disease, but it is only in 1880 that Alphonse Laveran, a French military physician, discovered the single-celled *Plasmodium* parasite as the real cause of malaria.[29] Years later, between 1889 and 1900, Italian researchers discovered that the *Anopheles* mosquitoes are responsible for transmitting the disease. [29,31,32]

There are more than 100 different species of plasmodium[29] but only five have been identified as being able to cause malaria in humans, these are *Plasmodium falciparum, vivax, malariae, ovale* and *knowlesi*.[30,33] *Plasmodium knowlesi* is predominantly a monkey species but can cause severe human infections with cases being reported in South-East Asia.[3435] *Plasmodium falciparum* is the most virulent, causing the most deaths due to malaria.[29,36] In Africa, children under the age of 5 years and pregnant women are the most at risk.[28,33] *Plasmodium vivax* is not as virulent as *P. falciparum,* but is the most geographically widespread of all the species[30] and is associated with relapses occurring up to three years with a debilitating chronic disease. *Plasmodium malariae* can persist asymptomatically in blood for a long time, while *Plasmodium ovale* is rare and also associated with relapses.[29,30,33,35]

In the mid 1950s and 1960s, the WHO started a worldwide campaign to eradicate malaria by controlling the transmitting vector and treating of infected people.[29,37] This was successful for a while with malaria being completely eradicated in some places.[32] However, this was short lived as some strains of *Anopheles* mosquitoes developed resistance to the insecticides used for their control, and the *Plasmodium* parasites became resistant to chloroquine, the mainstay of antimalarial drug treatment in humans at that time.[29,32,35]

Since then various antimalarial agents have been developed and used for the treatment of the disease.[36] However, the high cost of the drugs, severe side effects, toxicities, and the rapid spread of resistance to these drugs has seriously compromised their efficacy and use.[28] Of significance is the recent evidence of the possible emergence of resistance to the current first-line artemisinin-combination therapy (ACTs), in South-East Asia, which threatens the current clinical efficacy of these compounds and create the need for continuous search for novel and structurally diverse compounds with potent antiplasmodial activity.[30,33,35,38–40]

1.2.2 Epidemiology

Malaria has a worldwide distribution, being found in tropical areas, throughout sub-Saharan Africa and to a lesser extent in South Africa, South-East Asia, the Pacific islands, India and Central and South America.[30,36]

There were an estimated 219 million cases of malaria (range154–289 million) and 660 000 deaths from malaria (range 610 000–971000) in 2010.[30] Globally, an estimated 3.3 billion people were at risk of malaria in 2011, with populations living in sub-Saharan Africa at highest risk.[30] Approximately 80% of malaria cases and 90% of the deaths are estimated to occur in Africa.[30] Out of 43 countries in Africa with ongoing malaria transmission, only 8 countries have achieved a greater than 75% reduction in malaria case incidence or malaria admission rates.[30] Population migration due to business, commerce, and tourism has resulted in more people from non-endemic countries being exposed to malaria.[36]

Since malaria is associated with poverty, mortality rates are highest in developing nations, especially in countries where a higher proportion of the population is living in poverty. The prevalence of malaria infections in children less than 5 years of age is also highest in poorer populations and rural areas. [28,30,41,42] Malaria is prevalent in tropical and subtropical regions because rainfall, warm temperatures, and stagnant waters provide ideal mosquito habitats.[28,29,32]

1.2.3 Transmission and Pathogenesis

Human malaria occurs by transmission of *Plasmodium* sporozoites via a bite from an infected anopheles mosquito[43,44] (Figure 1.3). The sporozoites travel from the salivary glands of the mosquito through the bloodstream of the host to the liver, where they invade hepatocytes.[43,44] These cells divide repeatedly to form mature tissue schizonts, each containing thousands of daughter merozoites.[31,43] This is called the exoerythrocytic stage of infection and is asymptomatic[31,35,44]

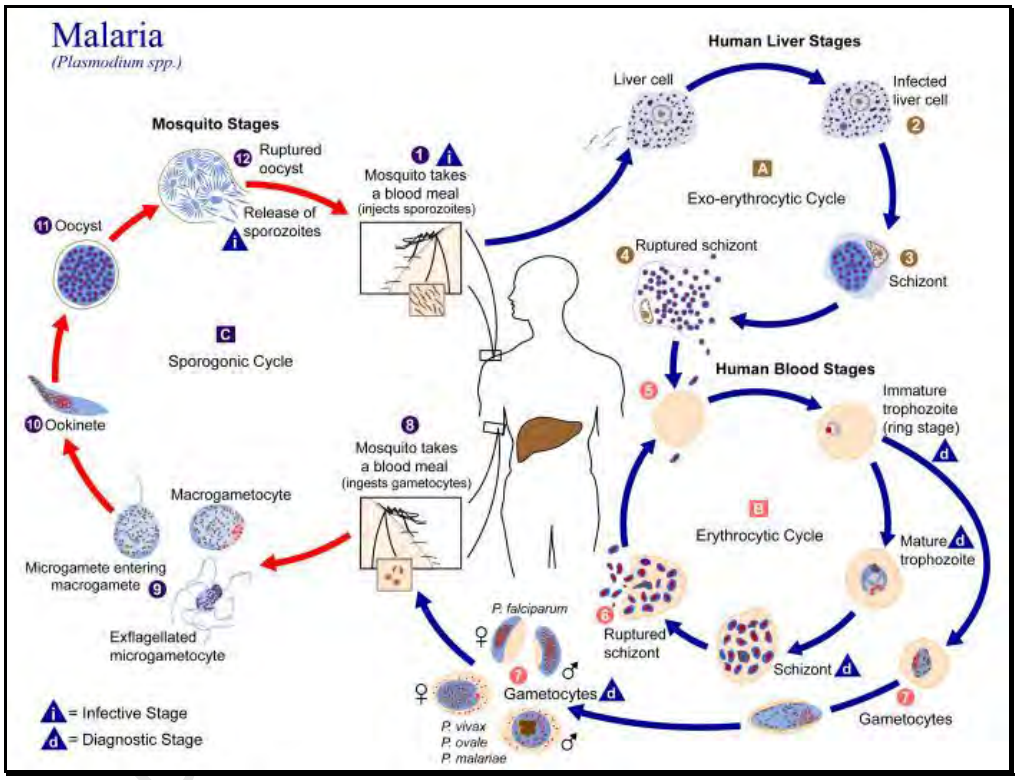

Figure 1.3: Malaria parasite life cycle-adapted from the CDC public health image library[45]

The liver schizonts rupture after one to two weeks in *P. falciparum*- longer in other species-and release merozoites into the bloodstream where they invade erythrocytes.[29,35] This is known as the erythrocytic stage of the infection.[44] In *P. vivax* and *P. ovale* infection, some parasites remain dormant in the liver as hypnozoites and can cause late relapse by reactivating after many months.[36,43] *P. malariae* doesn't form hypnozoites but can cause very late relapse due to sub patent infection that can become symptomatic years to decades later.[36]

Within the erythrocytes merozoites undergo a cycle of asexual reproduction, forming schizonts filled with more merozoites. When these schizont mature, the cell ruptures and merozoites together with the parasite's waste and cell debris are released into the blood stream, and are responsible for the clinical symptoms of malaria, such as high and periodic fevers, nausea and vomiting, chills, abdominal and back pain, headache, diarrhea, and anaemia.[29,43] The newly released merozoites invade other erythrocytes, and this process is repeated almost indefinitely and continues until it is brought under control, either by treatment or the body's immune system.[28,29]

The merozoites mature successively from ring forms to trophozoites to mature red cell schizonts, the asexual forms of the parasite, over 24 hours for *P. knowlesi*, 48 hours for *P. vivax, P. ovale,* and *P. falciparum* and 72 hours for *P. malariae*.[36,41,43] Within the erythrocytes the parasites digest hemoglobin.[29] The breakdown of hemoglobin in the parasite food vacuole leads to accumulation of toxic breakdown products which the parasite gets rid of by formation of hemozoin, a polarizable crystal as a detoxification mechanism.[43] A few merozoites differentiate into male or female gametocytes, the sexual form of the parasite, which cause no symptoms but can circulate in the bloodstream until they are ingested by a blood-feeding *Anopheles* mosquito.[29]

In the mosquito sporogony begins when the gametocytes mature into male and female gametes, which then can undergo fertilization to form a motile zygote (ookinete) inside the lumen of the mosquito gut.[31,36,43] The ookinete then penetrates the mosquito gut wall and develops into an oocyst which contains sporozoites that are released upon its rupture and migrate to the salivary glands ready for injection into a new host. The cycle is then repeated.[28,29,31,35,41,43,46]

1.2.4 Treatment

Malaria can be effectively controlled and treated.[30] Management of malaria requires a combination of preventive measures, vector control and active disease treatment. The widespread use of insecticide-treated bed nets and spraying of houses with environmentally

friendly insecticides have positively contributed to the reduction of the disease burden.[28,30,32,34] The prompt treatment of malaria with effective antimalarial drugs to completely cure the disease, prevent death, and get rid of the human reservoir of malaria infection and curbing its transmission is the objective of malaria chemotherapy.[34]

There are several broad classes of antimalarial drugs in clinical use based on their mode of action.[28,36,43] Quinolines and related compounds are thought to block parasite heme detoxification by preventing the formation of hemozoin.[47,48] This class of compounds includes some of the oldest known antimalarial agents such as **quinine**, **chloroquine**, **amodiaquine**, **mefloquine**, **piperaquine** and some newer agents like **lumefantrine**[36,43,44] (Figure 1.4).

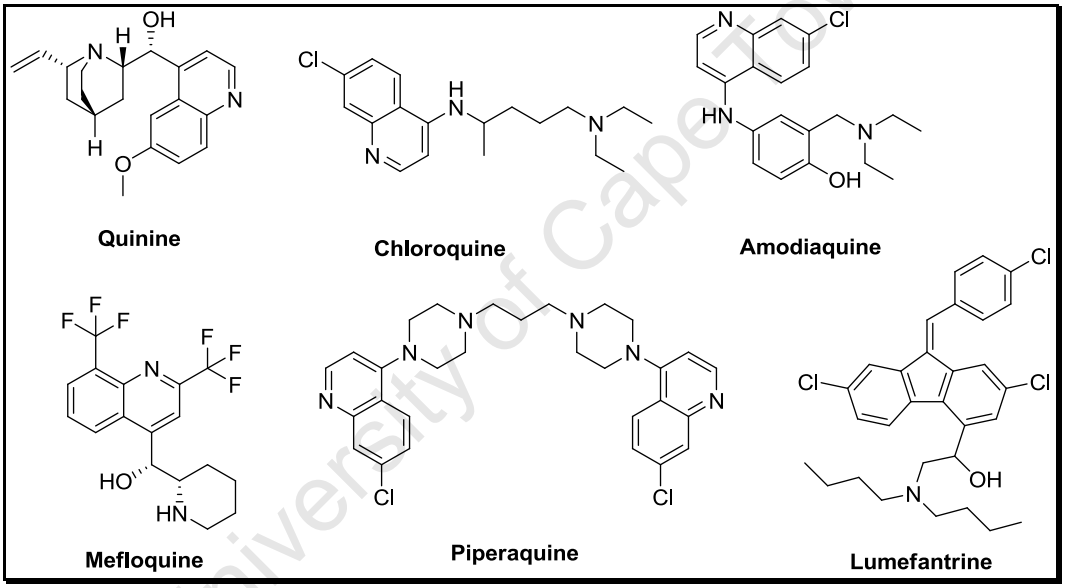

Figure 1.4: Chemical structures of quinolines and other related compounds[43]

Antifolates interfere with folate metabolism hence inhibiting nucleic acid synthesis, a pathway that is essential for malaria parasite survival.[47] This class includes **sulfadoxine** and **pyrimethamine**[36,43,44] (Figure 1.5).

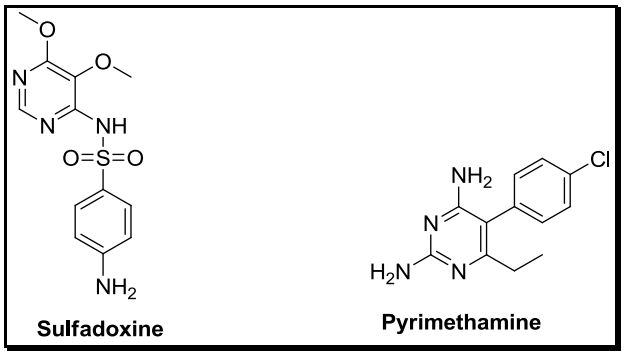

Figure 1.5: Chemical structures of antifolate antimalarial agents[43]

Artemisinine derivatives are the most recent class of antimalarial agents to enter the market and though their mode of action is not well understood, they are thought to interfere with heme detoxification via radical formation and/or heme alkylation although these mechanisms are not well understood.[47] The artemisinins include **artesunate**, **artemether**, and **Dihydroartemisinin**[36] (Figure 1.6).

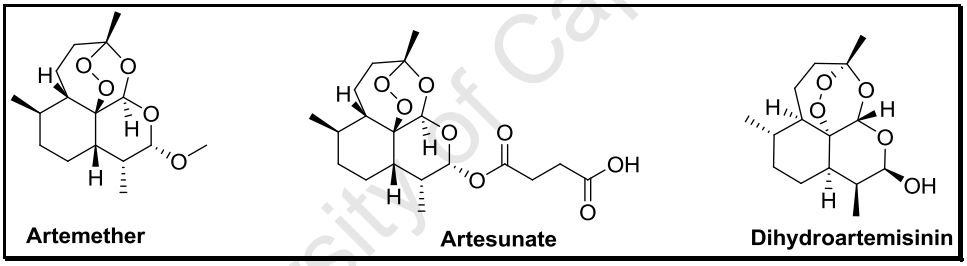

Figure 1.6: Chemical structures of artemisinin derivatives[43]

Atovaquone, a hydroxynaphthoquinone antiparasitic agent, interferes with cytochrome electron transport, and is combined with **proguanil** (Figure 1.7) for the treatment of malaria for synergistic effect.[34,47] Proguanil is a biguanide that is metabolized in the body via cytochrome P450 to the active metabolite, cycloguanil, which inhibits plasmodial dihydrofolate reductase. Proguanil has weak intrinsic antimalarial activity through an unknown mechanism.[34]

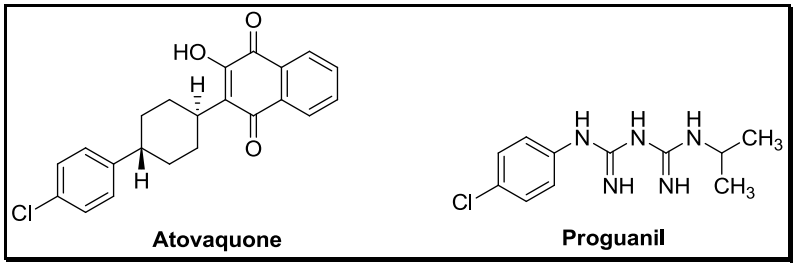

Figure 1.7: Chemical structures of atovaquone and proguanil which are used in combination in malaria treatment[43]

Antibiotics used in the treatment of malaria mainly act by inhibiting protein synthesis. They include the tetracycline's such as **tetracycline** and lincosamides such as **clindamycin** (Figure 1.8).[28,34–37,43,49,50]

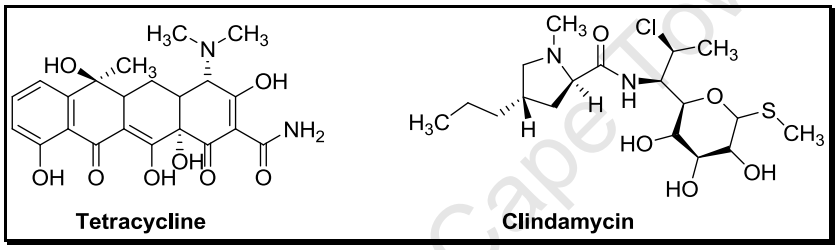

Figure 1.8: Chemical structures of antibiotics used in treatment of malaria[43]

To minimize the development of resistance to the drugs and cross resistance between structurally similar drugs, combinations of drugs with different mechanisms of action has been adopted in malaria chemotherapy.[28,30,33,48,51,52]

The guidelines provided by the WHO for the treatment of malaria are based on the classification of the disease as either uncomplicated or complicated. Uncomplicated malaria is symptomatic malaria without any signs or evidence of severity and/or vital organ dysfunction. The signs and symptoms are normally nonspecific and hence, uncomplicated malaria is clinically suspected mainly on the basis of fever or a history of fever. Complicated malaria presents with one or more of the features of vital organ dysfunction such as prostration, altered consciousness, respiratory distress, multiple generalized convulsions, severe anemia, hypoglycemia, and jaundice.[30,34]

Artemisinin combination therapies (ACTs) are recommended by the WHO as standard treatment for uncomplicated malaria.[28,34,51] The artemisinin derivative component of the combination must be given for at least three days for an optimum effect to be achieved.[34] Recommended ACTs include artemether plus lumefantrine, artesunate plus amodiaquine, artesunate plus mefloquine, artesunate plus sulfadoxine-pyrimethamine, and dihydrortemisinin plus piperaquine.[30,34]

For complicated malaria both in adults and children, the WHO recommends parenteral artesunate 2.4 mg/kg bodyweight given intravenously (IV) or intramuscularly (IM) on admission, at 12 hours, 24 hours, and once daily thereafter. Artemether or quinine are an acceptable alternative if parenteral artesunate is not available, and they should be administered as artemether 3.2 mg/kg IM given on admission then 1.6 mg/kg per day thereafter; or quinine 20 mg salt/kg on admission as an IV infusion or divided IM injections, then 10 mg/kg every 8 hours thereafter. The parenteral antimalarials should be administered for a minimum of 24 hours once started, irrespective of the patient's ability to tolerate oral medication earlier. Thereafter, once the patient can tolerate oral medication, a complete treatment with any of the ACTs should be administered.[30,34]

1.2.4.1 Treatment challenges

The rapid development of resistance to known antimalarials compared to the rate at which new agents are coming into the market is the biggest challenge in malaria drug discovery.[28] Currently, resistance to ACTs has already been documented in South-East Asia, yet there is no ready alternative to these drugs.[34,50] Multi-drug and cross-drug resistance, especially with aminoquinolines, also highlights the need for new agents with novel mechanisms of action.[48]

Access to antimalarial drugs is limited because of their cost and problems with distribution, especially in developing nations where the malaria burden is great.[51] Although pharmaceutical companies have provided subsidies in recent years, this may not be sustainable in the long run and efforts geared towards developing low cost drugs that will be easily accessible are needed.

Patient compliance to treatment is hampered due to severe side effects and toxicities of most antimalarial drugs such as anorexia and loss of balance with mefloquine, agranulocytosis with amodiaquine, and chinconism with quinine.[34,39] Compliance is also decreased due to the inability of patients, especially in rural settings, to follow treatment correctly and the unavailability of suitable formulations for children.[42]

To address these challenges there needs to be an effort to discover new antimalarial agents that are,

i. safe and well tolerated-especially by children and pregnant women
ii. orally bioavailable
iii. effective against drug resistant strains of *Plasmodium*
iv. acting via new mechanisms to prevent rapid development of resistance and/or cross-resistance
v. cheap and affordable in resource poor settings
vi. able to achieve cure within a short duration of time
vii. able to be formulated in combinations that are easy to administer in non-hospital settings.[33,48,50]

1.3 DRUG DISCOVERY STRATEGIES

1.3.1 Drug discovery through screening in treatment of TB and Malaria

There are a number of strategies that have been employed to fast track TB and malaria drug discovery efforts. One such strategy is the screening of pharmaceutical compound libraries to identify novel compounds with antimycobacterial or antiplasmodial activity (hits). This is known as a species specific platform for drug discovery. It is normally followed by synthesis, modification or derivatization of the identified hits to improve their activity and decrease any associated toxicities. It is quite common for drug discovery efforts to start from the identification of hits from high throughput screens.[8,16,19,52]

Recently this strategy has given rise to one of the most promising antituberculosis agents to enter clinical trials. Diarylquinolines were discovered to have antitubercular activity through whole cell screening of a library of compounds for potential anti-TB activity. Derivatization then led to the discovery of **TMC207**, [1,4,8,13,14,18] (Figure 1.9), the most potent compound of the series.

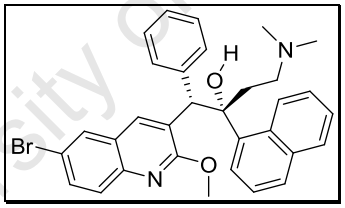

Figure 1.9: Chemical structure of **TMC207.**[7]

TMC207 has recently been approved as bedaquiline® by the US Food and Drug administration (FDA) through its regulatory path for accelerated review of limited efficacy data, as part of a combination regimen for management of MDR-TB where no other treatment options are available.[21] The benzothiazine **BTZ043**, which is currently in pre-clinical development, was also discovered through such screens.[8,21]

In malaria drug discovery high-throughput screening (HTS) efficacy models have been widely used at early stages of drug discovery and development.[48] This method recently resulted in the identification of an amino pyridine as a novel antiplasmodial scaffold through a phenotypic HTS

of a BioFocus DPI Soft Focus kinase library. Further work on these compounds led to the identification of the compound **MMV390048** [33,39,53] (Figure 2.0) which is currently in preclinical studies.

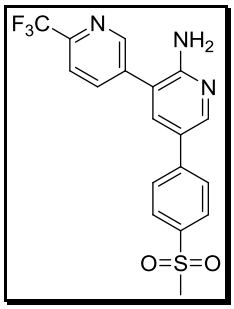

Figure 2.0: Chemical structure of **MMV390048**[39]

1.3.2 Drug repurposing and repositioning in the treatment of TB and malaria

A more common approach to identify TB and malaria drugs is by direct repurposing, or repositioning of existing antimicrobials and other drugs for non infectious indications. Drug repurposing is the investigation of new uses for existing drugs, whether in clinical use or not without any structural modification of the drug. Drug repositioning differs from repurposing in that the drug in question undergoes structural modifications to improve the desired activity.[25,26,52]

Drug repurposing and repositioning has been succefully applied in TB drug discovery in the past, and has become a useful tool in finding new drugs with decreased costs and duration of research.[4,25,26] In fact, some current drugs that are central in TB treatment were initially developed for other indications and repurposed or repositioned for management of TB.[8,21,25–27]

The repurposing of fluoroquinolones is a classic example. Fluoroquinolones were originally developed as broad spectrum antibiotics for treatment of severe bacterial infections. However, they are now the drugs of choice in the management of MDR-TB. Structural modifications of the original quinolones led to new compounds with improved activity. Two of these compounds, **gatifloxacin** and **moxifloxacin** (Figure 2.1), are said to have the potential to decrease treatment durations.[4,13,14,18,21,25–27]

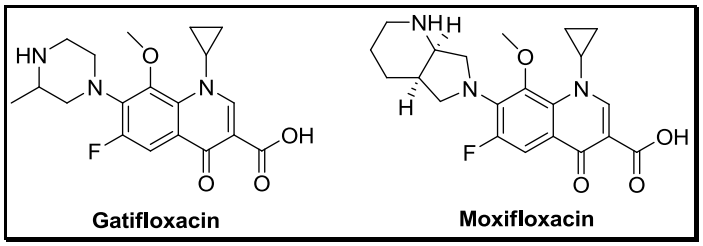

Figure 2.1: Chemical structures of fluoroquinolones with potential of shortening treatment duration.[21]

The repositioning of the oxazolidinone **linezolid** (Figure 2.2)**,** originally in clinical use for treatment of infections caused by methicillin-, vancomycin- and penicillin-resistant bacterial strains, is another success story. It was found to be active against *M.tb*. However, prolonged use was associated with toxicities such as anemia and peripheral neuropathies. Structural modifications of linezolid gave rise to sutezolid (**PNU100480**) which is believed to be more potent and safer, and is currently in phase II clinical trials.[4,8,13,14,21,25,26]

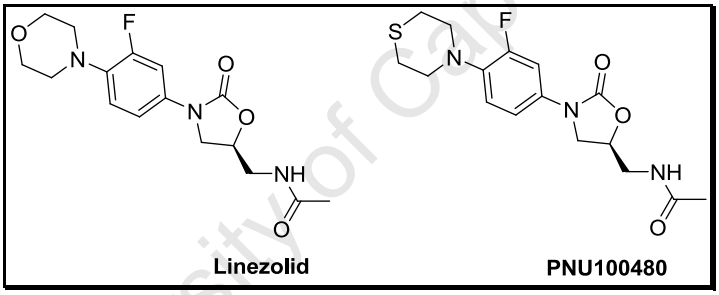

Figure 2.2: Chemical structures of linezolid and its active analogue **PNU100480**[21]

In malaria chemotherapy, repositioning and repurposing is well exemplified by the antibiotics currently in use both for malaria treatment and prophylaxis. **Doxycycline** (Figure 2.3) is the most widely used of the tetracycline antibiotics in the management of malaria. It has become the mainstay in malaria prophylaxis in cases where mefloquine is contra-indicated or in areas with multi-resistant *P. falciparum* strains.[25,43,52]

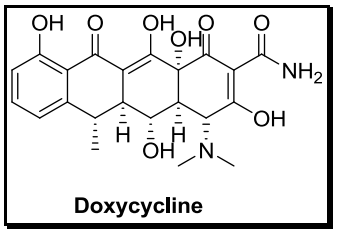

Figure 2.3: Chemical structure of doxycycline, an antibiotic used in malaria prophylaxis [25]

The antifolate class of antimalarials is another example of repurposing in malaria chemotherapy. Originally developed as antibacterial agents, these drugs have been repurposed in malaria treatment. They are successfully used in drug combination due to their synergistic effects although wide spread resistance has been reported.[25,43,44,52]

In the work presented in this dissertation two compounds of interest (Figure 2.4) were identified from different HTS campaigns conducted by the Tuberculosis Antimicrobial Acquisition and Coordinating Facility (TAACF), a programme established to allow researchers access to high quality screening services.[54] One of these compounds is metergoline, a drug in clinical use for non infectious conditions while the other belongs to the thiazole class of compounds which have diverse pharmacological application.

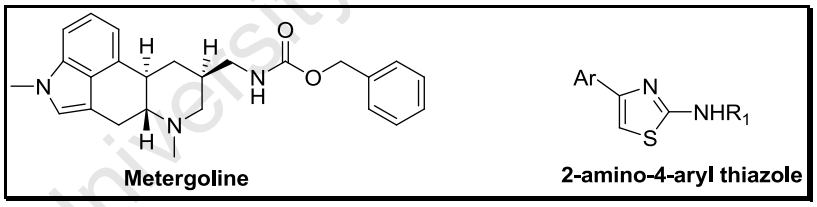

Figure 2.4: Chemical structures of metergoline and the thiazole scaffold of interest

The HTS demonstrated that metergoline and the 2-amino-4-heteroaryl thiazole scaffold (Figure 2.4) with an aryl or aryl alkyl substituent on the amino group at the position 2 exhibited antitubercular activity. It was therefore envisioned that through medicinal chemistry these compounds could be derivatized in an attempt to come up with analogues with improved antitubercular activity. The decision to test for antiplasmodial activity was based on the fact that there are reports of these compounds antiplasmodial activity in literature and in other screens.

CHAPTER 2: Design, Synthesis and Pharmacological evaluation of Thiazole Derivatives

2.1 Introduction

This chapter describes the design, synthesis and characterization of some novel thiazole derivatives, derived from the **2-amino-4-heteroaryl thiazole** scaffold (Figure 2.5). Structure-activity relationship studies were conducted to investigate the effect on activity of different structural motifs on the scaffold. Standard organic synthetic routes were used in the synthesis. All synthesized derivatives were evaluated for *in vitro* antimycobacterial and antiplasmodial activity as well as cytotoxicity, and also profiled for their physicochemical and Absorption, Distribution, Metabolism and Excretion (ADME) properties.

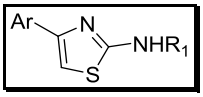

Figure 2.5: General structure of the 2-amino-4-aryl thiazole scaffold[54]

2.2 Background

Thiazole (Figure 2.6) is a heterocyclic compound containing both nitrogen and a sulfur atom as part of the aromatic five-membered ring. It's aromaticity is due to the delocalization of a lone pair of electrons from the sulfur atom giving the required 6 π electrons to satisfy Huckel's rule.[55]

Figure 2.6: Chemical structure of the thiazole ring[56]

Thiazoles are important for their wide range of pharmaceutical and biological properties,[57] and thiazole derivatives are known to exhibit an array of biological activities such as anticonvulsant, antimicrobial, anti-inflammatory, anticancer, antidiabetic, anti-Alzheimer's, antihypertensive, antioxidant, anti-HIV,[58] and are found in a number of clinically used drugs such as Sulfathiazole (antimicrobial drug), Ritonavir (antiretroviral drug), and Abafungin (antifungal drug) (Figure 2.7).[55]

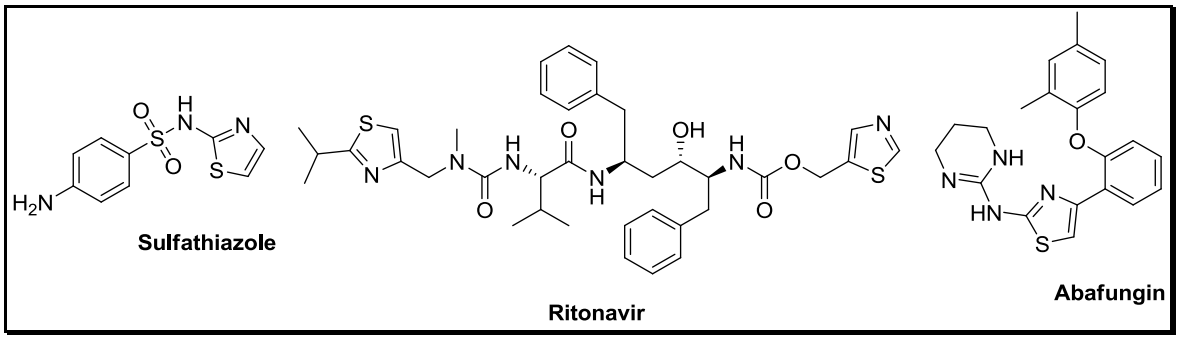

Figure 2.7: chemical structures of thiazole containing drugs in clinical use

2.2.1 Previous Studies on the Antimycobacterial Activity of Thiazoles

In a recent study conducted in 2011, *K.K.Roy et al*. demonstrated the antimycobacterial activity of some substituted 4-arylthiazol-2-amino derivatives. They synthesized and evaluated a series of analogues for antimycobacterial activity, and compounds **1** and **2** (Figure 2.8) both with an MIC_{99} of 6.25 µM effectively inhibited the growth of replicating *M.tb*.[24]

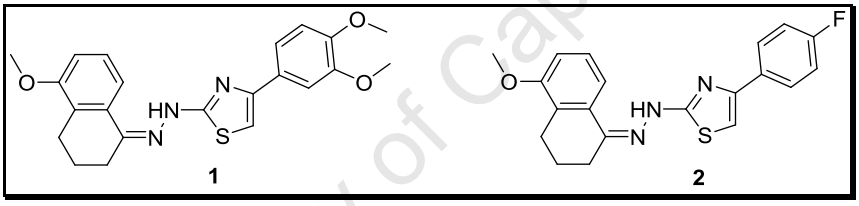

Figure 2.8: Chemical structures of 4-arylthiazol-2-amino analogues with antimycobacterial activity[24]

In a different study *G. Turan-zitouni et al* elicited antitubercular activity in compound **3** (Figure 2.9) which is an *N*-pyridyl-*N'*-thiazolylhydrazine derivative. The compound had an IC_{90} of 6.78µg/ml and further studies on it are still in progress.[19]

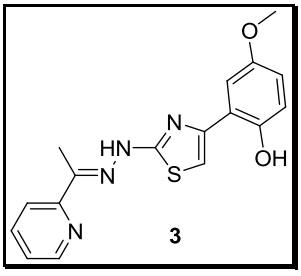

Figure 2.9: Chemical structure of an *N*-pyridyl-*N'*-thiazolylhydrazine analogue with antimycobacterial activity[19]

2.2.2 Previous Studies on the Antiplasmodial Activity of Thiazoles

A. Cohen et al. explored the antiplasmodial potential of new naphtho-[2,1-*d*] thiazole analogues and reported two hits, compounds **4** and **5** (Figure 3.0), with IC_{50} values of 4.8 and 2.7 µM *in vitro* activity against chloroquine and multi-drug resistant *P. falciparum* strain.[40]

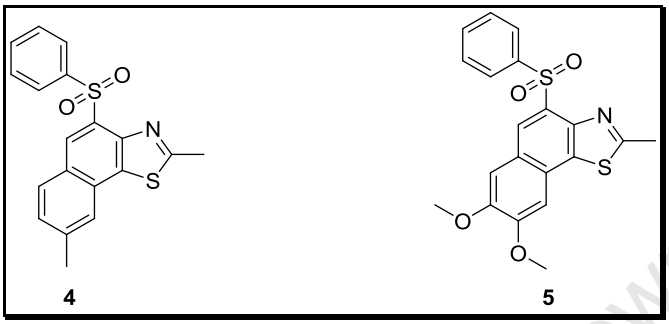

Figure 3.0: Chemical structures of naphtho-[2, 1-d] thiazole analogues with antiplasmodial activity[40]

D. Cabrera et al. demonstrated the antimalarial activity of an aminomethylthiazole pyrazole carboxamide **6** (Figure 3.1). The compound had good *in vitro* antiplasmodial activity with an IC_{50} of 0.08µM against the K1 (chloroquine and multi-drug resistant strain) and 0.07µM against the NF54 (chloroquine sensitive) *P.falciparum* strain and demonstrated *in vivo* efficacy in the *P.berghei* mouse model at a dose of 4 X 50mg/kg when administered orally.[38]

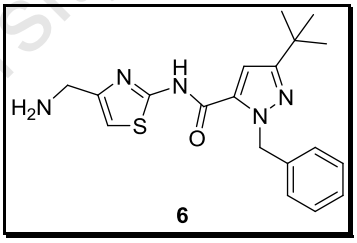

Figure 3.1: Chemical structure of an aminomethylthiazole pyrazole carboxamide with antimalarial activity[38]

2.3 Rationale

Substitutions on the thiazole ring have proven highly effective in improving potency as in the studies above. As mentioned in Chapter 1, a HTS conducted in 2009 by TAACF, demonstrated that the 2-amino-4-heteroaryl thiazole scaffold (Figure 2.5) possesses antimycobacterial activity. Out of 100,997compounds from the Chembridge library, and 1120 compounds from the Prestwick chemical library, 18 compounds were found to possess this scaffold. In the initial

single dose assay at 10µg/ml, 15 of these 18 compounds showed > 90% inhibition of growth. These 15 hits were screened in a dose-response assay from 50µg/ml to 0.098µg/ml and 13 of them had sub µg/ml TB IC_{90} values. Most of these compounds had a substituted phenyl or pyridyl group at the 2-amino position of the thiazole ring, and all active compounds had the 2-pyridyl group at position 4 of the thiazole ring. Some compounds which were 3-pyridyl and 4-pyridyl analogues (at position 4 of the thiazole ring) of the active compounds which were present in the library were found to be inactive, indicating optimum activity was with the 2-pyridyl group at this position.[54]

There are no Structure-Activity-Relationship (SAR) studies reported on this class of compounds to the best of our knowledge, therefore, in this study the SAR of the 2-amino-4-heteroaryl thiazole scaffold was conducted with the aim of validating the essentiality of each component attached to the scaffold for activity, expanding the SAR at the 2-amino position and investigating the findings from the HTS that the 2-pyridyl group at position 4 of the thiazole ring was optimum for activity (Figure 3.2)

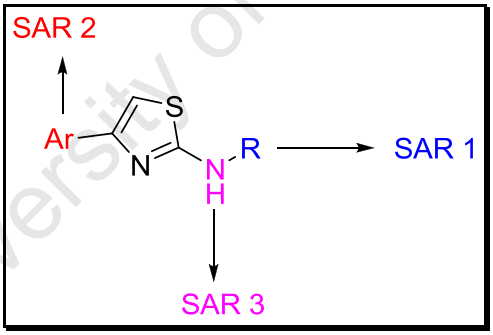

Figure 3.2: Investigated SAR series of the 2-amino-4-aryl thiazole scaffold.

The scaffold was investigated in the 3 different series described below:

i. Series 1 (SAR 1) - effect on activity of a substituted phenyl group at the 2-amino position
ii. Series 2 (SAR 2) - essentiality of the heteroaryl group at position 4 of the thiazole moiety
iii. Series 3 (SAR 3) - importance of the linker between the thiazole moiety and the substituted phenyl group via position 2 of the thiazole moiety.

2.4 Objective

Synthesis and SAR evaluation of 2-amino-4-heteroaryl thiazole derivatives as antimycobacterial and antiplasmodial agents.

2.4.1 Research Question

Is it possible to identify 2-amino-4-heteroaryl thiazole derivatives with potent antimycobacterial and/ or antiplasmodial activity and favorable drug metabolism and pharmacokinetic properties?

2.4.2 Specific Aims:

1. Synthesis of target compounds
2. Characterization of the target compounds using analytical and spectroscopic techniques
3. Conducting *in vitro* solubility profiling of synthesized compounds
4. Evaluating synthesized compounds for pharmacological (antimycobacterial and antiplasmodial) activity.
5. Performing *in vitro* microsomal metabolic stability profiling of the most potent analogues identified from pharmacological evaluation.

2.5 Series 1-Introduction, Synthesis and Characterization

2.5.1 Introduction

In determining the derivatives to be synthesized, it was envisioned that it would be advantageous if a rational approach could be followed in deciding which substituted analogues to make. The QSAR (quantitative structure-activity relationship) approach was used. QSAR tries to identify and quantify the physicochemical properties of a molecule and determine whether any of these properties has an effect on the biological activity. It allows some level of prediction by quantifying a linear relationship between a physicochemical property of a drug and its biological activity.[59]

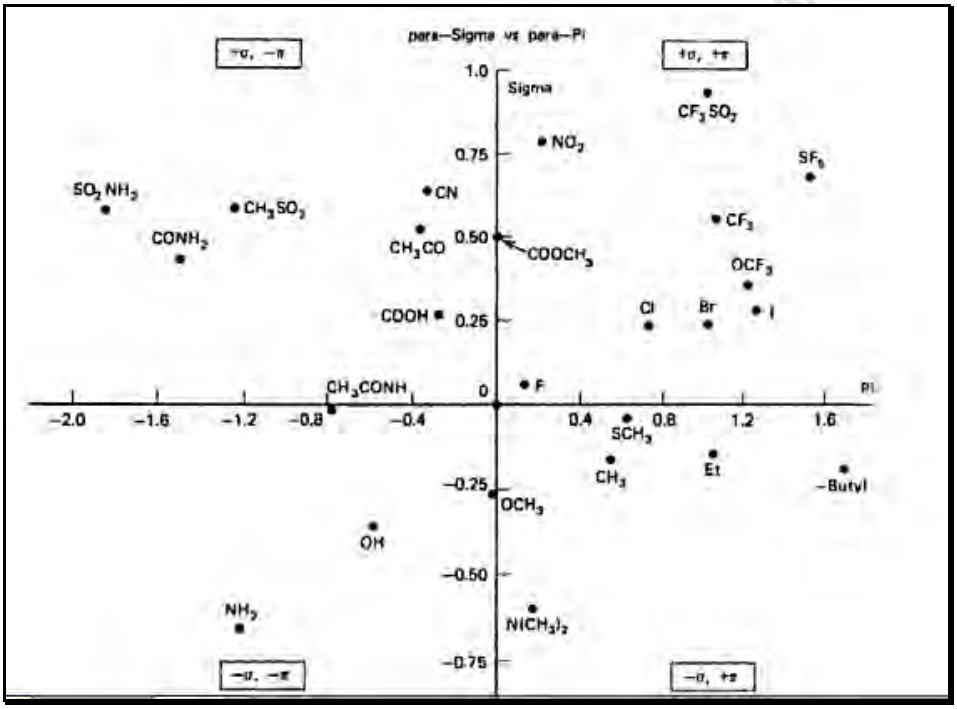

Figure 3.3: The Craig plot

Thus substituents on the phenyl ring, in this case, were selected by use of a Craig plot. This is a plot of π (pi) (substituent hydrophobicity constant) on the x axis and σ (sigma) (Hammett substitution constant,) of substituents on the y axis (Figure 3.3).

Pi is a measure of the hydrophobic character of a substituent and indicates how easily it crosses cell membranes, and interacts with receptors. Sigma is a measure of the electronic effects of a substituent and gives an idea of its ionization or polarity which in turn can indicate how easily it

can pass through cell membranes or how strongly it can bind to receptors. Changing substituents on a molecule may therefore have a significant effect on its hydrophobic and electronic character and hence its biological activity .[59]

Here derivatives of 2-amino-4-heteroaryl thiazoles with a phenyl group having substituents selected from the Craig plot were synthesized and profiled for physicochemical properties and pharmacological activity.

2.5.2 Synthesis of 4-R-N-[4-(2-pyridinyl)-2-thiazolyl]–benzamides

The desired targets were synthesized in a 3-step reaction sequence (Scheme 1.0) starting from commercially available 2-acetylpyridine, which was stirred in a mixture of 48% HBr and Br_2 for 1 hour at 65^{o}C, and then for a further 1 hour at room temperature to yield **FM001** as an orange solid in moderate yields.

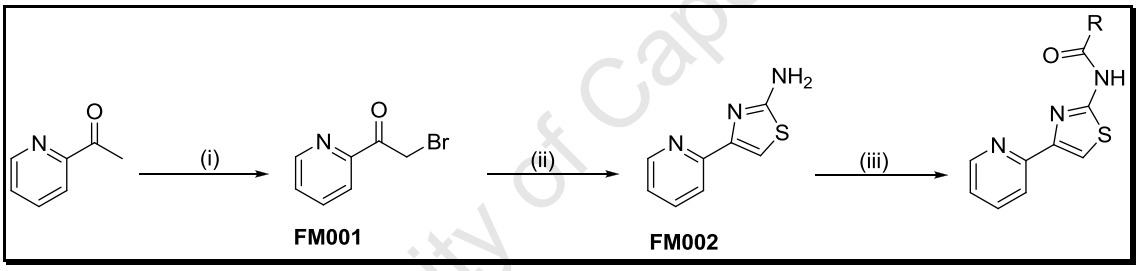

Scheme 1.0: Reagents and conditions; (i) HBr (48%), Br_2, 65^{o}C→RT, 2hr; (ii) Thiourea, EtOH, RT, 1hr; (iii)Appropriate carboxylic acid, EDCI, HOBt, DCM, RT, 24 hr.

The first step is an α-bromination reaction via enol formation to yield the α-bromoketone **FM001**. α-Haloketones are useful reagents in heterocyclic synthesis as they are highly reactive towards incoming nucleophiles. The reactivity of α-haloketones is due to the inductive effect of the carbonyl group which enhances the polarity of the carbon-halogen bond by increasing the electron deficiency at the α-carbon atom. In addition, the more polar the C-X bond, the faster the reaction with nucleophiles. Thus the formation of **FM001** is necessary to enhance reactivity during thiazole ring formation in the second step.[60] The HBr solvent acts to protonate the ketone, which promotes the reaction in two ways. First it increases the electrophilicity of the α-carbon on the ketone and second it generates the bromine ion (Br^-) which acts as a base

and picks up a beta proton, giving the enol tautomer, which is nuclephilic enough to attack Br_2, forming **FM001** as an HBr salt.

The second step of the reaction involves the formation of a thiazole ring when **FM001** is stirred at room temperature with thiourea in ethanol for 1 hour. The reaction proceeds via a Hantzsch synthesis[61] to yield the primary amine **FM002** as a pink powder in moderate yields.

FM002 is the key intermediate in this series, and it is formed via the condensation of the α-bromoketone **FM001** with thiourea (Figure 3.4).

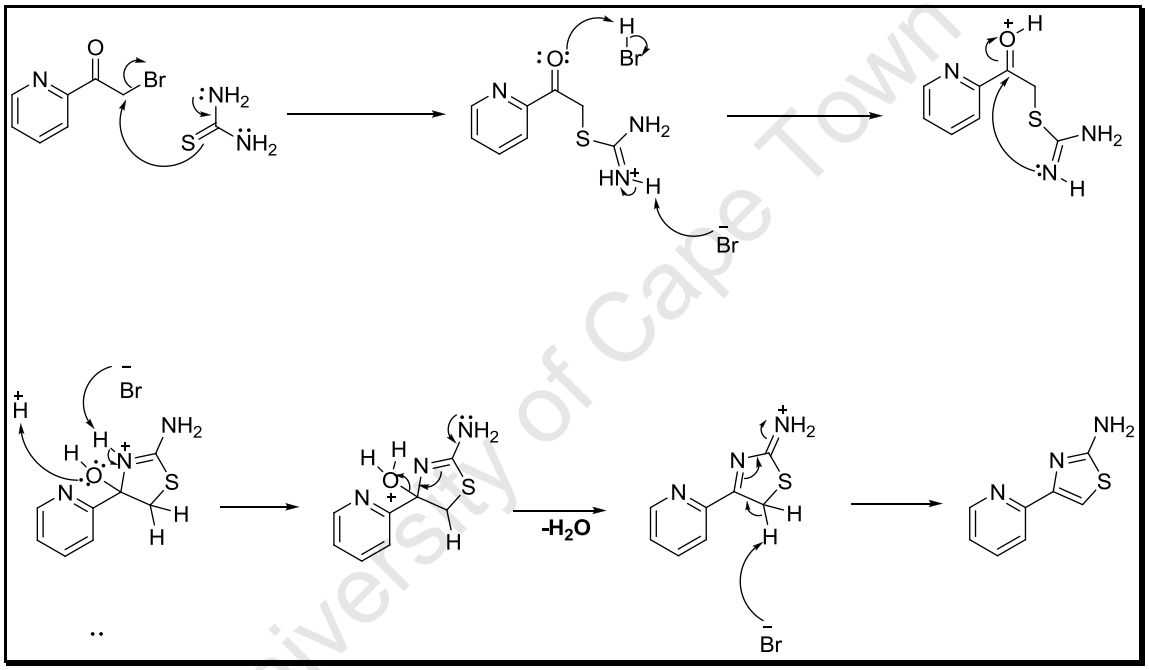

Figure 3.4: Proposed mechanism of formation of the 4-(pyridin-2-yl) thiazol-2-amine FM002.

The reaction is driven by the nucleophilicity of the amine groups attached to the sulfur atom in thiourea which causes it to attack the bromine bearing carbon of the α-bromoketone via an S_N2 mechanism thus displacing bromine and forming an S-C bond. This is followed by the deprotonation of the imminium ion intermediate to form an imine which enhances the nucleophilicity of the nitrogen, with generation of HBr. HBr enhances the polarization of the carbonyl by protonating it to form an oxonium ion. The electrophilic carbonyl carbon is then readily attacked by the nitrogen of the imine with concomitant ring closure. The bromide ion

then deprotonates the iminium and regenerates HBr. As the product still exists as an HBr salt at this point, sodium bicarbonate is used to neutralize the HBr to generate the final product as a free base.

The final step of the reaction is an EDCI (1-Ethyl-3-(3-dimethylaminopropyl) carbodiimide)-mediated coupling of **FM002** with a range of different appropriately substituted carboxylic acids. This was accomplished by adding the EDCI in small portions to a solution of the appropriate carboxylic acid and HOBt in dry DCM solvent and allowing this reaction mixture to stir for 10 minutes, followed by addition of the primary amine **FM002** as a solution in dry DCM. The reaction mixture was then left to stir for 24 hours at room temperature and the target benzamides isolated as solids in varying yields (Table 1.1).

EDCI is a coupling reagent used to activate carboxylic acid during amide synthesis by replacing the hydroxyl group of the carboxylic acid with a bulkier and better leaving group hence enhancing the acid reactivity. The initial step in the activation process is the addition of the carboxyl group to the carbodiimide to form an *O*-acylisourea intermediate which is then available for coupling with the incoming amine to yield the amide (Figure 3.5).

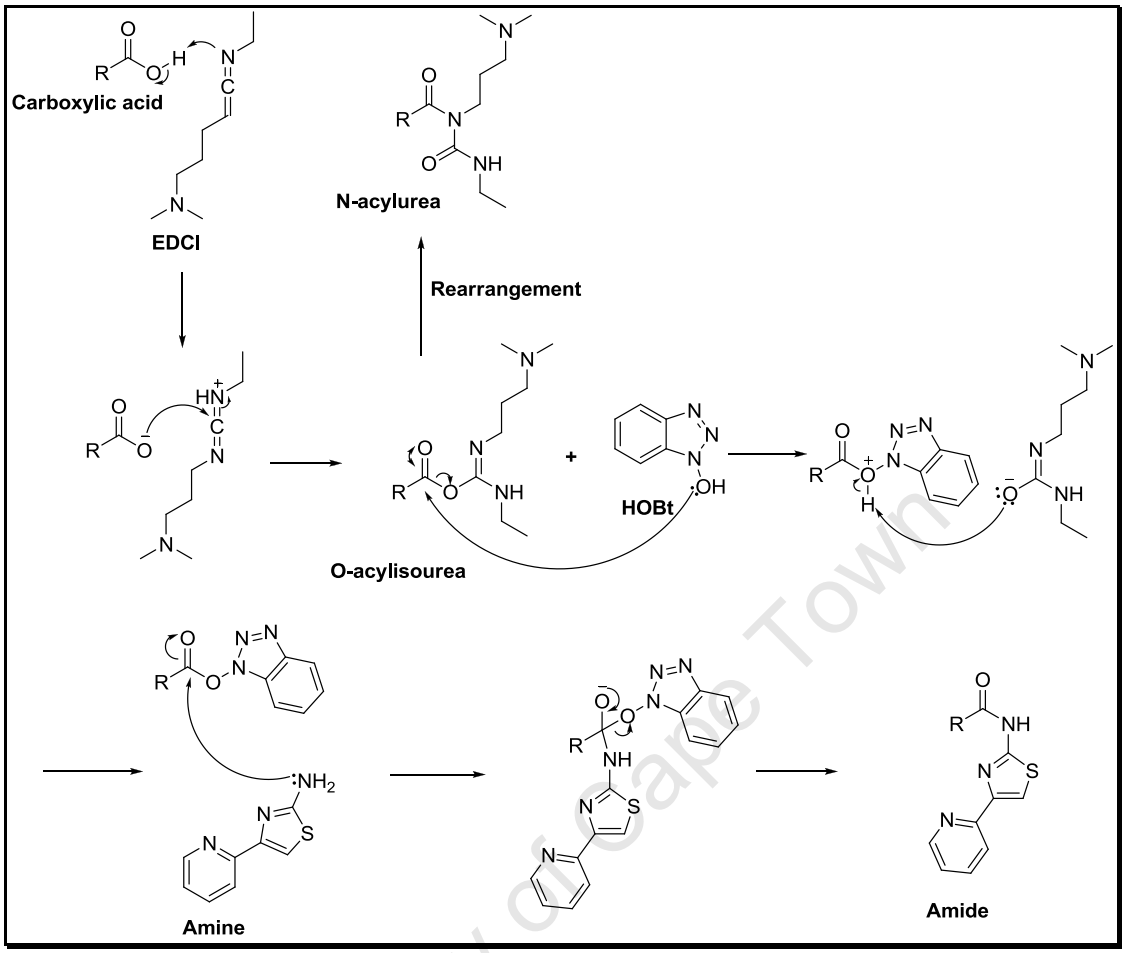

Figure 3.5: Proposed mechanism for the EDCI mediated coupling to form on amide bond

The EDCI and the carboxylic acid are left to react for ten minutes before the amine is added, in order to give time for this activated intermediate to form. The formation of the *O*-acylisourea is very fast and it then reacts with the incoming amine to form an amide bond. The *O*-acylisourea is very reactive and may undergo rearrangement via an intermolecular acyl transfer to form the more stable and unreative *N*-acylurea. If this occurs, it would lead to low reaction yields owing to decreased amounts of the *O*-acylisourea that the amine can react with to give the desired product. The addition of HOBt (1-hydroxybenzotriazole) is used to suppress the formation of this unreactive species, hence improving the yields. Yields may be further decreased when equilibrium is reached between the carboxylic acid, and the *O*-acylisourea. At equilibrium, formation of the symmetrical anhydride occurs because the reaction of the *O*-acylisourea with the unreacted carboxylic acid is faster than the addition of the acid to the carbodiimide.[62,63]

Table 1.1: Isolated yields, molecular ion peaks and melting points of the 4-(pyridine-2-yl)-2-thiazol amide derivatives

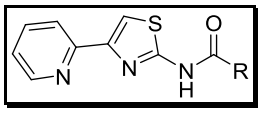

Compound code	R	% YIELD	$[M]^+$		Melting Point
			Expected	Found	(^oC)
RIZ 003		41	360.97	360.98	182-184
RIZ 004		42	406.96	406.95	200-202
RIZ 006	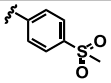	32	359.04	358.93	275-277
RIZ 007	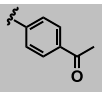	38	323.07	323.00	162-163
RIZ 008	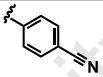	44	306.06	305.98	220-221
RIZ 009	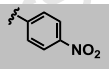	18	326.05	325.95	238-239
RIZ 010	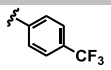	28	349.05	349.04	225-227
RIZ 011	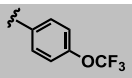	27	365.04	365.04	176-177
RIZ 012	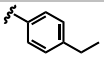	29	309.09	309.07	168-170
RIZ 013	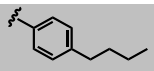	52	337.12	337.03	93-95
RIZ 015	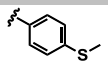	36	327.05	326.98	198-200

Compound code	R	% YIELD	[M]+		Melting Point
			Expected	Found	(°C)
RIZ 017	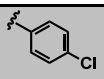	26	315.02	315.02	195-197
RIZ 018		21	299.05	299.03	179-181
RIZ 020		64	281.06	281.04	135-137
RIZ O21		56	360.97	360.91	178-180
RIZ 022	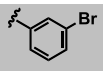	70	360.97	360.87	176-178
RIZ 023		62	282.06	281.94	148-150
RIZ 024		25	282.06	282.04	232-234
RIZ 025		22	282.06	282.01	215-217
RIZ 038		17	288.01	287.90	203-205
RIZ 039		12	271.05	270.77	229-231
RIZ 042		23	287.02	287.00	163-164

Spectroscopic Analysis of key intermediates and the final target compounds.

As the amides are derivatives of the same scaffold, many aspects of their NMR spectra are similar; therefore only one representative compound is described here. Most compounds in this series contained the thiazole ring, the amide linker, a phenyl ring substituted at *para* position and a 2-pyridine ring. These components give rise to characteristic peaks that allow for confirmation of the compounds being derivative of the 2-amino-*N*-(2-pyridinyl) thiazole scaffold.

The ^{1}H NMR spectrum of **FM001** agrees with that reported in literature.[64] The mass spectra gave the expected molecular ion peak with an *M/Z* ratio of 198.96 at 39.2% of the baseline, thus confirming the compound synthesized was the hydrobromide salt form.

The ^{1}H NMR spectrum for **FM002** shows the appearance of the NH_2 protons at 7.08 ppm as a broad singlet integrating for 2 H (Figure 3.6). Replacement of the keto group by a thiazole ring affects the relative shifts of the pyridyl protons. The thiazole being electron donating provides a shielding effect which results in a slight upfield proton shift relative to **FM001**. A sharp singlet at 4.97 ppm, corresponding to the $-CH_2$ in **FM001** disappears and there appears a new singlet in the aromatic region corresponding to H5 of the thiazole ring. The ^{13}C NMR spectrum indicates that all the expected carbons are present. The mass spectra gave the expected molecular ion peak with an *M/Z* ratio of 176.92 at 100% of the baseline, thus confirming the compound synthesized was the free primary amine. The melting point of the salt was found to be 174-176°C, which falls within range of the reported literature melting point of 173-174°C.[65]

The ^{1}H NMR spectrum of **RIZ015** shows the disappearance of the $-NH_2$ protons observed in **FM002** and the appearance of the –NH proton of the amide group appearing downfield at a high chemical shift value of 12.60 ppm, indicating the successful coupling between the amine and the carboxylic acid (Figure 3.6).

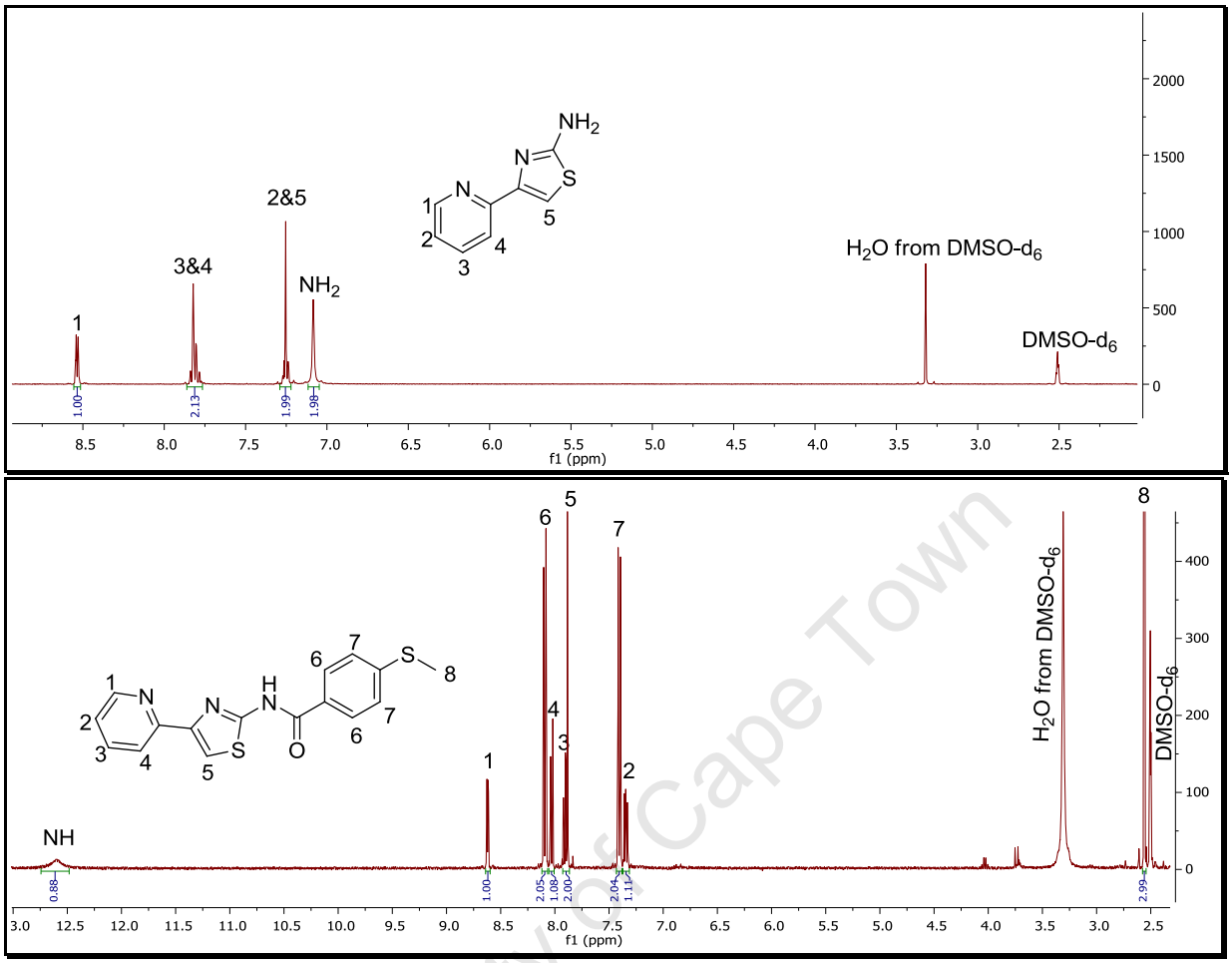

Figure 3.6: ^{1}H NMR of FM002 in DMSO-d_6 at 400 MH_Z (top) ^{1}H NMR of RIZ015 in DMSO-d_6 at 400 MH_Z (bottom)

The pyridyl protons remained in the same aromatic region with the single proton of the thiazole ring H5 appearing at 7.92-7.85 ppm with H3 as a multiplet. A singlet appearing at 2.56 ppm is representative of H8, the methyl protons of the methylthio group. The ^{13}C NMR spectrum indicates that all the expected carbons are present. The most upfield carbon in the spectrum is the $-CH_3$ group at 14.50 ppm, due to its attachment to the sulfur, while the most downfield carbon at 164.74 ppm corresponds to the carbonyl carbon. The mass spectra gave the expected molecular ion peak with an *M/Z* ratio of 326.98 at 25.3% of the baseline.

2.6 Series 2-Introduction, Synthesis and Characterization

2.6.1 Introduction

As mentioned earlier all active compounds from the HTS had a 2-pyridyl group at position 4 of the thiazole ring. Isomers of some of the active compounds with 3-pyridyl and 4-pyridyl groups at this position were present in the library and were found to be inactive, indicating optimum activity was with the 2-pyridyl group.[54] To investigate the findings from the HTS that the 2-pyridyl group at position 4 of the thiazole ring was optimum for activity, two analogues of the compound **RIZ 003** were synthesized where the 2-pyridyl group was replaced with a 3 and 4-pyridyl ring respectively. **RIZ 003** was selected as it had shown the best antimycobacterial activity in the preliminary screen.

2.6.2. Synthesis of 3-pyridyl and 4-pyridyl analogues of RIZ 003

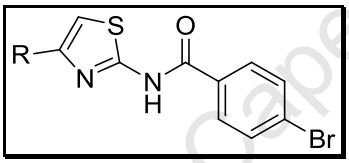

The compounds were synthesized in a 3 step reaction similar to the ones described for series 1 above in 2.5.2 but starting from commercially available 3-acetylpyridine and 4-acetylpyridine respectively (Scheme 1.1).

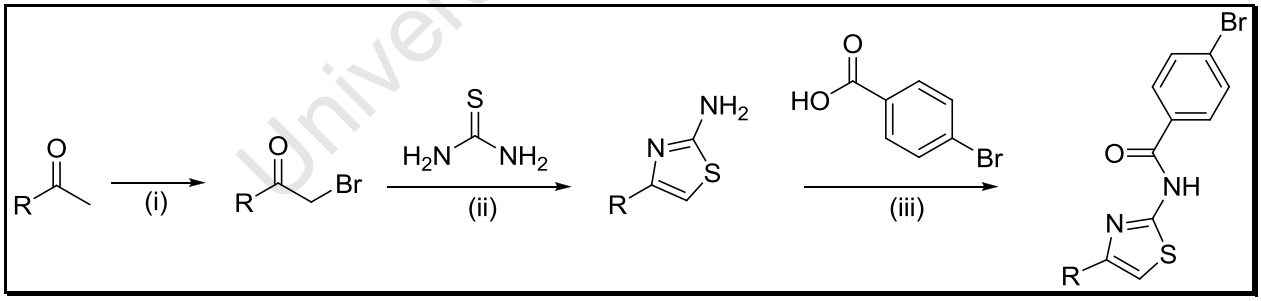

Scheme 1.1: Reagents and conditions; (i) HBr (48%), Br_2, 65^{o}C→RT, 2hr; (ii) EtOH, RT, 1hr; (iii) EDCI, HOBt, DCM, RT, 24 hr.

The compounds were isolated as solids in low yields (Table 1.2).

Table 1.2: Isolated yields, molecular ion peaks and melting points of the 3-pyridyl and 4-pyridyl analogues of RIZ003

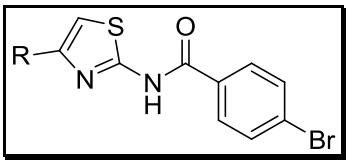

Compound code	R	% YIELD	[M]$^+$		Melting Point
			Expected	Found	(^{o}C)
RIZ 034		20	360.97	360.87	233-235
RIZ 035		23	360.97	360.86	251-253

Spectroscopic Analysis N-4-bromo-N-[4-(3-pyridinyl)-2-thiazolyl]-benzamide RIZ 034

The ^{1}H NMR spectrum shows the downfield appearance of the –NH proton of the amide group at a chemical shift value of 12.87 ppm as expected (Figure 3.7).

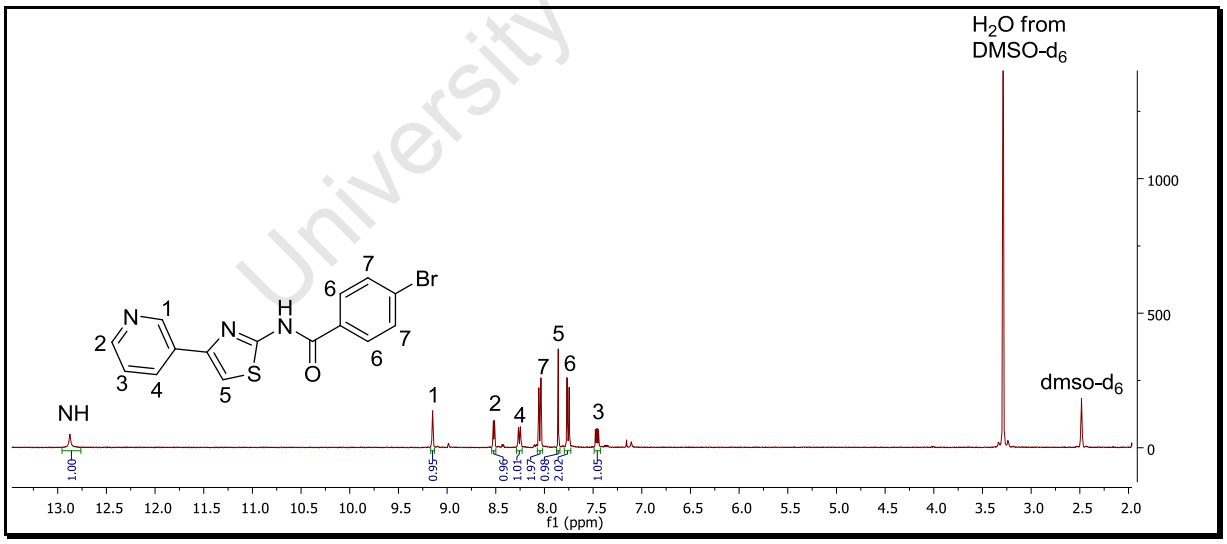

Figure 3.7: ^{1}H NMR of RIZ034 in DMSO-d_6 at 400 MH_Z

The pyridyl protons H1-H4 remained in the same aromatic region, but with extensive coupling, and a slightly downfield shift as their position relative to the nitrogen in the pyridyl group had

changed. The singlet appearing at 7.86 ppm is representative of the H5 of the thiazole ring. The ^{13}C NMR spectrum indicates that all the expected carbons are present within a similar high frequency range as expected since they are all –CH or tertiary carbons. The most downfield carbon is at 165.02 ppm and corresponds to the carbonyl carbon. There were also two sets of equivalent carbons of the phenyl ring. The mass spectra gave the expected molecular ion peak with an *M/Z* ratio of 360.87 at 38.0% of the baseline.

2.7 Series 3-Introduction, Synthesis and Characterization

2.7.1 Introduction

This series sought to investigate the effect of the linker between the thiazole moiety and the substituted aryl group via position 2 of the thiazole moiety. Here analogues of **RIZ 020** were synthesized with different bridges linking the 2-amino-4-(2-pyridyl) scaffold and the phenyl ring. **RIZ 020** was selected as the materials for synthesis were readily available.

2.7.2 Synthesis of RIZ 020 analogues with various linkers

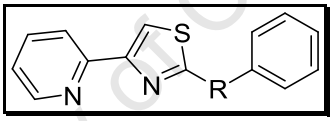

2.7.2.1. Synthesis of N-phenyl-[4-(2-pyridinyl) thiazole-2-amine, RIZ 020B

This compound was prepared by refluxing commercially available phenylthiourea and **FM001** in ethanol for 1 hour, (Scheme 1.2), and then cooling the mixture and adjusting its pH to approximately 8 using $NaHCO_3$, and then stirring for a further 2 hours at 20°C. **RIZ 020B** was isolated as a brown solid in 59% yield.

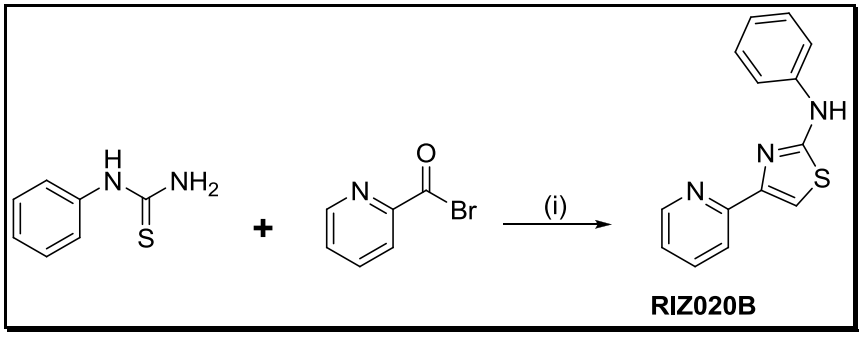

Scheme 1.2: Reagents and conditions; (i) EtOH, 90°C→20°C, 3 hr.

The reaction occurs in the same manner as described in step two of 2.5.2, but in this case an *N*-phenyl substituted thiourea was used.

Spectroscopic Analysis N-phenyl-[4-(2-pyridinyl) thiazole-2-amine, RIZ 020B

The ^{1}H NMR spectrum is as that reported in literature (Figure 3.8),[64] and shows the downfield appearance of the –NH proton of the amine at 10.27 ppm, slightly lower than the one observed with the amide group –NH as expected.

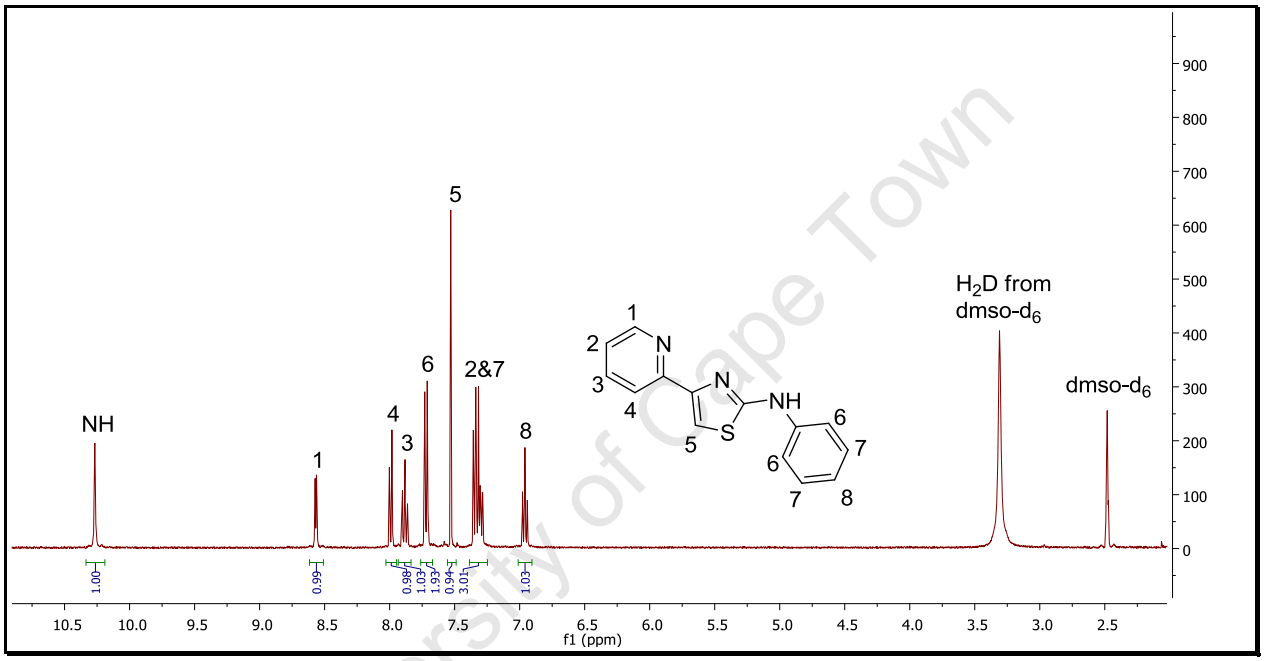

Figure 3.8: ^{1}H NMR of RIZ020B in DMSO-d_6 at 400 MH$_Z$

The pyridyl protons remained in the same aromatic region, some with extensive coupling hence appearing as multiplets. The singlet representing H5 appears at 7.53 ppm. The phenyl ring being unsubstituted gives 3 signals as expected. The ^{13}C NMR spectrum indicates that all the expected carbons are present within a similar high frequency range as expected since they are all –CH or tertiary carbons. The mass spectra gave the expected molecular ion peak with an *M/Z* ratio of 252.78 at 100.0% of the baseline. The melting point of the compound was found to be 142-144°C, the same as is reported in literature.[64]

2.7.2.2. Synthesis of 1-phenyl-3-[4-(2-pyridinyl) thiazol-2-yl) urea, RIZ 020C

This compound was synthesised by stirring phenylisocyanate and **FM002** at 56^0C for two hours, and then the heat was turned off and the reaction mixture left to stir at room temperature for 24 hours (Scheme 1.3). The phenylisocyanate was generated *in situ* by refluxing aniline and triphosgene in toluene for 8 hours, then cooling the mixture to 0^oC using ice before the addition of the amine **FM002.**

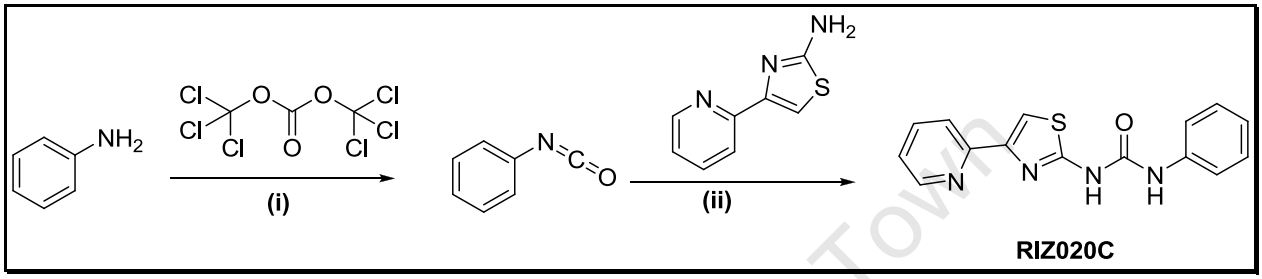

Scheme 1.3: Reagents and conditions; (i) Toluene, 120^oC→0^oC, 8 hr; (ii) 56^oC– RT, 26 hr.

Overnight the desired product precipitated out, and was recrystallized from absolute ethanol to yield the final pure product which was isolated as a pale-brown solid in 27% yield. The generation of the phenylisocyanate occurs via a nucleophilic substitution reaction while the last step to form the final compound is thought to be a nucleophilic addition reaction as depicted in figure 3.9.

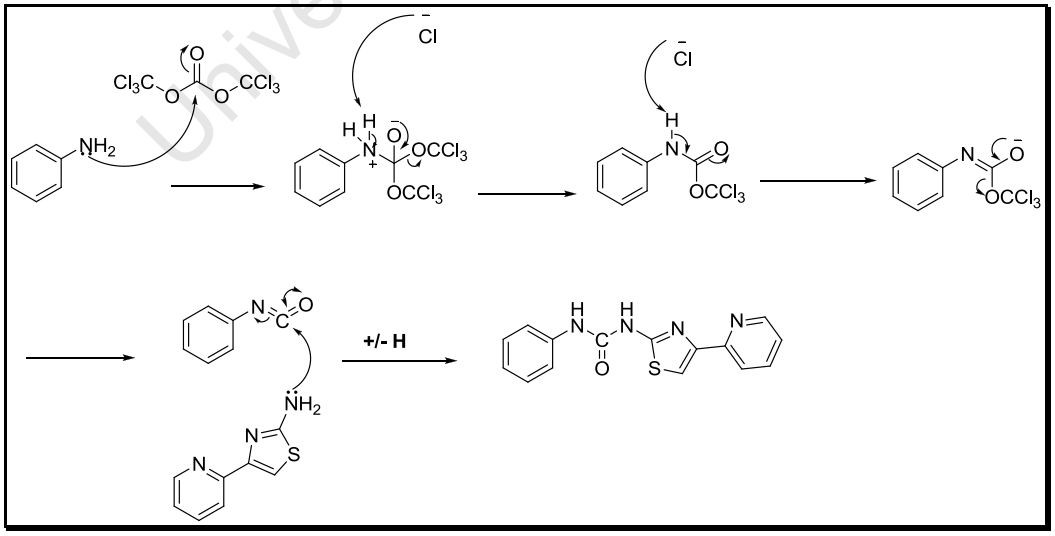

Figure 3.9: Proposed mechanism for the formation of 1-phenyl-3-[4-(2-pyridinyl) thiazol-2-yl) urea, **RIZ 020C**

2.7.2.3. Synthesis of N-[4-(2-pyridinyl) thiazol-2-ylcarbamothioyl) benzamide, RIZ 020F

The final target compound in this series was synthesized by refluxing commercially available benzoyl isothiocyanate and the amine **FM002** in acetone for 3 hours (Scheme 1.4) to yield the product as a pale green solid in 51% yield.

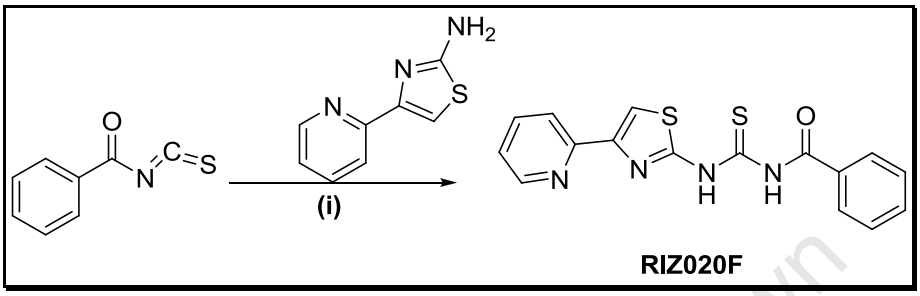

Scheme 1.4: Reagents and conditions; (i) Acetone, 70°C→0°C, 3 hr.

The reaction follows the same mechanism as the final step of the reaction mechanism described above in figure 3.9 with sulfur replacing the oxygen.

2.8. Physicochemical Properties, Pharmacological and Cytotoxicity Evaluation, and Microsomal Metabolic Stability Profiling

2.8.1 Physicochemical Properties

Physicochemical properties of a drug have an effect on the drug's pharmacological activity, and play an important role in the Absorption, Distribution, Metabolism, and Excretion (ADME) properties of the drug. Solubility is one of the most significant physicochemical properties of a drug candidate, and has long been noted as a limiting factor in the absorption process since only compounds in solution are readily available for permeation across the gastrointestinal membrane. Solubility is therefore related to the drugs' permeability and subsequently its pharmacological activity. However, there needs to be a balance between the solubility and lipophilicity of a drug to enable it not only be absorbed but to cross cell membranes and be effectively distributed.[66]

In this study the solubility of the synthesized compounds was determined experimentally by the turbidimetric assay and classified using the data described by Lipinski[67] as

- ≤ 5 µg/ml = low solubility
- 10-60 µg/ml = medium solubility
- ≥ 65 µg/ml = high solubility

Drug candidates with low aqueous solubility can yield misleading results during assays, with an increased risk of false hits and/or leads. Low solubility is typically associated with high plasma protein binding, slow tissue distribution, and drug-drug interactions generally leading to low biological activity. High solubility is desirable up to a certain limit beyond which permeability, and therefore activity, is decreased. It is therefore important to determine the solubility of compounds at an early stage of the drug development process to get an indication of the necessary balance required for activity and to avoid the risk of false hits or leads.[66]

From the results obtained it was observed that all the compounds in series 1 had low to moderate solubility, (Table 1.3), based on the nature of the substituent attached. Solubility is inversely proportional to the number and type of lipophilic functions within the molecule and also the tightness of the crystal packing of the molecule.

Table 1.3: Solubility of series 1 compounds

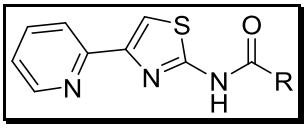

Compound code	R	Solubility (µg/mL)	Compound code	R	Solubility (µg/mL)
RIZ003	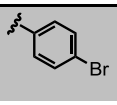	4.0	**RIZ017**	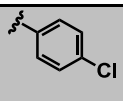	6.0
RIZ004	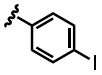	33.0	**RIZ018**	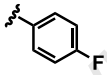	12.0
RIZ006	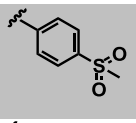	14.0	**RIZ020**		45.0
RIZ007	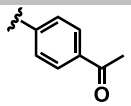	6.0	**RIZ021**		29.0
RIZ008	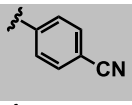	12.0	**RIZ022**	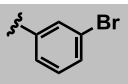	14.0
RIZ009	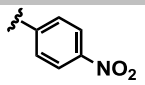	3.0	**RIZ023**		56.0
RIZ010	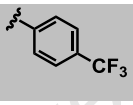	5.0	**RIZ024**		45.0
RIZ011	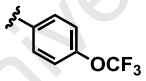	4.0	**RIZ025**		56.0
RIZ012	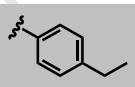	6.0	**RIZ038**	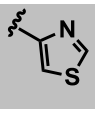	46.0
RIZ013	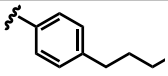	3.0	**RIZ039**		54.0
RIZ015	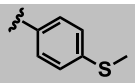	7.0	**RIZ042**		23.0

Based on the Craig plot substitutions, the electronic effect of the substituents didn't have influence on solubility of the compounds. Hydrophobicity of the substituents influenced

solubility to an extend as compounds with lipophilic groups such as halides had lower solubility compared to those with hydrophilic groups such as acetyl, or methylsulfonyl. Solubility was improved when the substituted phenyls were replaced by other heterocycles like the pyridine, thiophene, thiazole, and imidazole.

Series 2 compounds had moderate solubility (Table 1.4) probably due to the balance of the hydrophilic pyridine ring and the lipophilic bromo-substituted phenyl ring.

Table 1.4: Solubility of series 2 and 3 compounds

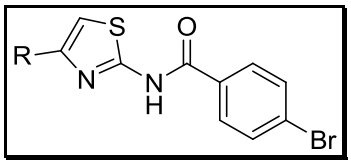

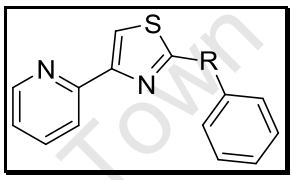

Series 2			Series 3		
Compound code	**R**	**Solubility (µg/mL)**	**Compound code**	**R**	**Solubility (µg/mL)**
RIZ034		14	**RIZ020B**	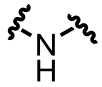	41
RIZ035		14	**RIZ020C**	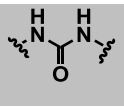	24
			RIZ020F	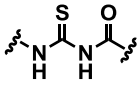	3

The solubility of compounds in series 3 decreased as the linker changed from an amine to urea, to acyl thiourea (Table 1.4) .These compounds were all less soluble than their amide analogue. This is probably due to the increase in tightness of the crystal packing of the molecule as the molecules tendancy for hydrogen bonding increased.

2.8.2 Pharmacological and Cytotoxicity Evaluation

The *in vitro* antimycobacterial activity of the synthesized compounds was measured in a micro plate-based assay where MIC_{99} (minimum concentration that will inhibit 99% of growth of

microorganism) was determined for all the compounds against *Mycobacterium tuberculosis* H37Rv strain. Rifampicin and Kanamycin were used as references for the assay.

The *in vitro* antiplasmodial activity of the compounds was performed in triplicate on one occasion against the chloroquine sensitive (CQS) *NF54* strain of *Plasmodium falciparum.* Chloroquine (CQ) was used as the reference drug in the assay. The cytotoxicity was tested against a mammalian Chinese Hamster Ovarian (CHO) cell-line using the 3-(4, 5-dimethylthiazol-2-yl)-2, 5-diphenyltetrazoliumbromide (MTT) assay.

2.8.2.1 Series 1 and 2

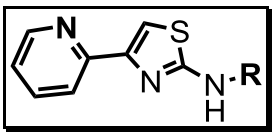

Antimycobacterial activity

The results obtained showed that compound in this series are active against *M.tb* within a range of between 1.25µM to 160µM. This activity is best with the phenyl substituted compounds with no significant variation based on the type of substituent at the *para* position (Table 1.5). This implies that the electronic effect and the hydrophobicity of the substituents didn't have an effect on activity. Compound **RIZ 003** had the best day 14 activity of 2.5µM. The non variation in activity could be due to the fact that the MIC_{99} values reported were determined based on a two-fold serial dilution of concentrations and not exact concentrations such that an MIC_{99} of 20µM represents concentrations of $10\mu M \leq MIC_{99} \leq 20\ \mu M$. This can be ruled out in future work where exact MIC_{99} values will be determined. It could also be that the activity is not dependent on whether the substituent on the phenyl ring is electron withdrawing or donating.

The position of the substituent, however, seems to have an effect on activity as demonstrated by the bromo-substituted compounds with day 7 activity of the *para*-bromo > *meta*-bromo > *ortho*-bromo.

Table 1.5: Series 1 Pharmacological Activity and Cytotoxicity

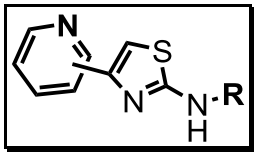

Compound	R	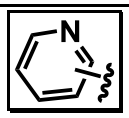	Antiplasmodial Activity NF54 IC_{50},µM(µg/ml)	Cytotoxicity (CHO) IC_{50},µM(µg/ml)	SI	Antimycobacterial $H_{37}Rv$ Activity MIC^{99} (µM)	
						Day 7	Day 14
RIZ 003	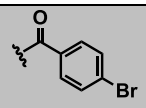	2-	5.3 (1.9)	3.6 (1.3)	0.7	1.25	2.5
RIZ 034	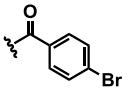	3-	15.9 (5.7)	89.0 (32.1)	5.6	>160	>160
RIZ 035	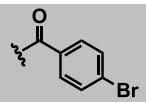	4-	3.5 (1.3)	34.4 (12.4)	9.8	>160	>160
RIZ 004	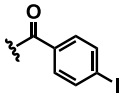	2-	3.9 (1.6)	7.9 (3.2)	2.0	5	5
RIZ 006	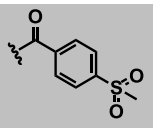	2-	5.9 (2.1)	19.7 (7.1)	3.3	10	20
RIZ 007	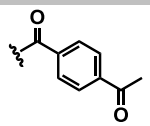	2-	14.8 (4.8)	2.1 (0.7)	0.1	10	10
RIZ 008	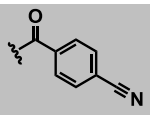	2-	0.8 (0.3)	3.1 (1.0)	3.9	5	10

Compound	R	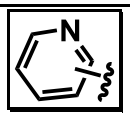	Antiplasmodial Activity NF54 IC_{50},µM(µg/ml)	Cytotoxicity (CHO) IC_{50},µM(µg/ml)	SI	Antimycobacterial $H_{37}Rv$ Activity MIC^{99} (µM)	
						Day 7	Day 14
RIZ 009	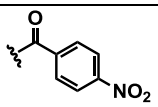	2-	6.1 (2.0)	2.2 (0.7)	0.4	5	5
RIZ 010	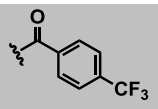	2-	18.6 (6.5)	2.0 (0.7)	0.1	5	5
RIZ 011	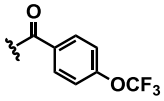	2-	5.5 (2.0)	23.3 (8.5)	4.2	2.5	5
RIZ 012	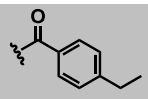	2-	6.5 (2.0)	6.5 (2.0)	1.0	2.5	5
RIZ 013	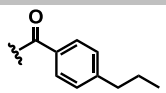	2-	7.4 (2.5)	3.4 (1.1)	0.5	20	20
RIZ 015	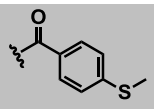	2-	7.6 (2.5)	4.5 (1.5)	0.6	5	5
RIZ 017	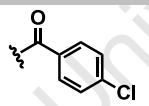	2-	1.3 (0.4)	3.2 (1.0)	2.5	5	5
RIZ 018	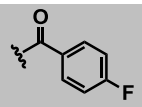	2-	1.8 (0.5)	3.1 (0.9)	1.7	5	5
RIZ 020	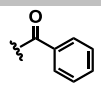	2-	1.0 (0.3)	3.0 (0.9)	3.0	5	5
RIZ 021	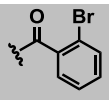	2-	2.2 (0.8)	3.4 (1.2)	1.5	5	5

Compound	R	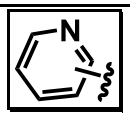	Antiplasmodial Activity NF54 IC_{50},µM(µg/ml)	Cytotoxicity (CHO) IC_{50},µM(µg/ml)	SI	Antimycobacterial $H_{37}Rv$ Activity MIC^{99} (µM)	
						Day 7	Day 14
RIZ 022	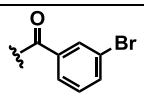	2-	1.6 (0.6)	2.8 (1.0)	1.8	2.5	5
RIZ 023	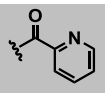	2-	>35.4 (>10)	9.2 (2.6)	0.3	80	80
RIZ 024	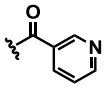	2-	>35.4 (>10)	0.7 (0.2)	0.02	10	10
RIZ 025	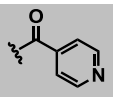	2-	1.9 (0.5)	0.0 (0.004)	0.005	5	5
RIZ 038	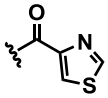	2-	13.8 (4.0)	14.3 (4.1)	1.0	160	160
RIZ 039	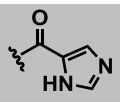	2-	35.0 (9.5)	1.4 (0.4)	0.04	160	160
RIZ 042	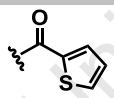	2-	0.9 (0.2)	2.8 (0.8)	3.1	*10	40
FM 002		2-	47.8 (8.5)	55.0 (9.8)	1.2	>160	>160

Selectivity index (SI) = IC_{50}µM CHO/IC_{50}µM NF54 * Precipitation

The solubility of the compounds didn't influence activity as most of the active compounds were poorly solube. Activity in this series decreased when the phenyl ring was replaced with other heterocycles such as the pyridine, thiophene, thiazole, and imidazole.

The 2-amino-4-(2-pyridyl) thiazole scaffold **FM002** was also tested along with the synthesized derivatives and was found to have an IC_{50} value of >160µM. This decreased activity compared to the other derivatives may be attributed to the fact that it doesn't contain any phenyl substitution at the 2-amino position of the thiazole ring. This therefore suggests that a substituted phenyl group at this position is essential for activity.

When the 2-pyridyl group at position 4 of the thiazole ring was replaced by the 3-pyridyl and 4-pyridyl analogues in series 2, activity was lost. This suggests that the 2-pyridyl group at this position is essential for antimycobacterial activity.

Antiplasmodial activity

The results showed that compounds in series 1 were active against the chloroquine sensitive (CQS) *NF54* strain of *Plasmodium falciparum* with IC_{50} values in the range of 0.2µg/ml to 10µg/ml (Table 1.5). This activity was best when the phenyl group is substituted with hydrophobic electron withdrawing groups, moderate when the phenyl group is substituted with hydrophilic electron withdrawing groups and least when the phenyl group is substituted with hydrophobic electron donating groups. The exception, however, was the most active compound **RIZ 008** which had an IC_{50} value of 0.8µM and contained a phenyl group substituted with a *para*-hydrophilic electron withdrawing -CN group. This suggests that the activity is influenced by the electronic effect of the substituent than its hydrophobocity.

The position of the substituent had an effect on activity as demonstrated by the bromo substituted compounds where activity of the *meta*-bromo > *ortho*-bromo > *para*-bromo. The solubility of the compounds didn't influence activity as some of the most active compounds were poorly solubility. Activity in this series decreased when the phenyl ring was replaced with other heterocycles like the 2-pyridine, 3-pyridine, thiazole, and imidazole. The thiophene and 4-pyridine ring, however, retained activity.

The 2-amino-4-(2-pyridyl) thiazole scaffold **FM002** was also tested along with the synthesized derivatives and was found to have an IC_{50} value of 47.8µM. This poor activity compared to the

other derivatives may suggest that a phenyl substitution at the 2-amino position of the thiazole ring may be essential for activity.

The antiplasmodial activity did not change significantly when the 2-pyridyl group at position 4 of the thiazole ring was replaced by the 3-pyridyl or 4-pyridyl in series 2. This suggests that the aryl group at this position may not be essential for antiplasmodial activity.

2.8.2.2 *Series 3*

Antimycobacterial activity

Varying the linker between the thiazole moiety and the substituted phenyl group from the amide to the amine, urea, and acylthiourea in series 3, resulted in compounds that were less active than the parent amide derivative (Table 1.6).

Table 1.6: Series 3 biological activity and cytotoxicity

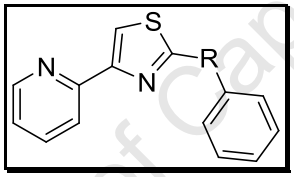

Compound	R	Antiplasmodial Activity NF54 IC_{50},µM(µg/ml)	Cytotoxicity (CHO) IC_{50},µM(µg/ml)	SI	Antimycobacterial $H_{37}Rv$ Activity MIC^{99} (µM)	
					Day 7	Day 14
RIZ 020B		3.2 (0.8)	1.3 (0.4)	0.4	160	160
RIZ 020C	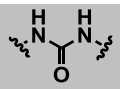	1.7 (0.5)	2.2 (0.7)	1.3	*10	80
RIZ 020F	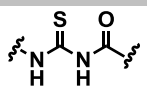	2.7 (0.9)	4.3 (1.5)	1.6	*20	80

Selectivity index (SI) = IC_{50}µM CHO/IC_{50}µM NF54 * Precipitation

As mentioned previously these compounds were all less soluble than their amide analogue and two of them precipitated out during testing making them not readily available in solution to exert activity on the *M.tb*.

Antiplasmodial activity

The antiplasmodial activity did not change significantly when linker was changed from amide to amine, urea, and acylthiourea in series 3. This suggests that the linker is not critical for the activity of the compounds. All tested compounds were less active than the reference drugs used and showed significant cytotoxicity on the (CHO) cell line and therefore had a low selectivity index. The antiplasmodial activity may therefore be due to the cytotoxic nature of the compounds and not due to any intrinsic antiplasmodial activity.

2.8.3 Metabolic Stability Profiling

The *in vitro* metabolic stability of a selected sample of the compounds was determined in human liver microsomes (HLM), rat liver microsomes (RLM), and mouse liver microsomes (MLM) separately. The samples were selected based on their antiplasmodial activity. Only compounds with an IC_{50} value of ≤ 2.0µM were tested.

Metabolic reactions were initiated by the addition of the co-factor NADPH to a mixture of the microsomes and the test compounds and incubated for 30 minutes.

From the obtained data, with the exception of **RIZ022**, the selected compounds exhibited instability across all species (Table 1.7). In addition **RIZ 017** and **RIZ 018** also show significant degradation (up to 20%) in buffer, while for **RIZ 020** it is about 5%.

Table 1.7: Metabolic Stability of Some Derivatives in Human, Rat, and Mouse Liver Microsomes.

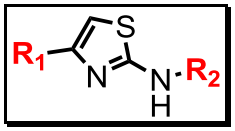

Compound	R_1	R_2	% remaining		
			HLM	RLM	MLM
RIZ 008		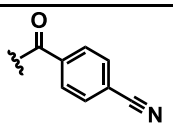	24.1	64.6	1.61
RIZ 017		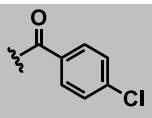	8.40	42.1	1.33
RIZ 018		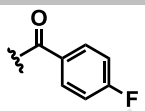	14.2	72.1	3.61
RIZ 020		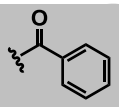	27.5	54.5	7.60
RIZ 022		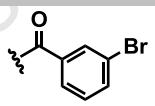	>99	>99	82.4
RIZ 025		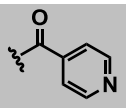	53.8	47.8	3.71

2.9. Conclusion

The SAR (Structure-Activity Relationship) study was conducted on the 2-amino-4-aryl thiazole scaffold by synthesizing a series of analogues with different motifs at the various positions of the scaffold.

The compounds were characterized using various spectroscopic and analytical techniques, such as ^{1}H, and ^{13}C NMR, melting point and mass spectrometry. Solubility of the compounds was also determined to establish its effect, if any, on the activity. The antiplasmodial, cytotoxicity and antimycobacterial activities as well as microsomal metabolic stability of the compounds were evaluated *in vitro*.

The compounds exhibited moderate antiplasmodial activity in the CQS strain of *P. falciparum*, and good antimycobacterial activity on the H37Rv strain of *M.tb*. It can be concluded that the 2-pyridyl group at position 4 of the thiazole ring is essential for antimycobacterial activity as is the presence of a substituted phenyl at position 2. The electronic effect of the substituents based on the Craig plot had no influence on either the solubility or the antimycobacterial activity of the compounds. However, the antiplasmodial activity was better with electron withdrawing substituents. The hydrophobicity of the substituents affected neither the antimycobacterial nor the antiplasmodial activity of the compounds but influenced their solubility as expected.

The linker between these two groups seems to affect solubility and hence antimycobacterial activity with little influence on the antiplasmodial activity. The antiplasmodial activity though good, could not be ascertained as intrinsic to the compounds due to their cytotoxic nature.

Most of the compounds had low to moderate solubility depending on the motifs attached to the scaffold. Most of the compounds were also unstable in HLM, RLM, and MLM, as well as in buffer.

An expansion of the SAR of this scaffold, to cover a wider chemical space and diversity, may be useful in order to draw detailed and useful insight.

CHAPTER 3: Design, Synthesis and Pharmacological evaluation of Metergoline Derivatives

3.1 Introduction

This chapter describes the design, synthesis and characterization of some new metergoline derivatives. Metergoline can be chemically viewed as an amine with a carboxybenzyl protecting group (Figure 4.0). The first step towards derivatization is therefore the removal of the carboxybenzyl protecting group to release the free amine that can then be derivatized. All synthesized derivatives were evaluated for *in vitro* antimycobacterial and antiplasmodial activity as well as cytotoxicity, and profiled for their solubility and microsomal metabolic stability.

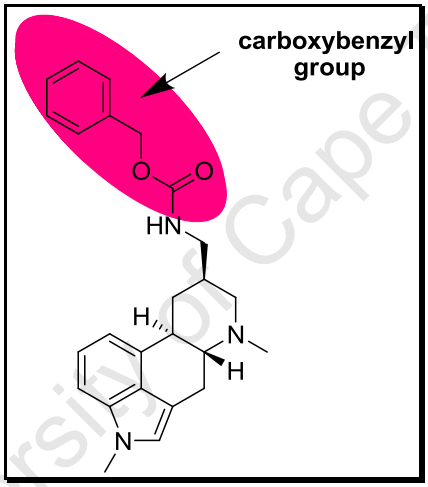

Figure 4.0: Chemical structure of metergoline

3.2 Background

Metergoline is a semi-synthetic ergoline alkaloid derived from the ergoline backbone (Figure 4.1). It is in clinical use for the management of hyperprolactinaemia and as a prophylaxis for migraine headaches.[68] Ergoline occurs naturally in lower fungi.

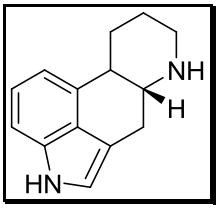

Figure 4.1: Chemical structure of the ergoline backbone

Ergoline alkaloids and their derivatives have broad clinical use such as: vasoconstriction in treatment of migraines (**ergotamine**),[69] management of Parkinson's disease (**bromocriptine**),[70] and as oxytoxics (**ergometrine**) [71] (Figure 4.2).

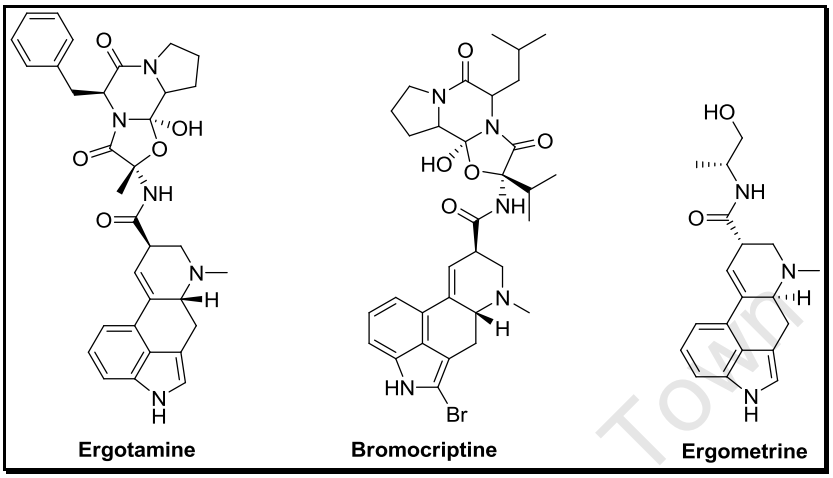

Figure 4.2: Chemical structures of drugs with an ergoline backbone in clinical use

Metergoline has been documented to have *in vitro* antifungal activity,[72,73] and has been investigated in the management of psychiatric disorders like obsessive compulsive disorder, carbon dioxide induced anxiety and premenstrual syndrome.[68,74–76] There is hardly any literature on its investigation as an antimicrobial or antiplasmodial agent, however, a HTS conducted by the TAACF on a vast library of compounds in 2009, found metergoline to have antimycobacterial activity with a MIC_{90} of between 5.6-6.0µg/ml.[77] In addition, a quantitative HTS for delayed death inhibitors of the malaria parasite plasmid, on a National Institute of Health (NIH) molecular library found metergoline to have antiplasmodial activity with an IC_{50} of 7.4µM.[78]

3.3 Rationale

There are a good number of compounds with an ergoline backbone in diverse clinical use as mentioned.[68–71] Metergoline being one of them demonstrated antimycobacterial activity in a HTS conducted by the TAACF, and antiplasmodial activity in a HTS for delayed death inhibitors of the malaria parasite plasmid on a NIH library as mentioned above.[77,78] Although there were more active compounds that metergoline in these screens, it nevertheless represents a good

starting point for drug repositioning through medicinal chemistry. There are no reports on any further studies on the potential of this compound and its derivatives as antimycobacterial and/or antiplasmodial agents after the HTS campaigns mentioned above. A clear advantage is that being in clinical use, the human system profile of the drug, and that of the ergoline backbone are already known thus making it attractive for repositioning. It was thus envisioned that structural modification could yield compounds with better antimycobacterial and antiplasmodial activity than the parent drug.

In this study, the ergoline backbone of metergoline was maintained and substitutions made on the free primary amine by incorporating various substituted aromatic rings. The QSAR approach[59] was used in determining the substituent on the aromatic ring.

3.4 Objective

To perform structural modifications on the ergoline backbone of metergoline, with a view to improving antimycobacterial and antiplasmodial activity and deriving analogues with favorable drug metabolism and pharmacokinetic properties.

3.4.1 Research Question

Is it possible to identify metergoline derivatives with potent antimycobacterial and/ or antiplasmodial activity and favorable drug metabolism and pharmacokinetic properties?

3.4.2 Specific Aims:

1. Synthesis of target compounds
2. Characterization of the target compounds using analytical and spectroscopic techniques
3. Conducting *in vitro* solubility profiling of synthesized compounds
4. Evaluating synthesized compounds for pharmacological (antimycobacterial and antiplasmodial) activity.
5. Performing *in vitro* microsomal metabolic stability profiling of the most potent analogues identified from pharmacological evaluation.

3.5 Introduction, Synthesis and Characterization of metergoline derivatives

3.5.1 Introduction

As already mentioned, metergoline is made up of an ergoline backbone and a carboxybenzyl group. Since this compound has these two distinct features the analogues synthesised were decided upon with the goal of retaining the similarity in features but with addition of groups that may improve activity.

3.5.2. Synthesis of the 4-R-N-((4,7-dimethyl-4,6,6a,7,8,9,10,10a-octahydroindolo[4,3-fg]quinolin-9-yl)methyl)benzamides

The desired benzamides were synthesized in a 2-step reaction sequence starting from commercially available metergoline which was catalytically cleaved by hydrogenation using Pd/C catalyst at room temperature (Scheme 1.5) to remove the benzyloxycarbamate group and yield the free amine **FRM000**.

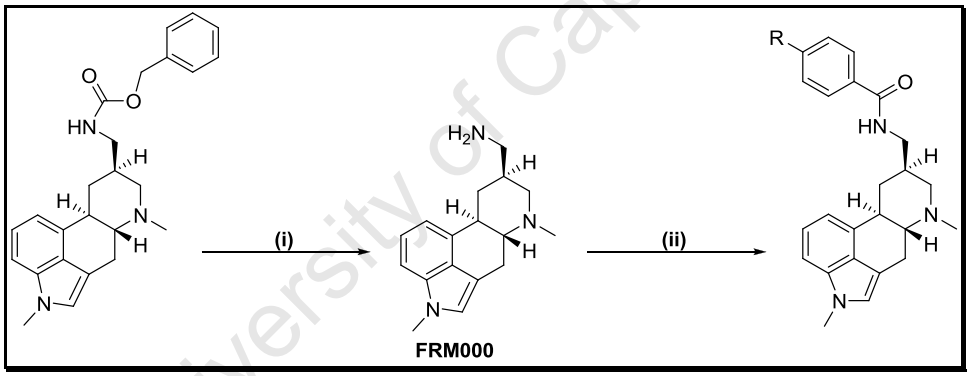

Scheme 1.5: Reagents and conditions; (i) EtOH:THF (1:1), H_2, 10% wt Pd/C, RT, 10 hr; (ii) Carboxylic acid, EDCI, HOBt, DCM, RT, 24 hr.

The second and final step of this reaction is an EDCI-mediated coupling of **FRM000** with a range of different appropriately substituted phenyl carboxylic acids. This was achieved by adding the EDCI in small portions to a solution of the appropriate carboxylic acid and HOBt in anhydrous DCM and letting this reaction mixture to stir for 10 minutes and then the primary amine **FRM000** was added as a solution in dry DCM (Scheme 1.5). The reaction mixture was then left to stir for 24 hours at room temperature and the different benzamides isolated as solids in varying yields (Table 1.8). The reaction proceeds as described in chapter 2, figure 3.5.

Table 1.8: Isolated yields, molecular ion peaks and melting points of 4-R-N-((4,7-dimethyl-4,6,6a,7,8,9,10,10a-octahydroindolo[4,3-fg]quinolin-9-yl)methyl)benzamides

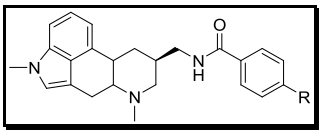

Compound code	R	% YIELD	$[M]^+$		Melting Point (^oC)
			Expected	Found	
FRM 001	**Br**	53	451.13	450.98	213-215
FRM 002	**CH_2CH_3**	37	401.25	401.07	192-194
FRM 003	**CN**	52	398.21	397.99	137-139
FRM 004	**NO_2**	37	418.20	417.93	228-230
FRM 005	**Cl**	35	407.18	406.87	224-226
FRM 006	**$N(CH_3)_2$**	78	416.26	415.92	258-260
FRM 007	**$(CH_2)_3CH_3$**	38	429.28	428.91	171-173
FRM 008	**SCH_3**	31	419.20	418.81	214-216
FRM 009	**I**	46	499.11	498.98	227-229
FRM 010	**SO_2CH_3**	44	451.19	451.16	209-211
FRM 011	**OCH_3**	41	403.23	403.12	212-214
FRM 012	**CF_3**	43	441.20	440.94	228-230
FRM 013	**$COCH_3$**	41	415.23	414.79	198-200
FRM 014	**F**	28	391.21	391.18	212-214
FRM 015	**H**	27	373.22	373.13	205-207
FRM 016	**OCF_3**	23	457.20	457.15	182-184

Spectroscopic Analysis of key intermediates and the final target compounds.

As the benzamides are derivatives of the ergoline backbone they contain the characteristic features as described for the key intermediate **FRM000**, and additional features based on the substituted phenyl group added. These additional features helped ascertain that the coupling to form the amides had successfully occurred. Since all compounds in this series contained the ergoline backbone, an amide linker, a phenyl ring substituted at the *para* position, only one representative compound is described here.

The ^{1}H NMR spectrum of **FRM000** is comparable to that reported in literature (Figure 4.3).[79] It has four characteristic aromatic protons as expected for H2, H10, H11 and H12. It shows two sharp singlets corresponding to the methyl groups H1 and H5 at chemical shift values of 3.71 ppm and 2.44 ppm respectively. H1 is more downfield by virtue of being attached to a nitrogen atom of an aromatic ring system. The aliphatic protons are in the region of 1.0-3.5 ppm as expected. The $-NH_2$ appeared upfield at approximately 1.75ppm. The ^{13}C NMR spectrum contains 17 carbon atoms as expected with the methyl carbons appearing slightly downfield due to being directly attached to a nitrogen atom. The mass spectra gave the expected molecular ion peak with an *M/Z* ratio of 269.15 at 100% of the baseline.

The ^{1}H NMR spectrum of **FRM012** shows the disappearance of the NH_2 protons of the amine group and the appearance of the NH proton of the amide group lying downfield at a chemical shift value of 6.36 ppm, indicating the successful coupling between the amine and the carboxylic acid (Figure 4.3). The aromatic protons of the ergoline backbone appear as in **FRM000** with some slight variation in the chemical shifts; however, the pattern is maintained.

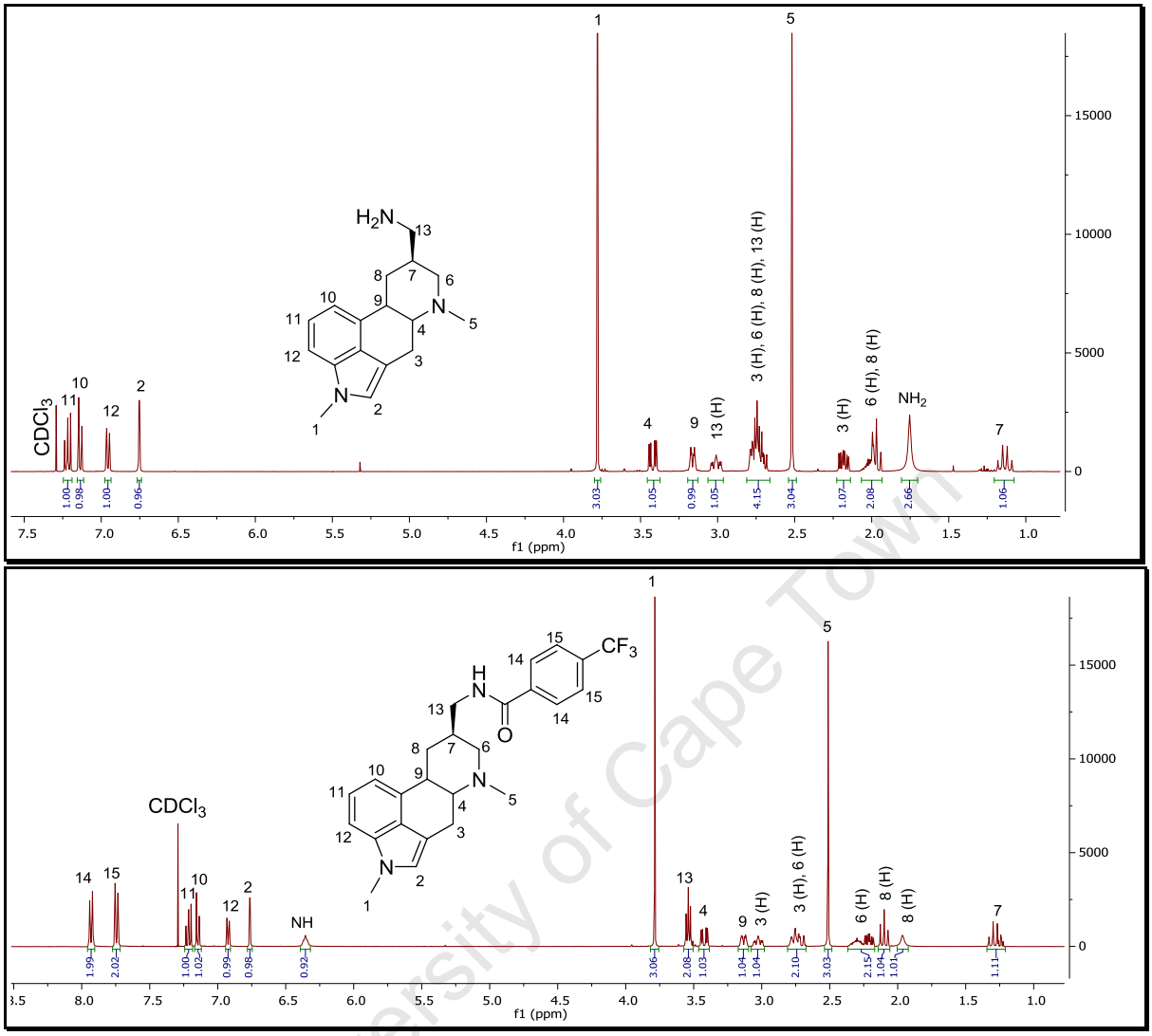

Figure 4.3: ^{1}H NMR of **FRM000** in $CDCl_3$ at 400 MH_Z (top). ^{1}H NMR of **FRM012** in $CDCl_3$ at 400 MH_Z (bottom)

The appearance of two doublets H14 and H15 representing the two sets of equivalent protons of the substituted phenyl ring further confirming successful coupling. ^{13}C NMR spectrum indicates that all the expected carbons are present. The most downfield carbon at a chemical shift value of 166.47 ppm corresponds to the carbonyl carbon. The mass spectra gave the expected molecular ion peak with an *M/Z* ratio of 440.94 at 100.0% of the baseline.

3.5.3. Synthesis of the 4-chloro-N-((4,7-dimethyl-4,6,6a,7,8,9,10,10a-octahydroindolo[4,3-fg]quinolin-9-yl)methyl)aniline, FRM017.

To investigate the importance of the linker between the ergoline backbone and the substituted phenyl group, an analogue of **FRM005** was synthesized with an amine linker. This was achieved via reductive amination where **FRM000** and 4-chlorobenzaldehyde were stirred for 2 hours at room temperature in dry DCM under nitrogen (Scheme 1.6), then cooled to 0^{o}C using ice. Sodium borohydride was then added to the imine generated *in situ* and the reaction left to warm to room temperature again and stirred for 24 hours. The final compound **FRM017** was isolated as a brown solid in moderate yield.

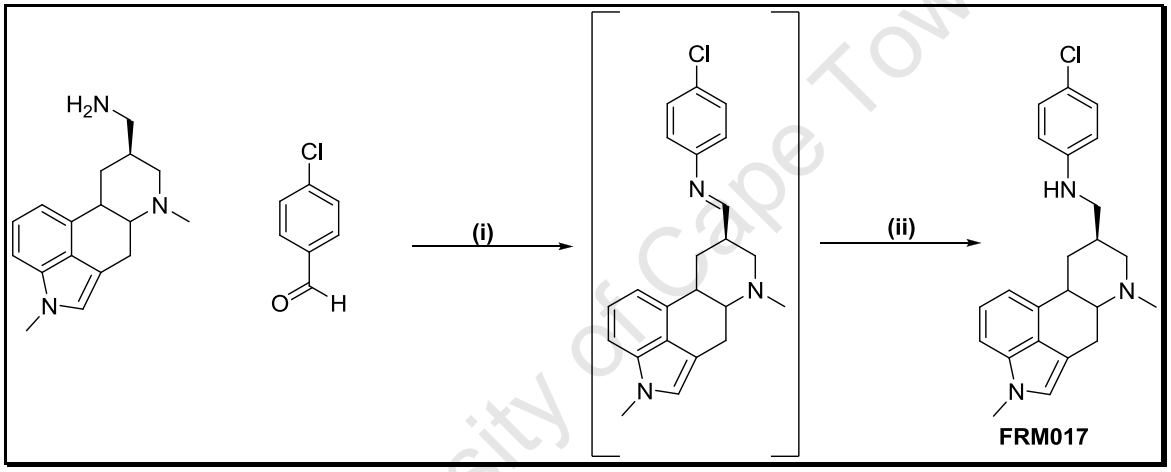

Scheme 1.6: Reagents and conditions; (i) N_2, DCM, RT→0^{o}C, 2 hr; (ii) $NaBH_4$, RT, 24 hr.

Spectroscopic Analysis of FRM017

The ^{1}H NMR spectrum shows the disappearance of the NH_2 protons of the primary amine group and the appearance of the NH proton of the secondary amine group lying upfield at a chemical shift value of 1.8 ppm, indicating a successful reductive amination (Figure 4.4). The ergoline backbone protons appear as in **FRM000** with some slight variation in the chemical shifts, however, the pattern is maintained. The appearance of a doublet at 7.34 ppm integrating for four protons corresponding to H15 and H16 further confirms a successful reaction. In addition there is the appearance of a doublet at a chemical shift value of 3.84 ppm corresponding to H14. The ^{13}C NMR spectrum indicates that all the expected carbons are present. The mass

spectra gave the expected molecular ion peak with an *M/Z* ratio of 392.95 at 100.0% of the baseline.

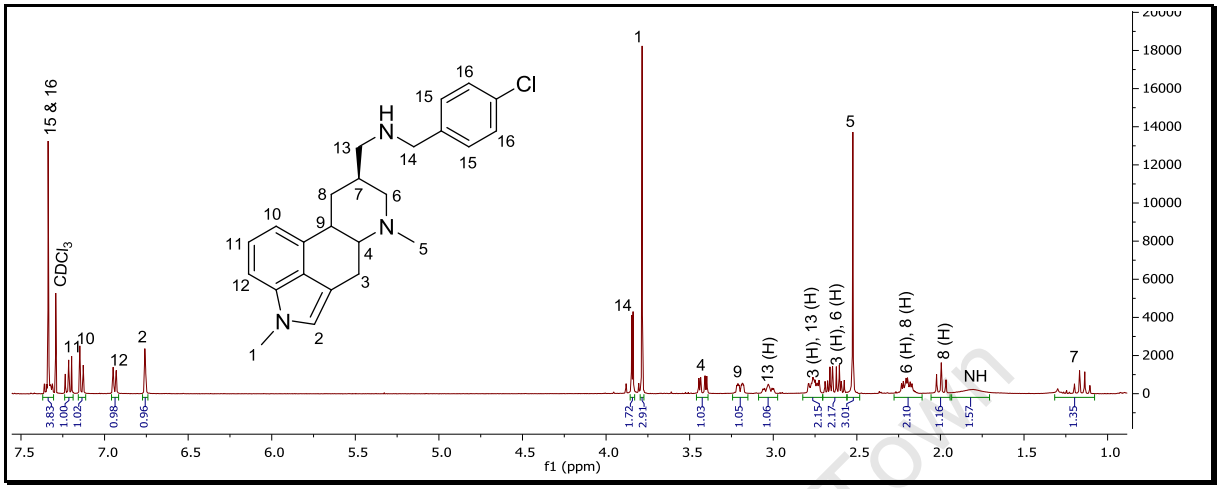

Figure 4.4: ^{1}H NMR of FRM017 in $CDCl_3$ at 400 MH_Z

3.6. Physicochemical Properties, Biological and Cytotoxicity Evaluation, and Microsomal Metabolic Stability Profiling

3.6.1 Physicochemical Properties

The solubility of the compounds was determined experimentally by the turbidimetric solubility assay and classified as

- ≤ 5 µg/ml = low solubility
- 10-60 µg/ml = medium solubility
- ≥ 65 µg/ml = high solubility[67]

The results obtained showed that the compounds had low to moderate solubility (Table 1.9).

Table 1.9: Solubility of metergoline amide analogues

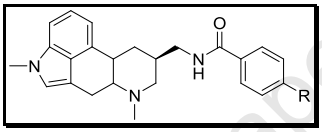

Compound code	R	Solubility (µg/mL)	Compound code	R	Solubility (µg/mL)
FRM 001	**Br**	4.0	FRM010	**SO_2CH_3**	12.0
FRM002	**CH_2CH_3**	33.0	FRM011	**OCH_3**	45.0
FRM003	**CN**	14.0	FRM012	**CF_3**	29.0
FRM004	**NO_2**	6.0	FRM013	**$COCH_3$**	14.0
FRM005	**Cl**	12.0	FRM014	**F**	56.0
FRM006	**$N(CH_3)_2$**	3.0	FRM015	**H**	45.0
FRM007	**$(CH_2)_3CH_3$**	5.0	FRM016	**OCF_3**	56.0
FRM008	**SCH_3**	4.0	Metergoline		32.0
FRM009	**I**	6.0	Unsubstituted amine FRM000		54.0

The free amine **FRM000** had a moderate solubility of 54µg/ml, while the compound **FRM017** which is an analogue of **FRM005** with an amine linker had a high solubility of 79µg/ml. This can be explained by the presence of the primary and secondary amine respectively which makes them hydrophilic due to the availability of the lone pair of electrons. The parent compound metergoline had a moderate solubility of 32µg/ml.

3.6.2 Pharmacological and Cytotoxicity Evaluation

In vitro Antimycobacterial Activity

The results obtained showed that compounds were active against *M.tb* H37Rv strain (Table 2.0) within MIC_{99} values in the range of 19µM-50µM. This suggests that the carboxybenzyl protecting group is not essential for activity. Activity is best with compounds that have the phenyl ring substituted with a hydrophobic electron withdrawing or donating group. This suggests that the electronic property of the substituent had no influence on activity. The hydrophobicity of the substituents, however, influenced activity since compounds that had hydrophilic substituents were less active than those with hydrophobic substituents. The hydrophobicity of the substituent may be enhancing activity by aiding the transport of the compounds across the cell wall and cell membrane of *M.tb* to the site of action. The free amine **FRM000** was also tested alongside the synthesized analogues and was found to be inactive at the maximum concentration of 50µM, suggesting that the presence of an aryl group attached to the nitrogen of the amine is essential for activity. However, since all compounds were less active than the parent metergoline (based on reported literature values), optimization of the aryl group is needed for optimized activity.

In vitro Antiplasmodial and Cytotoxicity Activity

The compounds were active against the chloroquine sensitive (CQS) *NF54* strain of *Plasmodium falciparum* with IC_{50} values in the range of 0.5µM-34µM *(*Table 2.0). Compounds with hydrophobic substituents were more active than those with hydrophilic substituents with the exception of the most active compound **FRM003** which had a hydrophilic substituent. The electronic property of the substituent and the solubility of the compounds did not affect activity.

Table 2.0: Summary of Pharmacological Activity and Cytotoxicity Evluation

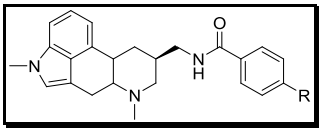

Compound	R	Antiplasmodial Activity NF54 IC_{50},µM(µg/ml)	Cytotoxicity (CHO) IC_{50},µM(µg/ml)	SI	Antimycobacterial $H_{37}Rv$ Activity MIC^{99} (µM)	
					Day 14	Day 21
FRM 001	**Br**	2.6 (1.2)	5.1 (2.3)	2.0	19	25
FRM 002	**CH_2CH_3**	4.3 (1.7)	5.6 (2.2)	1.3	19	25
FRM 003	**CN**	0.6 (0.2)	103.6 (41.3)	187.7	37	50
FRM 004	**NO_2**	0.5 (0.2)	5.0 (2.1)	10.7	37	50
FRM 005	**Cl**	1.3 (0.5)	4.3 (1.7)	3.3	19	25
FRM 006	**$N(CH_3)_2$**	33.8 (14.1)	132.5 (55.2)	3.9	25	50
FRM 007	**$(CH_2)_3CH_3$**	2.0 (0.9)	14.5 (6.2)	7.3	19	25
FRM 008	**SCH_3**	4.7 (2.0)	6.0 (2.5)	1.3	19	50
FRM 009	**I**	3.0 (1.5)	5.5 (2.7)	1.8	19	25
FRM 010	**SO_2CH_3**	14.2 (6.4)	221.5 (100)	15.6	37	>50
FRM 011	**OCH_3**	8.4 (3.4)	7.4 (3.0)	0.9	19	37
FRM 012	**CF_3**	2.7 (1.2)	4.9 (2.2)	1.8	19	37
FRM 013	**$COCH_3$**	12.3 (5.1)	151.9 (63.1)	12.4	19	50
FRM 014	**F**	12.5 (4.9)	7.3 (2.9)	0.6	37	50
FRM 015	**H**	24.4 (9.1)	27.0 (10.1)	1.1	37	50
FRM 016	**OCF_3**	4.2 (1.9)	12.8 (5.8)	3.1	25	50
*FRM 017	**Cl**	0.4 (0.15)	3.3 (1.3)	8.7		
Unsubstituted amine		3.6 (1.0)	26.1 (7.0)	7.0	50	>50
Metergoline		3.7 (1.5)	16.6 (6.7)	4.5	ND	ND

Selectivity index (SI) = IC_{50}µM CHO/IC_{50}µM NF54. *amine linker instead of an amide. ND-Not determined

Compounds which had the phenyl ring substituted with a hydrophobic group showed significant cytotoxicity on the CHO cell line and therefore had a low selectivity index while those with hydrophilic groups had a good selectivity index. The activity of these compounds could therefore be due to their cytotoxic effect. Metergoline and the free amine **FRM000** had IC_{50} of 3.7µM and 3.6µM respectively. The derivatization of the amine was thus beneficial as it gave some analogues with improved activity.

The best combination of activity and selectivity was compound **FRM003** with an activity of 0.6µM and a selectivity index of 188. This compound contained a phenyl ring substituted with a *para*-hydrophilic electron withdrawing a -CN group. **FRM017** with an amine linker was found to have an IC_{50} of 0.4µM and a selectivity index of 8.7 suggesting that the linker does not affect activity.

3.6.3 Metabolic Stability Profiling

The *in vitro* metabolic stability of the compounds was determined in human liver microsomes (HLM) and mouse liver microsomes (MLM) separately. Metabolic reactions were initiated by the addition of the co-factor NADPH to a mixture of the microsomes and the test compounds and incubated for 30 minutes.

From the obtained data, based on the HLM results, compounds with hydrophobic electron withdrawing and hydrophilic electron withdrawing substituents had better stability than those with hydrophobic electron donating groups (Table 2.1). Aromatic hydroxylation generally parallels electron density[80] with compounds having greater electron density undergoing faster metabolism. This may explain why electron withdrawing substituents increased metabolic stability,[81] assuming that metabolism proceeds through aromatic hydroxylation for these compounds. **FRM017** with an amine linker instead of an amide was unstable compared to its amide analogue **FRM005.** Metergoline was found to be unstable, and derivatization was successful in enhancing stability.

Table 2.1: Metabolic Stability of Some Derivatives in Human, Rat, and Mouse Liver Microsomes.

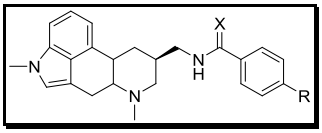

Compound code	R	X	% remaining		Compound code	R	X	% remaining	
			HLM	MLM				HLM	MLM
FRM 001	**Br**	**O**	60	82	FRM009	**I**	**O**	78	>99
FRM002	**CH_2CH_3**	**O**	45	61	FRM010	**SO_2CH_3**	**O**	>99	95
FRM003	**CN**	**O**	68	44	FRM011	**OCH_3**	**O**	58	82
FRM004	**NO_2**	**O**	69	>99	FRM012	**CF_3**	**O**	90	>99
FRM005	**Cl**	**O**	54	>99	FRM013	**$COCH_3$**	**O**	44	92
*FRM 017	**Cl**	**CH_2**	22	38	FRM014	**F**	**O**	20	78
FRM006	**$N(CH_3)_2$**	**O**	ND	ND	FRM015	**H**	**O**	5	63
FRM007	**$(CH_2)_3CH_3$**	**O**	22	>99	FRM016	**OCF_3**	**O**	79	>99
FRM008	**SCH_3**	**O**	14	50	metergoline			1.2	20

ND-Not determined. *amine linker instead of an amide

3.9. Conclusion

Structural modifications were performed on the ergoline backbone of metergoline, and a number of analogues synthesized with different *para* substituted phenyls.

The compounds were characterized using various spectroscopic and analytical techniques, such as ^{1}H, and ^{13}C NMR, melting point and mass spectrometry. Solubility of the compounds was also determined using the turbidimetric solubility method. The antiplasmodial, cytotoxicity and antimycobacterial activities as well as microsomal metabolic stability of the compounds were evaluated *in vitro*.

The compounds exhibited moderate antiplasmodial activity in the CQS strain of *P. falciparum*, and moderate antimycobacterial activity on the H37Rv strain of *M.tb*. The electronic effect of the substituent didn't have an influence on antimycobacterial activity while the hydrophobicity did have an effect since compounds that had hydrophilic groups were less active than those with hydrophobic groups. The presence of a substituted phenyl group attached to the nitrogen atom of the amine was found to be essential for antimycobacterial activity as the free unsubstituted amine was inactive at the maximum concentration of 50μM. The substituted phenyl group however didn't confer optimum activity as the compounds were less active than metergoline, hence a wider chemical space should be investigated. The antiplasmodial activity of the compounds wasn't influenced by the electronic property of the aromatic substituents whereas the hydrophobicity of the substituents enhanced activity although with significant cytotoxicity. Changing the linker to an amine group didn't have any significant effect on antiplasmodial activity. Derivatization led to analogues with better antiplasmodial activity than metergoline. As expected compounds with hydrophobic electron withdrawing substituents had better microsomal metabolic stability than those with hydrophobic electron donating groups.

An expansion of the diversity of structural motifs on the ergoline backbone to cover a wider chemical space may be useful in establishing SAR and aid the design and synthesis of more potent and metabolically stable derivatives. In addition further work will include *ortho* and *meta* substituted derivatives of some of the synthesized compounds.

CHAPTER 4: Summary and Future Prospects

4.1 General Summary and Conclusion

A SAR study was conducted on the 2-amino-4-aryl thiazole scaffold by synthesizing a series of analogues with different motifs at the various positions of the scaffold. Structural modifications were performed on the ergoline backbone of metergoline, and a number of analogues were synthesized with different substituted phenyls.

Standard organic synthetic routes were used and the compounds characterized using various spectroscopic and analytical techniques, such as ^{1}H, and ^{13}C NMR, melting point and mass spectrometry to ascertain their identity. Aqueous solubility of the compounds was determined experimentally by the turbidimetric solubility method. The *in vitro* antiplasmodial, cytotoxicity and antimycobacterial activities as well as the microsomal metabolic stability of the compounds were also evaluated.

In vitro results from the 2-amino-4-aryl thiazole scaffold studies indicate that,

i. For antimycobacterial activity:
   - The 2-pyridyl moiety at position 4 of the thiazole ring is essential
   - A substituted phenyl ring at the 2-amino position of the thiazole ring enhanced activity with the electronic effect and hydrophobicity of the substituent on the phenyl ring having no effect on activity
   - The solubility of the compounds was influenced by the hydrophobicity of the substituents
   - The linker between the thiazole moiety and the substituted aryl group via position 2 of the thiazole moiety affected solubility.

ii. For antiplasmodial activity:
   - The group attached at position 4 of the thiazole ring did not influence activity
   - A substituted phenyl ring at the 2-amino position of the thiazole ring enhanced activity with electron withdrawing substituents being the most active, while the hydrophobicity of the substituents had no effect.

- The solubility of the compounds was influenced by the hydrophobicity of the substituents
- The linker between the thiazole moiety and the substituted aryl group via position 2 of the thiazole moiety did not affect activity.

The compounds had low to moderate solubility depending on the motifs attached to the scaffold and were unstable in HLM, RLM, and MLM.

In vitro results from the metergoline analogues suggests

iii. For antimycobacterial activity:

- The presence of a substituted phenyl ring attached to the nitrogen of the amine enhanced activity as the unsubstituted amine was inactive
- The electronic property of the substituent on the phenyl ring had no effect on activity while the hydrophobicity enhanced activity
- The solubility of the compounds had no effect on activity
- The linker between the ergoline backbone and the substituted phenyl ring did not affect activity.

iv. For antiplasmodial activity

- The presence of a substituted phenyl ring attached to the nitrogen of the amine was not essential for activity as the unsubstituted amine was active
- The electronic property of the substituent on the phenyl ring had no effect on activity while the hydrophobicity enhanced activity
- The solubility of the compounds had no effect on activity
- The linker between the ergoline backbone and the substituted phenyl ring did not affect activity.

Compounds with hydrophobic substituents had moderate solubility while those with hydrophilic groups had high solubility. Compounds with electron withdrawing substituents had better stability than those with electron donating groups.

4.2 Future Outlook

An expansion of the SAR of the 2-amino-4-aryl thiazole scaffold and the structural modifications on the ergoline backbone, to cover a wider chemical space and incorporate chemical diversity, may be useful in future to draw detailed and useful insight as to the drivers of the SAR. In addition, testing the compounds against chloroquine and multi-drug resistant strains of *P. falciparum* and clinical isolates of drug resistant *M.tb* will give an indication of the usefulness of these compounds for investigation for drug resistant cases of malaria and tuberculosis. Lastly *ortho* and *meta* derivatives of some of the synthesized metergoline analogues will be synthesized to investigate the effect of the position of the substituent on the phenyl ring.

CHAPTER 5: Experimental

5.1. General comments

All reagents and solvents were obtained from commercial sources and used as received. All dry solvents were obtained from an SP-1 stand alone solvent purification system from LC Technology Solutions Inc. Reactions were monitored by thin layer chromatography (TLC) using Merck TLC silica gel 60 F_{254} aluminium-backed precoated plates and were visualized by ultraviolet light at 254 nm.

Nuclear Magnetic Resonance (NMR) spectra were recorded on a Varian Unity XR400 MHz (^{1}H at 400 MHz, ^{13}C at 100 MHz), or a Bruker Ultrashield 400 Plus spectrometer (^{1}H at 400 MHz, ^{13}C at 100 MHz). Chemical shifts for ^{1}H and ^{13}C NMR were reported using tetramethylsilane (TMS) as the internal standard. NMR data is presented as chemical shift in ppm on the δ scale relative to $^{\delta}$TMS = 0, intergration, multiplicity (s = singlet, d = doublet, t = triplet, q = quartet, and m = multiplet), coupling constant (*J*/ Hz).COSY experiments were used in some cases to fully interpret spectra for related compounds.

Melting points were determined using a Reichert-Hung Thermovar Hot Stage Microscope and are uncorrected. Mass Spectrometry was recorded on a JEOL GCmatell in Electron Ionisation mode. High Performance Liquid Chromatography (HPLC) was done using a Waters HPLC 2727 instrument with a Waters 2424 PDA detector and a Waters X-bridge C18 column (19mm x 250mm x 5µM, preparative). HPLC grade solvents were used to prepare 10mMol ammonium acetate in water and 10mMol ammonium acetate in methanol which were used as eluents.

The HPLC-MS system used for metabolic stability assay was Agilent 1200 Rapid Resolution (600 bar) HPLC with a diode array detector (DAD) coupled to an AB SCIEX 4000 QTRAP MS, equipped with a Turbo V™ ion source. Analyst 1.5.1 software was used for instrument control and data acquisition. Uv-vis absorbance readings for solubility assay were taken using a spectraMax 340PC[384].

5.2. Synthesis of 4-R-*N*-[4-(2-pyridinyl)-2-thiazolyl]–benzamides

5.2.1. General procedure for the synthesis of 2-bromo-1-(pyridin-2-yl) ethanone (FM001)

To a solution of 2-acetylpyridine (16.5 mmol) in 48% HBr (8 ml) was added Br_2 (16.5 mmol) in 48% HBr (3.2 ml).The reaction mixture was stirred at 65^{o}C for one hour, and then stirred at room temperature for an additional hour. It was then quenched with ice and the solvent reduced under reduced pressure. Ether was added and induced precipitation. The off-white solid **FM001** was filtered and washed with cold ether.

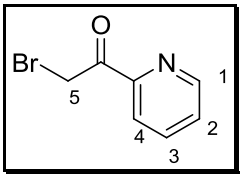

Off-white powder (3.1 g, 68%); m.p 205 – 207^{o}C; δ_H (400 MHz, DMSO): 8.71 (1H, ddd, *J* = 4.8, 1.7, 0.9 Hz, H-1), 8.08 - 8.03 (1H, m, H-3), 8.00 - 7.96 (1H, m, H-4), 7.71 (1H, ddd, *J* = 7.5, 4.8, 1.4 Hz,H-2), 4.97 (2H, s, H-5); δ_C(100 MHz, DMSO): 149.92, 149.16, 138.97, 129.47, 128.77, 124.40, 65.62; LRMS (EI+): *m/z* = 198.96 (39.2 %) [M+] calculated for C_7H_6BrNO 198.96 [M^+].

5.2.2. General procedure for the synthesis of 4-(pyridin-2-yl) thiazol-2-amine (FM002)

To a solution of **FM001** (11.2 mmol) in 25 ml of ethanol at room temperature was added thiourea (13.4 mmol).The reaction mixture was stirred at room temperature for 1 hour, quenched with water and washed with dichloromethane. The aqueous phase was concentrated *in vacuo* to give a yellow solid HBr salt. The salt was then dissolved in minimal amount of water and 10% NaOH added drop wise until a white precipitate **FM002** formed (approximately at pH 8).The precipitate was then filtered and dried.

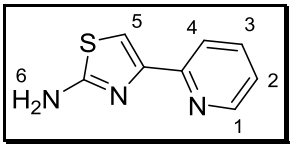

Pink powder (1.3 g, 67%); m.p 164 – 166^{o}C; δ_H (400 MHz, DMSO): 8.54 (1H, ddd, *J* = 3.1, 1.5, 1.0 Hz, H-1), 7.87 – 7.77 (2H, m, H-3, 4), 7.29 – 7.20 (2H, m, H-2, 5), 7.08 (2H, s, NH_2); δ_C (100 MHz, DMSO): 168.88, 152.94, 150.62, 149.70, 137.45, 122.70, 120.58, 105.85; LRMS (EI+): *m/z* = 176.92 (100.0%) [M+] calculated for $C_8H_7N_3S$ 177.04 [M^+].

5.2.3. General procedure for the synthesis of 4-R-N-[4-(2-pyridinyl)-2-thiazolyl] – benzamides

EDCI (1.7 mmol) was added in small batches to a solution of the carboxylic acid (1.4 mmol) and HOBt (1.7 mmol) in dry DCM or DMF (5 ml), and the reaction mixture was stirred for 10 minutes at room temperature. A solution of the amine (1.1 mmol) in 5 ml of dry DCM or DMF was added in small portions and the reaction mixture left to stir for 24 hr at room temperature (monitored by TLC until completion). The reaction mixture was then washed with saturated aqueous sodium bicarbonate (3 x 10ml), saturated aqueous sodium chloride (2 x 10ml), dried with anhydrous Na_2SO_4 and concentrated under reduced pressure. Purification by column silica gel chromatography (EtOAc/Hexane, 40:60) afforded the products as solids.

1. **4-bromo-N-[4-(2-pyridinyl)-2-thiazolyl]-benzamide (RIZ 003)**

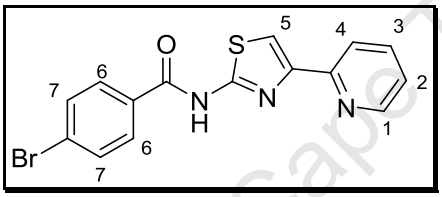

Pale-yellow crystals (83.5 mg, 41%); m.p 182 – 184^{o}C; δ_H (400 MHz, DMSO): 12.87 (1H, s, NH), 8.62 (1H, ddd, *J* = 4.8, 1.8, 1.0 Hz, H-1), 8.07 (2H, d, *J* = 8.6 Hz, H-6), 8.02 (1H, dt, *J* = 7.8, 1.0 Hz, H-4), 7.90 (1H, s, H-5), 7.89 (1H, td, *J* = 7.8, 1.8 Hz, H-3), 7.78 (2H, d, *J* = 8.6 Hz, H-7), 7.35 (1H, ddd, *J* = 7.8, 4.8, 1.0 Hz, H-2); δ_C (100 MHz, DMSO): 165.03, 159.30, 152.53, 150.01 (2C), 137.74(2C), 132.10 (2C), 131.71, 130.75 (2C), 127.05, 120.55, 112.72; LRMS (EI$^+$): *m/z* = 360.98 (48.9%) [M$^+$] calculated for $C_{15}H_{10}BrN_3OS$ 360.97 [M$^+$]; HPLC Purity: 99% (t_r = 14.87 min).

2. **4-iodo-N-[4-(2-pyridinyl)-2-thiazolyl]-benzamide (RIZ 004)**

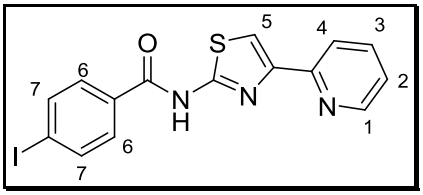

Pale-yellow crystals (94.6 mg, 42%); m.p 200 – 202^{o}C; δ_H (400 MHz, DMSO): 12.85 (1H, s, NH), 8.62 (1H, ddd, *J* = 4.8, 1.8, 1.0 Hz, H-1), 8.02 (1H, dt, *J* = 7.7, 1.0 Hz, H-4), 7.97 – 7.94 (2H, m, H-6), 7.93 – 7.88 (4H, m, H-3, 5, 7), 7.35 (IH, ddd, *J* = 7.7, 4.8, 1.0 Hz, H-2); δ_C (100 MHz, DMSO): 165.30, 159.15, 152.53, 150.01, 149.89, 137.97 (2C), 137.74, 131.96, 130.50 (2C), 123.34,

120.55, 112.72, 100.25; LRMS (EI$^+$): *m/z* = 406.95 (63.6%) [M$^+$] calculated for $C_{15}H_{10}IN_3OS$ 406.96 [M$^+$]; HPLC Purity: 99% (t_r = 15.24 min).

3. **4-methylsulfonyl-N-[4-(2-pyridinyl)-2-thiazolyl]-benzamide(RIZ006)**

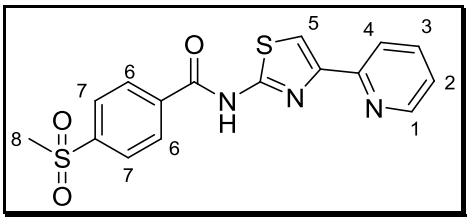

Off-white crystals (34.3 mg, 32%); m.p 275 – 277^{o}C; δ_H (400 MHz, DMSO): 13.05 (1H, s, NH), 8.61 (1H, ddd, *J* = 4.8, 1.8, 1.0 Hz, H-1), 8.33 (2H, d, *J* = 8.7 Hz, H-7), 8.09 (2H, d, *J* = 8.7 Hz, H-6), 8.01 (1H, dt, *J* = 7.8, 1.0 Hz, H-4), 7.92 (1H, s, H-5), 7.89 (1H, td, *J* = 7.8, 1.8 Hz, H-3) 7.34 (1H, ddd, *J* = 7.8, 4.8, 1.0 Hz, H-2), 3.30 (3H, s, H-8); δ_C (100 MHz, DMSO): 164.74, 159.03, 152.47, 150.04, 144.48, 137.78, 137.00, 129.73 (2C), 127.60(2C), 123.40, 120.58, 112.93, 43.68; LRMS (EI+): *m/z* = 358.93 (77.6%) [M+] calculated for $C_{16}H_{13}N_3O_3S_2$ 359.04 [M$^+$]; HPLC Purity: 99% (t_r = 8.45 min).

4. **4-acetyl-N-[4-(2-pyridinyl)-2-thiazolyl]-benzamide (RIZ 007)**

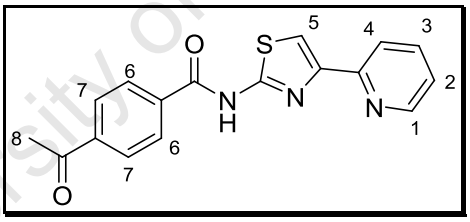

Pale-brown crystals (139.6 mg, 38%); m.p 162 – 163^{o}C; δ_H (400 MHz, DMSO): 13.00 (1H, s, NH), 8.65 (1H, ddd, *J* = 4.7, 1.7, 0.9 Hz, H-1), 8.27 (2H, d, *J* = 8.3 Hz, H-6), 8.12 (2H, d, *J* = 8.3 Hz, H-7), 8.05 (1H, m, H-4), 7.97 – 7.89 (2H, m, H-3,5), 7.37 (1H, ddd, *J* = 7.2, 4.7, 0.9 Hz, H-2), 2.68 (3H, s, H-8); δ_C (100 MHz, DMSO): 198.15, 165.14, 152.50, 150.01, 149.56, 140.07, 137.77, 129.05 (2C), 128.70 (2C), 123.37, 122.77, 120.58, 112.84, 105.99, 27.49; LRMS (EI+): *m/z* = 323.00 (41.8%) [M+] calculated for $C_{17}H_{13}N_3O_2S$ 323.07 [M$^+$]; HPLC Purity: 99% (t_r = 13.17 min).

5. **4-cyano-N-[4-(2-pyridinyl)-2-thiazolyl]-benzamide (RIZ 008)**

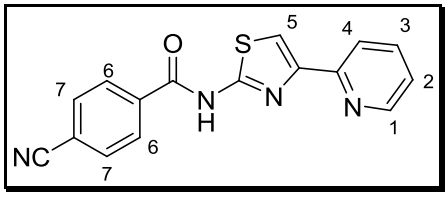

Dark-brown crystals (151.5 mg, 44%); m.p 220 – 221°C; δ_H (400 MHz, DMSO): 13.02 (1H, s, NH), 8.60 (1H, ddd, *J* = 4.8, 1.8, 1.1 Hz, H-1), 8.24 (2H, d, *J* = 8.2 Hz, H-6), 8.05 – 7.97 (3H, m, H-4, 7) 7.92 (1H, s, H-5), 7.89 (1H, td, *J* = 7.6, 1.8 Hz, H-3), 7.33 (1H, ddd, *J* = 7.6, 4.8, 1.1 Hz, H-2); δ_C (100 MHz, DMSO): 164.63, 152.44, 150.03, 137.78, 136.55, 133.02 (2C), 129.49 (2C), 122.72, 120.58, 118.61, 115.25, 112.95, 105.90, 72.47; LRMS (EI+): *m/z* = 305.98 (92.3%) [M+] calculated for $C_{16}H_{10}N_4OS$ 306.06 [M^+]; HPLC Purity: 99% (t_r = 13.13 min).

6. **4-nitro-N-[4-(2-pyridinyl)-2-thiazolyl]-benzamide (RIZ 009)**

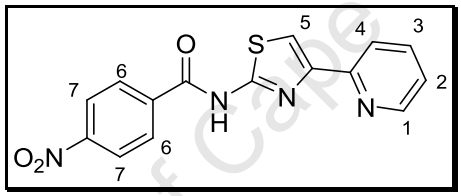

Deep-yellow crystals (66.6 mg, 18%); m.p 238 – 239°C; δ_H (400 MHz, DMSO): 13.15 (1H, s, NH), 8.63 (1H, ddd, *J* = 4.8, 1.3, 1.3 Hz, H-1), 8.42 – 8.31 (2H, m, H-6, 7), 8.03 (1H, dt, *J* = 7.8, 1.3, Hz, H-4), 7.95 (1H, s, H-5), 7.91 (1H, td, *J* = 7.8 1.3 Hz, H-3), 7.36 (1H, ddd, *J* = 7.8, 4.8, 1.3 Hz, H-2); δ_C (100 MHz, DMSO): 164.40, 158.93, 152.43, 150.20, 150.05, 138.17, 137.79, 130.28 (2C), 124.07 (2C), 123.42, 120.57, 113.00; LRMS (EI+): *m/z* = 325.95 (100.0%) [M+] calculated for $C_{15}H_{10}N_4O_3S$ 326.05 [M^+]; HPLC Purity: 99% (t_r = 13.80 min).

7. **4-trifluoromethyl-N-[4-(2-pyridinyl)-2-thiazolyl]-benzamide (RIZ 010)**

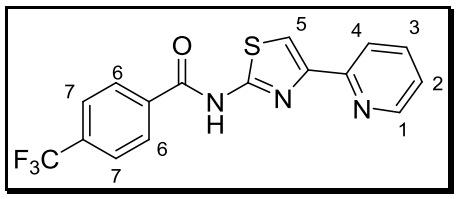

White crystals (111.6 mg, 28%); m.p 225 – 227°C; δ_H (400 MHz, DMSO): 13.05 (1H, s, NH), 8.63 (1H, ddd, *J* = 4.8, 1.7, 0.8 Hz, H-1), 8.32 (2H, d, *J* = 8.3 Hz, H-6), 8.03 (1H, m, H-4), 7.96 – 7.87 (4H, m, H-3, 5, 7), 7.35 (1H, m, H-2); δ_C (100 MHz, DMSO): 164.80, 159.03, 152.48, 150.02,

137.76, 136.34, 132.83, 132.51, 129.64 (4C), 126.04, 123.38, 120.57, 112.89; LRMS (EI+): *m/z* = 349.04 (77.4%) [M+] calculated for $C_{16}H_{10}F_3N_3OS$ 349.05 [M^+]; HPLC Purity: 99% (t_r = 14.91 min).

8. **4-trifluoromethoxy-N-[4-(2-pyridinyl)-2-thiazolyl]-benzamide (RIZ 011)**

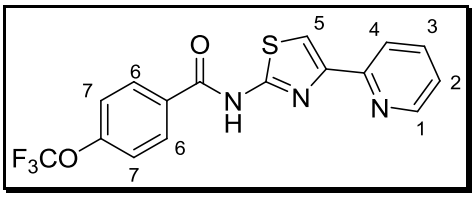

Brown crystals (109.5 mg, 27%); m.p 176 – 177^{o}C; δ_H (400 MHz, DMSO): 12.91 (1H, s, NH), 8.62 (1H, ddd, *J* = 4.8, 1.8, 1.1 Hz, H-1), 8.27 (1H, d, *J* = 8.4 Hz, H-6), 8.03 (1H, dt, *J* = 7.7, 1.1, Hz, H-4), 7.92 (1H, s, H-5), 7.90 (1H, td, *J* = 7.7, 1.8 Hz, H-3) 7.55 (2H, d, *J* = 8.4 Hz, H-7), 7.35 (1H, ddd, *J* = 7.7, 4.8, 1.1 Hz, H-2); δ_C (100 MHz, DMSO): 164.64, 159.14, 152.51, 151.68, 150.01, 149.89, 137.75, 131.55, 131.19 (2C), 123.35, 121.17 (2C), 120.57, 112.76; LRMS (EI+): *m/z* = 365.04 (72.6%) [M+] calculated for $C_{16}H_{10}F_3N_3O_2S$ 365.04 [M^+]; HPLC Purity: 99% (t_r = 15.15 min).

9. **4-ethyl-N-[4-(2-pyridinyl)-2-thiazolyl]-benzamide (RIZ 012)**

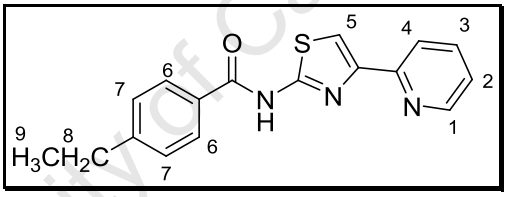

Pale-yellow crystals (100.5 mg, 29%); m.p 168 – 170^{o}C; δ_H (400 MHz, DMSO): 12.70 (1H, s, NH), 8.62 (1H, m, H-1), 8.08 (2H, d, *J* = 8.2 Hz, H-6), 8.03 (1H, d, *J* = 7.7 Hz, H-4), 7.90 (1H, td, *J* = 7.7, 1.6 Hz, H-3), 7.89 (1H, s, H-5) 7.39 (1H, d, *J* = 8.2 Hz, H-7), 7.34 (1H, m, H-2), 2.70 (2H, q, *J* = 7.5 Hz, H-8), 1.22 (3H, t, *J* = 7.5 Hz, H-9); δ_C (100 MHz, DMSO): 165.66, 159.35, 152.61, 149.99, 149.84, 149.46, 137.72, 129.88, 128.81 (2C), 128.45 (2C), 123.29, 120.56, 112.52, 28.59, 15.61 ; LRMS (EI+): *m/z* = 309.07 (72.6%) [M+] calculated for $C_{17}H_{15}F_3N_3OS$ 309.09 [M^+]; HPLC Purity: 99% (t_r = 14.78 min).

10. **4-butyl-N-[4-(2-pyridinyl)-2-thiazolyl]-benzamide (RIZ 013)**

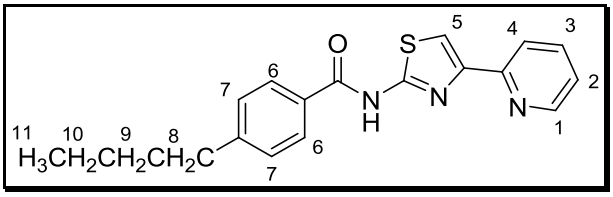

Off-white crystals (199.7 mg, 52%); m.p 93 – 95^{o}C; δ_H (400 MHz, DMSO): 12.66 (1H, s, NH), 8.60 (1H, ddd, *J* = 4.8, 1.8, 1.0 Hz, H-1), 8.05 (2H, d, *J* = 8.3 Hz, H-6), 8.01 (1H, dt, *J* = 7.9, 1.0 Hz, H-4), 7.91 – 7.81 (2H, m, H-3, 5), 7.37 – 7.27 (2H, m, H-2, 7), 2.65 (2H, t, *J* = 7.4 Hz, H-8), 1.57 (2H, q, *J* = 7.4, Hz, H-9) 1.30 (2H, m, H-10) 0.89 (3H, t, *J* = 7.4 Hz, H-11) ; δ_C (100 MHz, DMSO): 165.67, 159.36, 152.61, 149.99, 149.83, 148.11, 137.72, 129.87, 128.96(2C), 128.74(2C), 123.29, 120.56, 112.51, 35.19, 33.17, 22.21, 14.19; LRMS (EI+): *m/z* = 337.03 (36.4%) [M+] calculated for $C_{19}H_{19}F_3N_3OS$ 337.12 [M^+]; HPLC Purity: 97% (t_r = 11.98 min).

11. **4-methylthio-N-[4-(2-pyridinyl)-2-thiazolyl]-benzamide (RIZ 015)**

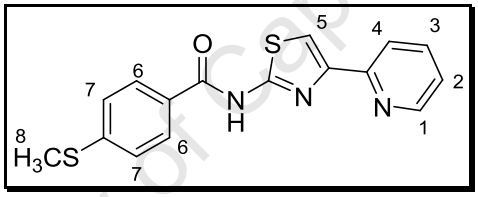

Pale-yellow crystals (133.3 mg, 36%); m.p 198 – 200^{o}C; δ_H (400 MHz, DMSO): 12.60 (1H, s, NH), 8.62 (1H, ddd, *J* = 4.8, 1.7, 1.0 Hz, H-1), 8.09 (2H, d, *J* = 8.5 Hz, H-6), 8.03 (1H, d, *J* = 7.7 Hz, H-4), 7.94 – 7.85 (2H, m, H-3, 5), 7.41 (2H, d, *J* = 8.5 Hz, H-7), 7.34 (1H, ddd, *J* = 7.7, 4.8, 1.2 Hz, H-2), 2.56 (3H, s, H-8); δ_C (100 MHz, DMSO): 165.25, 159.38, 152.61, 150.00, 149.83, 145.20, 137.72, 129.11 (2C), 128.30, 125.40 (2C), 123.29, 120.55, 112.55, 14.50; LRMS (EI+): *m/z* = 326.98 (25.3%) [M+] calculated for $C_{16}H_{13}N_3OS_2$ 327.05 [M^+]; HPLC Purity: 99% (t_r = 14.32 min).

12. **4-chloro-N-[4-(2-pyridinyl)-2-thiazolyl]-benzamide (RIZ 017)**

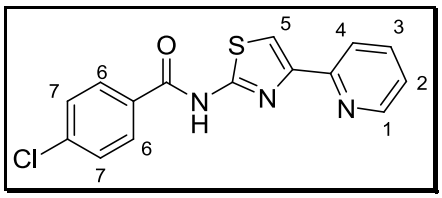

Light-yellow crystals (92.7 mg, 26%); m.p 195 - 197^{o}C; δ_H (400 MHz, DMSO): 12.85 (1H, s, NH), 8.60 (1H, m, H-1), 8.13 (2H, d, *J* = 8.5 Hz, H-6), 8.00 (1H, d, *J* = 8.0 Hz, H-4), 7.93 – 7.83 (2H, m,

H-3,5), 7.61 (2H, d, *J* = 8.5 Hz, H-7), 7.32 (1H, m, H-2); δ_C (100 MHz, DMSO): 164.87, 159.15, 152.51, 150.00, 149.87, 138.04, 137.76, 131.29, 130.61 (2C), 129.17 (2C), 123.35, 120.57, 112.74; LRMS (EI+): *m/z* = 315.02 (51.4%) [M+] calculated for $C_{15}H_{10}ClN_3OS$ 315.02 [M^+]; HPLC Purity: 99% (t_r = 14.69 min).

13. **4-fluoro-N-[4-(2-pyridinyl)-2-thiazolyl]-benzamide (RIZ 018)**

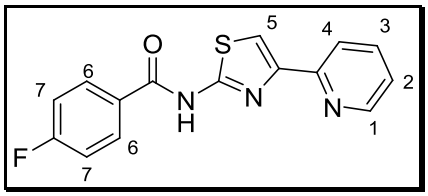

Light-yellow crystals (69.6 mg, 21%); m.p 179 - 181^{o}C; δ_H (400 MHz, DMSO): 12.79 (1H, s, NH), 8.60 (1H, ddd, *J* = 4.8, 1.8, 1.1 Hz, H-1), 8.20 (2H, m, H-6), 8.00 (1H, dt, *J* = 7.7, 1.1, Hz, H-4), 7.92 – 7.83 (2H, m, H-3, 5), 7.38 (2H, m, H-7), 7.32 (1H, ddd, *J* = 7.7, 4.8, 1.1 Hz, H-2); δ_C (100 MHz, DMSO): 166.42, 164.76, 163.93, 159.23, 152.55, 150.01, 137.75, 131.61, 131.52, 129.01, 123.33, 120.56, 116.21, 116.00, 112.66; LRMS (EI+): *m/z* = 299.03 (98.7%) [M+] calculated for $C_{15}H_{10}FN_3OS$ 299.05 [M^+]; HPLC Purity: 99% (t_r = 13.74 min).

14. **N-[4-(2-pyridinyl)-2-thiazolyl]-benzamide (RIZ 020)**

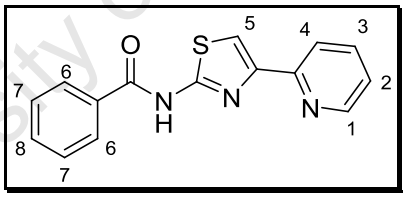

Pale-yellow crystals (204.8 mg, 64%); m.p 135 – 137^{o}C; δ_H (400 MHz, DMSO): 12.79 (1H, s, NH), 8.64 (1H, ddd, *J* = 4.8, 1.8, 1.0 Hz, H-1), 8.19-8.12 (2H, m, H-6), 8.05 (1H, dt, *J* = 7.9, 1.1 Hz, H-4), 7.96 – 7.87 (2H, m, H-3, 5), 7.71-7.63 (1H, m, H-8), 7.62-7.54 (2H, m, H-7), 7.36 (1H, ddd, *J* = 7.5, 4.8, 1.1 Hz, H-2); δ_C (100 MHz, DMSO): 165.82, 159.28, 152.58, 150.00, 137.74, 133.29, 132.44, 129.72, 129.06 (2C), 128.67 (2C), 123.32, 120.57, 112.61; LRMS (EI+): *m/z* = 281.04 (73.4%) [M+] calculated for $C_{15}H_{11}N_3OS$ 281.06 [M^+]; HPLC Purity: 99% (t_r = 13.28 min).

15. **2-bromo-N-[4-(2-pyridinyl)-2-thiazolyl]-benzamide (RIZ 021)**

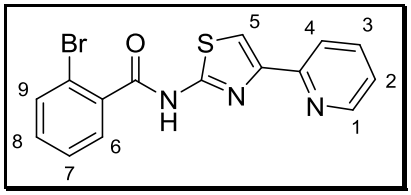

Off-white crystals (228.7 mg, 56%); m.p 178 - 180^{o}C; δ_H (400 MHz, DMSO): 12.85 (1H, s, NH), 8.60 (1H, m, H-1), 7.94 (1H, m, H-4), 7.90 (1H, s, H-5), 7.87 (1H, td, *J* = 7.5, 1.7 Hz, H-3), 7.72 (1H, dd, *J* = 7.6, 1.4 Hz, H-6), 7.62 (1H, dd, *J* = 7.6, 1.4 Hz, H-9), 7.50 (1H, td, *J* = 7.6, 1.4 Hz, H-7), 7.47 – 7.42 (1H, m, H-8), 7.32 (1H, ddd, *J* = 7.5, 4.8, 1.0 Hz, H-2); δ_C (100 MHz, DMSO): 166.42, 158.39, 152.43, 150.01, 149.87, 137.76, 136.96, 133.31, 132.45, 129.85, 128.12, 123.38, 120.57, 119.66, 112.68; LRMS (EI+): *m/z* = 360.91 (31.1%) [M+] calculated for $C_{15}H_{10}BrN_3OS$ 360.97 [M^+]; HPLC Purity: 99% (t_r = 13.24 min).

16. **3-bromo-N-[4-(2-pyridinyl)-2-thiazolyl]-benzamide (RIZ 022)**

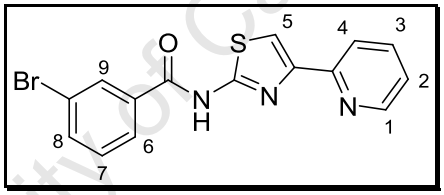

Off-white crystals (284.9 mg, 70%); m.p 176 – 178^{o}C; δ_H (400 MHz, DMSO): 12.87 (1H, s, NH), 8.60 (1H, ddd, *J* = 4.8, 1.8, 1.1 Hz, H-1), 8.32 (1H, t, *J* = 1.8 Hz, H-9), 8.10 (1H, ddd, *J* = 7.9, 1.8, 1.0 Hz, H-6), 8.00 (1H, dt, *J* = 7.7, 1.1 Hz, H-4), 7.91 – 7.85 (2H, m, H-3,5), 7.83 (1H, ddd, *J* = 7.9, 1.8, 1.0 Hz, H-8), 7.51 (1H, t, *J* = 7.9 Hz, H-7), 7.33 (1H, ddd, *J* = 7.7, 4.8, 1.1 Hz, H-2); δ_C (100 MHz, DMSO): 164.41, 159.05, 152.51, 150.01, 149.89, 137.75, 135.75, 134.66, 131.33, 131.24, 127.78, 123.36, 122.30, 120.55, 112.80; LRMS (EI+): *m/z* = 360.87 (49.1%) [M+] calculated for $C_{15}H_{10}BrN_3OS$ 360.97 [M^+]; HPLC Purity: 99% (t_r = 14.93 min).

17. **N-[4-(2-pyridinyl)-2-thiazolyl]-picolinamide (RIZ 023)**

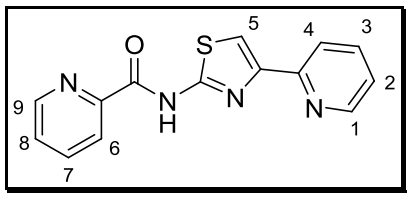

Off-white crystals (197.1 mg, 62%); m.p 148 – 150^{o}C; δ_H (400 MHz, DMSO): 11.99 (1H, s, NH), 8.75 (1H, ddd, *J* = 4.7, 1.6, 1.0 Hz, H-9), 8.59 (1H, ddd, *J* = 4.8, 1.7, 1.0 Hz, H-1), 8.18 (1H, dd, *J* = 7.7, 1.0 Hz H-4), 8.08 (1H, td, *J* = 7.7, 1.6 Hz, H-7), 8.01 (1H, d, *J* = 7.7 Hz, H-6), 7.92 (1H, s, H-5), 7.87 (1H, td, *J* = 7.7, 1.7 Hz, H-3), 7.70 (1H, ddd, *J* = 7.7, 4.8, 1.0 Hz, H-2), 7.31 (1H, ddd, *J* = 7.7, 4.7, 1.0 Hz, H-8); δ_C (100 MHz, DMSO): 163.31, 157.93, 152.38, 150.02, 149.96, 149.45, 148.27, 138.74, 137.72, 128.24, 123.40 (2C), 120.74, 112.95; LRMS (EI+): *m/z* = 281.94 (68.0%) [M+] calculated for $C_{14}H_{10}N_4OS$ 282.06 [M^+]; HPLC Purity: 99% (t_r = 13.19 min)

18. **N-[4-(2-pyridinyl)-2-thiazolyl]-nicotinamide (RIZ 024)**

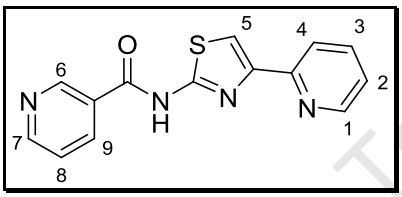

Off-white crystals (17.2 mg, 5%); m.p 232 – 234^{o}C; δ_H (400 MHz, DMSO): 13.00 (1H, s, NH), 9.2 (1H, m, H-6), 8.79 (1H, dd, *J* = 4.7, 1.4 Hz, H-7), 8.61 (1H, dd, *J* = 4.5, 1.2 Hz, H-1) 8.44 (1H, m, H-9), 8.01 (1H, m, H-4), 7.92 – 7.84 (2H, m, H-3,5), 7.58 (1H, dd, *J* = 7.4, 4.7 Hz, H-8), 7.33 (1H, m, H-2); δ_C (100 MHz, DMSO): 164.58, 158.98, 153.42, 152.48, 150.03, 149.89, 149.66, 137.78, 136.38, 128.47, 124.05, 123.39, 120.57, 112.83; LRMS (EI+): *m/z* = 282.04 (88.2%) [M+] calculated for $C_{14}H_{10}N_4OS$ 282.06 [M^+]**;** HPLC Purity: 99% (t_r = 11.75 min).

19. **N-[4-(2-pyridinyl)-2-thiazolyl]-isonicotinamide (RIZ 025)**

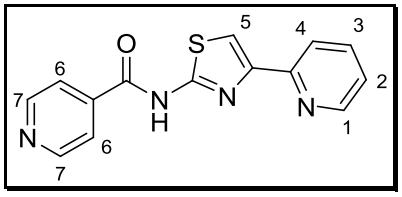

Off-white crystals (68.6 mg, 22%); m.p 215 – 217^{o}C; δ_H (400 MHz, DMSO): 13.09 (1H, s, NH), 8.80 (2H, dd, *J* = 4.5, 1.7 Hz, H-7), 8.60 (1H, m, H-1), 8.04-7.96 (2H, m, H-4, 6), 7.92 (1H, s, H-5), 7.88 (1H, td, *J* = 7.7, 1.8 Hz, H-3), 7.32 (1H, ddd, *J* = 7.7, 4.7, 1.1 Hz, H-2); δ_C (100 MHz, DMSO): 164.54, 158.87, 152.43, 150.88 (2C), 150.03, 149.95, 139.64, 137.78, 123.41, 122.26 (2C), 120.59, 113.03; LRMS (EI+): *m/z* = 282.01 (100.0%) [M+] calculated for $C_{14}H_{10}N_4OS$ 282.06 [M^+]**;** HPLC Purity: 99% (t_r = 12.01 min).

20. **N-(4-(2-pyridinyl)thiazol-2-yl)thiazole-2-carboxamide (RIZ 038)**

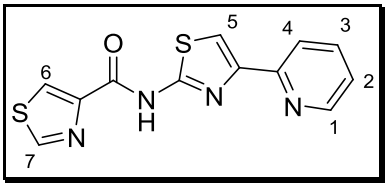

Off-white crystals (55.9 mg, 17%); m.p 203 – 205^{o}C; δ_H (400 MHz, DMSO): 12.21 (1H, s, NH), 9.28 (1H, d, *J* = 1.9 Hz, H-7), 8.74 (1H, d, *J* = 1.9 Hz, H-6), 8.6 (1H, ddd, *J* = 4.7, 1.7, 1.0 Hz, H-1), 8.01 (1H, dd, *J* = 7.6, 1.0 Hz, H-4), 7.93 – 7.83 (2H, m, H-3, 5), 7.33 (1H, ddd, *J* = 7.6, 4.7, 1.0 Hz, H-2); δ_C (100 MHz, DMSO): 170.76, 159.60, 158.22, 156.04, 152.47, 149.98, 148.86, 137.72, 127.68, 123.36, 120.66, 112.85; LRMS (EI+): *m/z* = 287.90 (100.0%) [M+] calculated for $C_{12}H_8N_4OS_2$ 288.01 [M^+]**;** HPLC Purity: 99% (t_r = 9.00 min).

21. **N-(4-(2-pyridinyl)thiazol-2-yl)-1H-imidazole-5-carboxamide (RIZ 039)**

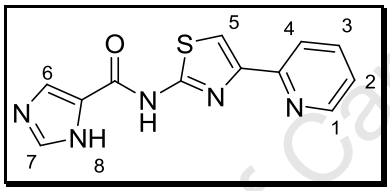

Pale-yellow crystals (37.7 mg, 12%); m.p 229 – 231^{o}C; δ_H (400 MHz, DMSO): 12.72 (1H, s, NH), 11.54 (1H, s, H-8), 8.59 (1H, m, H-1), 8.07 (1H, s, H-6), 7.99 (1H, d, *J* = 7.8 Hz, H-7) 7.91– 7.76 (3H, m, H-3, 4, 5) 7.31 (1H, m, H-2); δ_C (100 MHz, DMSO): 160.89, 158.43, 152.55, 149.95, 149.69, 137.69, 137.43,128.67, 123.27, 122.32, 120.61, 112.25; LRMS (EI+): *m/z* = 270.77 (63.2%) [M+] calculated for $C_{12}H_9N_5OS$ 271.05 [M^+]**;** HPLC Purity: 99% (t_r = 7.40 min).

22. **N-(4-(2-pyridinyl)thiazol-2-yl)thiophene-2-carboxamide (RIZ 042)**

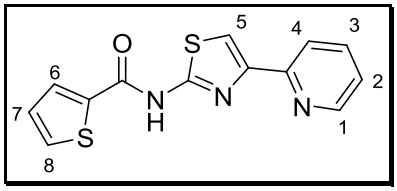

Pale-brown crystals (73.3 mg, 23%); m.p 163 – 165^{o}C; δ_H (400 MHz, DMSO): 12.86 (1H, s, NH), 8.60 (1H, ddd, *J* = 4.8, 1.3, 0.9 Hz, H-1), 8.29 (1H, dd, *J* = 3.8, 1.1 Hz, H-8), 8.00 (1H, dt, *J* = 7.7, 1.3 Hz, H-4), 7.96 (1H, dd, *J* = 5.0, 1.1 Hz, H-7), 7.91 – 7.85 (2H, m, H-3,5), 7.32 (1H, ddd, *J* = 7.7, 4.8, 1.3 Hz, H-2), 7.25 (1H, dd, *J* = 5.0, 3.8 Hz, H-6); δ_C (100 MHz, DMSO): 160.34, 158.96,

152.53, 150.01, 149.87, 137.73, 137.59, 134.17, 131.45, 129.05, 123.32, 120.54, 112.70; LRMS (EI+): *m/z* = 287.00 (58.5%) [M+] calculated for $C_{13}H_9N_3OS_2$ 287.02 [M^+]**;** HPLC Purity: 99% (t_r = 9.43 min).

23. **N-4-bromo-N-[4-(3-pyridinyl)-2-thiazolyl]-benzamide (RIZ 034)**

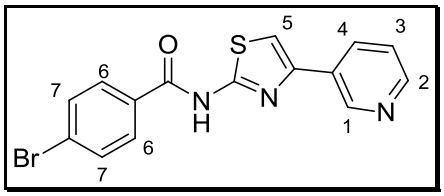

White crystals (79.0 mg, 20%); m.p 233 – 235^{o}C; δ_H (400 MHz, DMSO): 12.87 (1H, s, NH), 9.29-8.94 (1H, m, H-1), 8.52 (1H, dd, *J* = 4.7, 1.7 Hz, H-2), 8.26 (1H, dt, *J* = 8.0, 1.7 Hz, H-4), 8.05 (1H, d, *J* = 8.6 Hz, H-7), 7.86 (1H, S, H-5), 7.76 (1H, d, *J* = 8.6 Hz, H-6), 7.50-7.42 (1H, m, H-3); δ_C (100 MHz, DMSO): 165.02, 159.44, 149.18, 147.52, 147.34, 133.40, 132.12 (2C), 131.62, 130.76 (2C), 130.45, 127.10, 124.29, 110.72 ; LRMS (EI^+): *m/z* = 360.87 (38.0%) [M^+] calculated for $C_{15}H_{10}BrN_3OS$ 360.97 [M^+]; HPLC Purity: 95% (t_r = 10.44 min).

24. **N-4-bromo-N-[4-(4-pyridinyl)-2-thiazolyl]-benzamide (RIZ 035)**

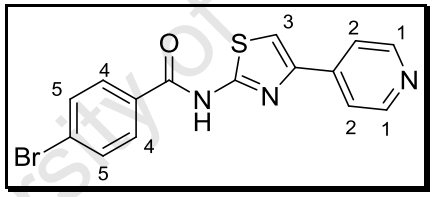

Off-white crystals (93.5 mg, 23%); m.p 251 – 253^{o}C; δ_H (400 MHz, DMSO): 12.88 (1H, s, NH), 8.62 (2H, dd, *J* = 4.5, 1.6 Hz, H-1), 8.07-8.02 (3H, m, H-3, 5), 7.87 (1H, dd, *J* = 4.5, 1.6 Hz, H-2), 7.77-7.74 (2H, m, H-4); δ_C (100 MHz, DMSO): 165.12, 159.45, 150.75 (2C), 147.21, 141.45, 132.12 (2C), 130.77 (2C), 127.14, 120.50 (2C), 113.33; LRMS (EI^+): *m/z* = 360.86 (32.6%) [M^+] calculated for $C_{15}H_{10}BrN_3OS$ 360.97 [M^+]; HPLC Purity: 99% (t_r = 10.18 min).

5.3. General procedure for the synthesis of N-phenyl-[4-(2-pyridinyl) thiazole-2-amine (RIZ 020B)

A mixture of **FM001** (1.78 mmol) and phenylthiourea (1.78 mmol) in 10 ml of ethanol was refluxed for 1 hr, the mixture was then cooled to 20^{o}C and diluted with 25 ml of water. The pH of the mixture was then adjusted to approximately 8 using saturated $NaHCO_3$, and the mixture

stirred for 2 hr at 20°C and a precipitate formed. The precipitate was filtered and washed with 5 ml of water and dried. Purification was done via column chromatography: EtOAc: Hexane (30:70)

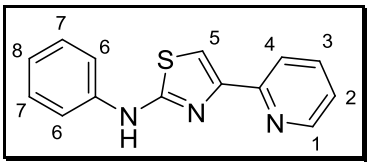

Brown crystals (264.2 mg, 59%); m.p 142 – 144°C; δ_H (400 MHz, DMSO): 10.27 (1H, s, NH), 8.64-8.49 (1H, m, H-1), 7.99 (1H, d, *J* = 7.7 Hz, H-4), 7.88 (1H, td, *J* = 7.7, 1.8 Hz, H-3), 7.72 (2H, d, *J* = 7.6 Hz, H-6), 7.53 (1H, s, H-5), 7.38 – 7.27 (3H, m, H-2,7), 6.96 (1H, t, *J* = 7.4, H-8); δ_C (100 MHz, DMSO): 163.90, 152.57, 150.76, 149.78, 141.62, 137.80, 129.49 (2C) ,123.10, 121.79, 120.87, 117.40 (2C), 107.30; LRMS (EI+): *m/z* = 252.78 (100%) [M+] calculated for $C_{14}H_{11}N_3S$ 253.07 [M^+]; HPLC Purity: 98% (t_r = 7.66 min).

5.4. General procedure for the synthesis of 1-phenyl-3-[4-(2-pyridinyl) thiazol-2-yl) urea (RIZ 020C)

A mixture of aniline (2.15 mmol) and triphosgene (2.15 mmol) in 10 ml of toluene was refluxed for 8 hr to generate the phenylisocyanate *in situ*; the mixture was then cooled to 0°C using ice and the amine **FM002** (2.15 mmol) added. The mixture was then warmed to 56°C and left to stir at this temperature for 2 hr, the heat was then turned off and the mixture left to stir at room temperature for 24 hr. Overnight a precipitate formed. The precipitate was filtered and recrystallized from absolute ethanol to yield the desired product.

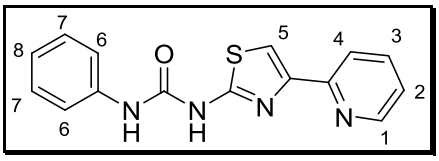

Pale-brown crystals (172.0 mg, 27%); m.p 215 – 217°C; δ_H (400 MHz, DMSO): 10.99 (1H, s, NH-thiazole), 9.97 (1H, s, NH-phenyl), 8.68 (1H, m, H-1), 8.39-8.19 (3H, m, H-3, 4, 5), 7.69 (1H, m, H-2), 7.49 (2H, d, *J* = 8.3 Hz, H-6), 7.31 (2H, t, *J* = 7.3 Hz, H-7), 7.10-6.96 (1H, m, H-8); δ_C (100 MHz, DMSO): 160.63,152.19, 148.03, 145.06,143.47,138.98, 129.42 (2C), 124.79, 123.76, 123.35,

122.97, 119.11, 119.00, 116.33; LRMS (EI+): *m/z* = 295.95 (13.7%) [M+] calculated for $C_{15}H_{12}N_4OS$ 296.07 [M^+]; HPLC Purity: 99% (t_r = 9.42 min).

5.5. General procedure for the synthesis of N-[4-(2-pyridinyl) thiazol-2-ylcarbamothioyl) benzamide (RIZ 020F)

A solution of benzoylisothiocyanate (3.1 mmol) and **FM002** (2.82 mmol) in 10 ml of acetone was refluxed for 3 hr. The resulting precipitate was filtered off yielding the desired product.

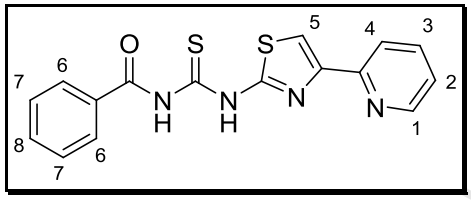

Pale-green crystals (484.4 mg, 51%); m.p 205 – 207^{o}C; δ_H (400 MHz, DMSO): 12.13 (1H, s, NH), 8.60 (1H, ddd, *J* = 4.8, 1.8, 1.0 Hz, H-1), 8.05-7.97 (3H, m, H-4, 6), 7.91 (1H, s, H-5), 7.88 (1H, td, *J* = 7.6, 1.8 Hz, H-3), 7.67 (1H, m, H-8), 7.59-7.52 (2H, m, H-7), 7.34 (1H, ddd, *J* = 7.6, 4.8, 1.0 Hz,H-2); δ_C (100 MHz, DMSO): 176.75, 169.25, 159.19, 152.30, 150.10, 149.97, 137.65, 133.80, 132.44, 129.24 (2C), 128.93 (2C), 123.48, 120.78, 112.76; LRMS (EI+): *m/z* = 339.63 (69.9%) [M+] calculated for $C_{16}H_{12}N_4OS_2$ 340.05 [M^+]; HPLC Purity: 99% (t_r = 11.22 min).

5.6. Synthesis of the 4-R-N-((4,7-dimethyl-4,6,6a,7,8,9,10,10a-octahydroindolo[4,3-fg]quinolin-9-yl)methyl)benzamides

5.6.1 Synthesis of (4,7-dimethyl-4,6,6a,7,8,9,10,10a-octahydroindolo[4,3-fg]quinolin-9-yl) methanamine (FRM 000)

Metergoline (1.6mmol) was dissolved in 20mls of a 1:1 mixture of EtOH and THF. 16% Pd/C was added, the flask purged three times with hydrogen gas, sealed under an atmosphere of hydrogen and stirred at room temperature for 10 hours. The reaction mixture was then filtered through celite, and the solvent removed under reduced pressure. The resulting residue was dissolved in a small volume of ethyl acetate, and the final compound precipitated out using ether to yield an off white solid.

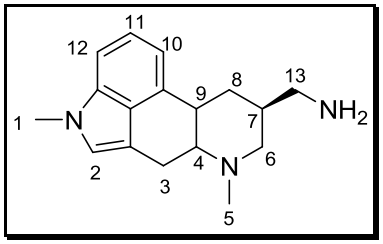

Off-white powder (554.8mg, 78%); m.p 151 – 153^{o}C; δ_H(400 MHz, $CDCl_3$): 7.22 (1H, dd, *J* = 8.1, 7.1 Hz, H-11), 7.14 (1H, d, *J* = 8.2 Hz, H-10), 6.96 (1H, d, *J* =7.1 Hz, H-12), 6.75 (1H, d, *J* = 1.5 Hz, H-2), 3.78 (3H, s, H-1), 3.42 (1H, dd, *J* = 14.7, 4.3 Hz, H-4), 3.16 (1H, dd, *J* = 7.6, 2.0 Hz, H-9), 3.07 – 2.95 (1H, m, H-13 (H)), 2.81 – 2.63 (4H, m, H-3 (H), H-6 (H), H-8 (H), H-13 (H),), 2.52 (3H, s, H-5), 2.18 (1H, ddd, *J* = 11.0, 9.7, 4.4 Hz, H-3 (H)), 2.10 – 1.92 (2H, m, H- 6 (H), H-8 (H)), 1.75 (2H, s, NH_2), 1.14 (1H, q, *J* = 12.2 Hz, H-7); δ_C(100 MHz, $CDCl_3$): 134.57, 133.67, 126.66, 122.71, 122.38, 112.57, 110.94, 106.64, 67.67, 61.83, 46.59, 43.19, 40.57, 39.26, 32.61, 32.25, 27.00; LRMS (EI+): *m/z* = 269.15 (100.0%) [M+] calculated for $C_{17}H_{23}N_3$ 269.19 [M^+]; HPLC Purity: 99% (t_r = 4.75 min).

5.6.2 Synthesis of the 4-R-N-((4,7-dimethyl-4,6,6a,7,8,9,10,10a-octahydroindolo[4,3-fg]quinolin-9-yl)methyl)benzamides.

EDCI (1.5 mmol) was added in small batches to a solution of the carboxylic acid (1.2 mmol) and HOBt (1.5 mmol) in 5 ml dry DCM. The reaction mixture was stirred for 10 minutes at room temperature, then a solution of the amine (1.0 mmol) in 5 ml of dry DCM was added in small portions and the reaction mixture left to stir for 24 hr at room temperature (monitored by TLC until completion). The reaction mixture was washed with saturated aqueous sodium bicarbonate (2 x 10ml), saturated aqueous sodium chloride (1 x 10ml), dried with anhydrous Na_2SO_4 and concentrated under reduced pressure. Purification by column silica gel chromatography (MeOH/DCM, 5:95) afforded the products as solids.

1. **4-bromo-N-((4,7-dimethyl-4,6,6a,7,8,9,10,10a-octahydroindolo[4,3-fg]quinolin-9-yl)methyl)benzamide (FRM 001)**

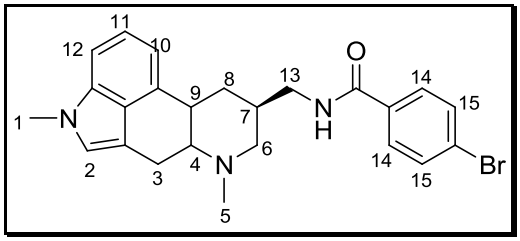

Off-white powder (45.2 mg, 53%); m.p 213 – 215^{o}C; δ_H(400 MHz, $CDCl_3$): 7.75 (2H, d, *J* = 8.3 Hz, H-14), 7.52 (2H, d, *J* = 8.3 Hz, H-15), 7.18 – 7.11 (2H, m, H-11, NH), 7.09 (1H, d, *J* = 7.9 Hz, H-10), 6.83 (1H, d, *J* = 7.4 Hz, H-12), 6.71 (1H, s, H-2), 3.71 (3H, s, H-1), 3.67 (2H, q, *J* = 7.0 Hz), 3.56 – 3.43 (1H, m), 3.38 (2H, dd, *J* = 14.8, 4.3 Hz), 3.33 – 3.22 (1H, m), 3.06 – 2.92 (1H, m), 2.66 (3H, s, H-5), 2.63 – 2.52 (1H, m), 2.38 – 2.28 (1H, m), 1.20 (1H, dd, *J* = 13.4, 6.4 Hz), 0.86 (1H, d, *J* = 6.2 Hz); δ_C(100 MHz, $CDCl_3$): 167.03, 134.43, 133.12, 131.19 (2C), 131.12, 128.92 (2C), 126.19, 126.09, 124.98, 122.94, 112.89, 108.66, 107.42, 67.48, 60.62, 43.35, 42.06, 39.38, 35.12, 33.44, 32.83, 26.74; LRMS (EI+): *m/z* = 450.98 (100.0%) [M+] calculated for $C_{24}H_{26}BrN_3O$ 451.13 [M^+]; HPLC Purity: 99% (t_r = 13.33 min).

2. **4-ethyl-N-((4,7-dimethyl-4,6,6a,7,8,9,10,10a-octahydroindolo[4,3-fg]quinolin-9-yl)methyl)benzamide (FRM 002)**

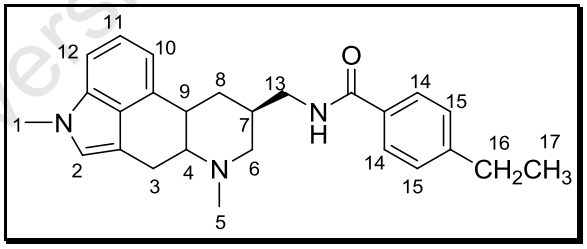

Pale brown powder (49.1mg, 37%); m.p 192 – 194^{o}C; δ_H(400 MHz, $CDCl_3$): 7.72 (2H, d, *J* = 8.1 Hz, H-14), 7.21 (2H, d, *J* = 7.6 Hz, H-15), 7.17 – 7.10 (1H, m, H-11), 7.07 (1H, d, *J* = 8.1 Hz, H-10), 6.83 (1H, d, *J* = 7.0 Hz, H-12), 6.69 (1H, s, H-2), 6.65 – 6.58 (1H, m, NH), 3.70 (5H, m,), 3.54 – 3.29 (4H, m), 3.24 (1H, d, *J* = 10.9 Hz), 3.19 – 3.08 (1H, m), 2.90 – 2.77 (1H, m), 2.73 – 2.59 (3H, m), 2.54 (3H, s, H-5), 2.44 – 2.25 (2H, m), 2.20 (1H, m,), 1.21 (1H, q, *J* = 7.9 Hz); δ_C(100 MHz, $CDCl_3$): 167.83, 148.17, 134.43, 132.19, 131.86, 128.07 (2C), 127.50 (2C), 126.29, 122.81, 122.73, 112.73, 109.63, 107.10, 67.45, 61.06, 43.40, 42.59, 39.79, 36.07, 32.78, 31.80, 28.76,

26.25, 15.28; LRMS (EI+): *m/z* = 401.07 (100.0%) [M+] calculated for $C_{26}H_{31}N_3O$ 401.25 [M^+]; HPLC Purity: 98% (t_r = 13.39 min).

3. **4-cyano-N-((4,7-dimethyl-4,6,6a,7,8,9,10,10a-octahydroindolo[4,3-fg]quinolin-9-yl)methyl)benzamide (FRM 003)**

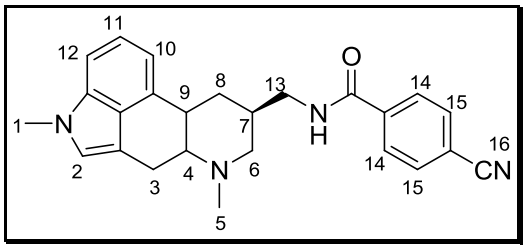

Brown powder (68.7mg,52.2%); m.p 137 – 139°C; δ_H(400 MHz, $CDCl_3$): 8.00 (2H, d, *J* = 8.2 Hz, H-14), 7.66 (2H, d, *J* = 8.1 Hz, H-15), 7.30 (1H, m, NH), 7.18 – 7.13 (1H, m, H-11), 7.11 (1H, d, *J* = 8.2 Hz, H-10), 6.84 (1H, d, *J* = 6.6 Hz, H-12), 6.74 (1H, s, H-2), 3.73 (3H, s, H-1), 3.59 – 3.47 (3H, m), 3.47 – 3.36 (2H, m), 3.36 – 3.27 (1H, m), 3.02 (1H, dd, *J* = 13.7, 12.5 Hz), 2.69 (3H, s, H-5), 2.68 – 2.58 (1H, m), 2.43 – 2.33 (1H, m), 1.32 (1H, q, *J* = 11.9 Hz), 1.24 – 1.18 (1H, m); δ_C(100 MHz, $CDCl_3$): 166.13, 138.09, 134.45, 132.33 (2C), 131.79, 130.90, 129.91, 128.01 (2C), 126.04, 123.04, 122.96, 112.84, 108.42, 107.57 67.57, 60.66, 43.48, 42.04, 39.42, 35.11, 32.87, 31.44, 25.67; LRMS (EI+): *m/z* = 397.99 (100.0%) [M+] calculated for $C_{25}H_{26}N_4O$ 398.21 [M^+]; HPLC Purity: 95% (t_r = 11.60 min).

4. **4-nitro-N-((4,7-dimethyl-4,6,6a,7,8,9,10,10a-octahydroindolo[4,3-fg]quinolin-9-yl)methyl)benzamide (FRM 004)**

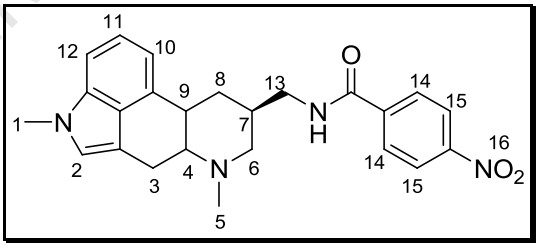

Orange powder (51.6mg,37.4%); m.p 228 – 230°C; δ_H(400 MHz, $CDCl_3$): 8.21 (2H, d, *J* = 8.6 Hz, H-14), 7.95 (2H, d, *J* = 8.5 Hz, H-15), 7.17 – 7.11 (1H, m, H-11), 7.08 (1H, d, *J* = 8.1 Hz, H-10), 6.83 (1H, d, *J* = 7.2 Hz), 6.79 (1H, s, NH), 6.70 (1H, s, H-2), 3.72 (3H, s, H-1), 3.48 (2H, t, *J* = 6.2 Hz), 3.36 (1H, dd, *J* = 14.5, 4.4 Hz), 3.22 (1H, d, *J* = 11.0 Hz), 3.13 – 3.05 (1H, m), 2.83 – 2.67 (2H, m), 2.54 (3H, s, H-5), 2.45 – 2.37 (1H, m), 2.36 – 2.28 (1H, m), 2.18 (1H, t, *J* = 11.5 Hz), 1.30 – 1.18

(1H, m); δ_C(100 MHz, $CDCl_3$): 165.81, 149.60, 140.02, 134.44, 132.11, 128.27 (2C), 126.28, 123.75 (2C), 122.79 (2C), 112.61, 109.65, 107.18 67.50, 61.22, 43.90, 42.82, 40.01, 36.17, 32.78, 31.93, 26.45; LRMS (EI+): *m/z* = 417.94 (100.0%) [M+] calculated for $C_{24}H_{26}N_4O$ 418.20 [M^+]; HPLC Purity: 98% (t_r = 12.48 min).

5. **4-chloro-N-((4,7-dimethyl-4,6,6a,7,8,9,10,10a-octahydroindolo[4,3-fg]quinolin-9-yl)methyl)benzamide (FRM 005)**

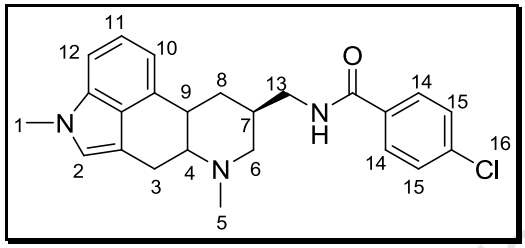

Off-white powder (52.5mg,34.8%); m.p 224 – 226°C; δ_H(400 MHz, $CDCl_3$): 7.76 (2H, d, *J* = 8.3 Hz, H-14), 7.35 (2H, d, *J* = 8.4 Hz, H-15), 7.26 (1H, s, NH), 7.16 – 7.10 (1H, m, H-11), 7.07 (1H, d, *J* = 8.2 Hz, H-10), 6.83 (1H, d, *J* = 6.9 Hz, H-12), 6.69 (1H, s, H-2), 3.70 (3H, s, H-1), 3.41 – 3.30 (3H, m), 3.23 (1H, d, *J* = 10.4 Hz), 3.10 – 3.00 (1H, m), 2.82 – 2.72 (1H, m), 2.65 (1H, d, *J* = 12.6 Hz), 2.49 (3H, s, H-5), 2.27 (2H, td, *J* = 10.7, 4.2 Hz), 2.13 – 2.03 (1H, m), 1.27 – 1.13 (1H, m); δ_C(100 MHz, $CDCl_3$): 166.71, 137.74, 134.46, 132.95, 132.51, 128.85 (2C), 128.48 (2C), 126.39, 122.80, 122.69 112.62, 110.01, 107.07 67.41, 61.20, 43.77, 42.83, 40.24, 36.17, 32.78, 31.97, 26.52; LRMS (EI+): *m/z* = 406.87 (100.0%) [M+] calculated for $C_{24}H_{26}ClN_3O$ 407.18 [M^+]; HPLC Purity: 99% (t_r = 13.19 min).

6. **4-dimethylamino-N-((4,7-dimethyl-4,6,6a,7,8,9,10,10a-octahydroindolo[4,3-fg]quinolin-9-yl)methylbenzamide (FRM 006)**

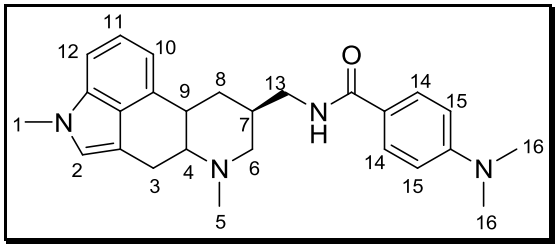

Off-white powder (120.9mg,78.4%); m.p 258 – 260°C; δ_H(400 MHz, $CDCl_3$): 7.66 (2H, d, *J* = 8.7 Hz, H-14), 7.18 – 7.11 (1H, m, H-11), 7.07 (1H, d, *J* = 8.2 Hz, H-10), 6.86 (1H, d, *J* = 6.9 Hz, H-12), 6.68 (1H, s, H2), 6.65 (2H, d, *J* = 8.6 Hz, H-15), 6.10 – 6.02 (1H, m, NH), 3.71 (3H, s, H-1), 3.47 –

3.40 (3H, m), 3.34 (1H, dd, *J* = 14.7, 4.4 Hz), 3.07 (1H, d, *J* = 10.6 Hz), 2.98 (6H, s, H-16), 2.73 – 2.61 (2H, m), 2.43 (3H, s, H-5), 2.25 – 2.17 (1H, m), 2.18 – 2.10 (1H, m), 2.07 – 1.98 (1H, m), 1.24 – 1.13 (1H, m); δ_C(100 MHz, $CDCl_3$): 167.59, 152.52, 134.45, 133.29, 128.35 (2C), 126.53, 122.73, 122.49, 121.51 112.60, 111.18 (2C), 110.69, 106.79 67.45, 61.60, 43.57, 43.28, 40.58, 40.12, 36.97, 32.74, 32.22, 26.95, 15.26; LRMS (EI+): *m/z* = 415.92 (63.0%) [M+] calculated for $C_{26}H_{32}N_4O$ 416.26 [M^+]; HPLC Purity: 99% (t_r = 12.54 min).

7. **4-butyl-N-((4,7-dimethyl-4,6,6a,7,8,9,10,10a-octahydroindolo[4,3-fg]quinolin-9-yl)methyl)benzamide (FRM 007)**

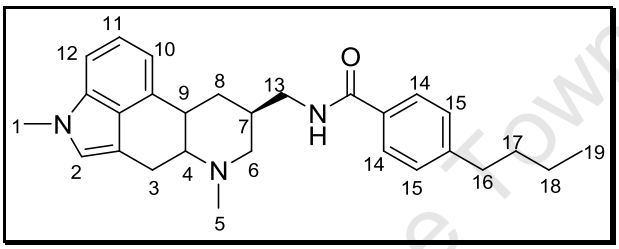

Dark brown powder (60.4mg,38.0%); m.p 171 – 173^{o}C; δ_H(400 MHz, $CDCl_3$): 7.70 (2H, d, *J* = 8.0 Hz, H-14), 7.21 (2H, d, *J* = 7.8 Hz, H-15), 7.18 – 7.11 (1H, m, H-11), 7.07 (1H, d, *J* = 7.9 Hz, H-10), 6.86 (1H, d, *J* = 6.9 Hz, H-12), 6.69 (1H, s, H-2), 6.39 – 6.31 (1H, m, NH), 3.71 (3H, s, H-1), 3.52 – 3.40 (2H, m), 3.40 – 3.31 (1H, m), 3.18 (1H, dd, *J* = 10.6, 1.7 Hz), 3.11 – 3.00 (1H, m), 2.80 – 2.65 (2H, m), 2.65 – 2.59 (2H, m), 2.48 (3H, s, H-5), 2.24 (1H, td, *J* = 11.2, 4.6 Hz), 2.08 (1H, t, *J* = 11.4 Hz), 1.58 (2H, p, *J* = 7.8 Hz), 1.36 – 1.29 (2H, m), 1.25 – 1.20 (2H, m), 0.90 (3H, t, *J* = 7.4 Hz); δ_C(100 MHz, $CDCl_3$): 167.74, 146.82, 134.45, 132.84, 132.01, 128.63 (2C), 126.98 (2C), 126.45, 122.77, 122.60 112.63, 110.29, 106.94 67.42, 61.30, 43.65, 42.96, 40.29, 36.43, 35.63, 35.52, 33.34, 32.06, 26.64, 22.29, 13.88; LRMS (EI+): *m/z* = 428.91 (100.0%) [M+] calculated for $C_{28}H_{35}N_3O$ 429.28 [M^+]; HPLC Purity: 99% (t_r = 14.69 min).

8. **4-methylthio-N-((4,7-dimethyl-4,6,6a,7,8,9,10,10a-octahydroindolo[4,3-fg]quinolin-9-yl)methyl)benzamide (RIZ 008)**

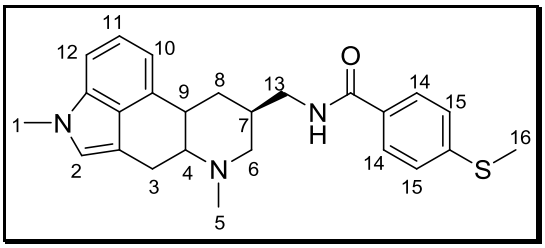

Pale brown powder (47.6mg,30.7%); m.p 214 – 216^{o}C; δ_H(400 MHz, $CDCl_3$): 7.71 (2H, d, *J* = 7.9 Hz, H-14), 7.24 (2H, d, *J* = 8.2 Hz, H-15), 7.18 – 7.11 (1H, m, H-11), 7.08 (1H, d, *J* = 7.8 Hz, H-10), 6.86 (1H, d, *J* = 6.5 Hz, H-12), 6.69 (1H, s, H-2), 6.34 (1H, s, NH), 3.71 (3H, s, H-1), 3.50 – 3.39 (2H, m), 3.36 (1H, dd, *J* = 14.7, 4.6 Hz), 3.18 (1H, d, *J* = 9.9 Hz), 3.09 – 2.98 (1H, m), 2.78 – 2.64 (2H, m), 2.48 (3H, s, H-16), 2.47 (3H, s, H-5), 2.34 – 2.20 (2H, m), 2.08 (1H, t, *J* = 11.5 Hz), 1.26 – 1.19 (1H, m); δ_C(100 MHz, $CDCl_3$): 167.18, 143.40, 134.45, 132.81, 127.38 (2C), 126.44, 125.61 (2C), 125.12, 122.77, 122.62 112.61, 110.28, 106.96 67.42, 61.33, 43.71, 40.34, 36.44, 32.76, 32.06, 26.66, 15.14; LRMS (EI+): *m/z* = 418.81 (100.0%) [M+] calculated for $C_{25}H_{29}N_3OS$ 419.20 [M^+]; HPLC Purity: 99% (t_r = 12.94 min).

9. **4-iodo-N-((4,7-dimethyl-4,6,6a,7,8,9,10,10a-octahydroindolo[4,3-fg]quinolin-9-yl)methyl)benzamide (RIZ 009)**

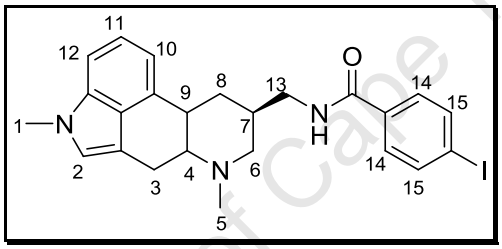

Off-white powder (84.6mg,45.8%); m.p 227 – 229^{o}C; δ_H(400 MHz, $CDCl_3$): 7.80 (2H, d, *J* = 7.5 Hz, H-14), 7.60 (2H, d, *J* = 8.4 Hz), 7.23 – 7.15 (1H, m, H-11), 7.12 (1H, d, *J* = 8.0 Hz, H-10), 6.89 (1H, d, *J* = 7.3 Hz, H-12), 6.75 (1H, s, H-2), 6.65 (1H, s, NH), 3.76 (3H, s, H-1), 3.52 – 3.33 (4H, m), 3.22 – 3.10 (1H, m), 2.93 – 2.81 (1H, m), 2.72 (1H, d, *J* = 13.5 Hz), 2.58 (3H, s, H-5), 2.49 – 2.34 (1H, m), 2.25 – 2.13 (1H, m), 1.37 – 1.24 (1H, m), 1.21 (1H, t, *J* = 7.0 Hz); δ_C(100 MHz, $CDCl_3$): 166.99, 137.80 (2C), 137.18, 134.46, 133.93, 132.26, 128.70 (2C), 126.34, 122.83, 122.74 112.67, 109.76, 107.14 67.40, 61.06, 43.71, 42.64, 40.12, 35.89, 32.79, 31.87, 26.34; LRMS (EI+): *m/z* = 498.98 (100.0%) [M+] calculated for $C_{24}H_{26}IN_3O$ 499.11 [M^+]; HPLC Purity: 99% (t_r = 13.68 min).

10. **4-methylsulfonyl-N-((4,7-dimethyl-4,6,6a,7,8,9,10,10a-octahydroindolo[4,3-fg]quinolin-9-yl)methyl)benzamide (FRM 010)**

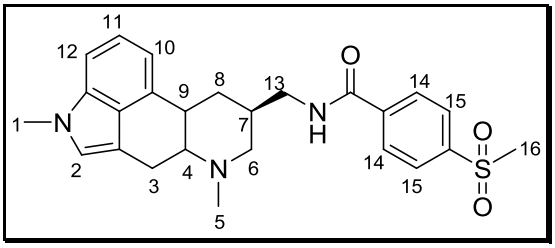

Pale brown powder (73.9mg,44.2%); m.p 209 – 211°C; δ_H(400 MHz, $CDCl_3$): 8.01 – 7.93 (4H, m, H-14, H-15), 7.21 – 7.15 (1H, m, H-11), 7.11 (1H, d, *J* = 8.2 Hz, H-10), 6.88 (1H, d, *J* = 7.1 Hz, H-12), 6.73 (1H, d, *J* = 1.2 Hz, H-2), 6.53 (1H, s, NH), 3.75 (3H, s, H-1), 3.54 – 3.46 (2H, m), 3.38 (1H, dd, *J* = 14.7, 4.3 Hz), 3.14 – 3.07 (1H, m), 3.05 (3H, s, H-16), 3.03 – 2.89 (1H, m), 2.77 – 2.64 (2H, m), 2.48 (3H, s, H-5), 2.33 – 2.21 (1H, m), 2.18 (1H, td, *J* = 10.4, 4.4 Hz), 2.06 (1H, t, *J* = 11.3 Hz), 1.35 – 1.17 (1H, m); δ_C(100 MHz, $CDCl_3$): 166.14, 142.95, 139.79, 134.46, 133.05, 128.10 (2C), 127.75 (2C), 126.51, 122.71, 122.62, 112.49, 110.56, 106.93, 67.40, 61.51, 44.40, 44.10, 43.30, 40.55, 36.68, 32.76, 32.20, 26.96; LRMS (EI+): *m/z* = 451.16 (100.0%) [M+] calculated for $C_{25}H_{29}N_3O_3S$ 451.19 [M^+]; HPLC Purity: 99% (t_r = 10.66 min).

11. **4-methoxy-N-((4,7-dimethyl-4,6,6a,7,8,9,10,10a-octahydroindolo[4,3-fg]quinolin-9-yl)methyl)benzamide (FRM 011)**

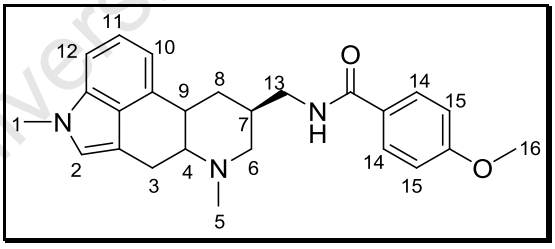

Pale brown powder (61.8mg,41.4%); m.p 212 – 214°C; δ_H(400 MHz, $CDCl_3$): 7.76 (2H, d, *J* = 8.8 Hz, H-14), 7.21 – 7.15 (1H, m, H-11), 7.11 (1H, d, *J* = 8.2 Hz, H-10), 6.94 (2H, d, *J* = 8.8 Hz, H-15), 6.90 (1H, d, *J* = 7.1 Hz, H-12), 6.72 (1H, d, *J* = 1.3 Hz, H-2), 6.18 (1H, t, *J* = 5.8 Hz, NH), 3.85 (3H, s, H-16), 3.75 (3H, s, H-1), 3.48 (2H, q, *J* = 7.0 Hz), 3.38 (1H, dd, *J* = 14.7, 4.3 Hz), 3.11 (1H, ddd, *J* = 11.6, 3.3, 2.1 Hz), 3.03 – 2.95 (1H, m), 2.77 – 2.64 (2H, m), 2.47 (3H, s, H-5), 2.30 – 2.21 (1H, m), 2.21 – 2.14 (1H, m), 2.06 (1H, t, *J* = 11.3 Hz), 1.21 (1H, t, *J* = 7.0 Hz); δ_C(100 MHz, $CDCl_3$): 167.21, 162.21, 134.45, 133.21, 128.67 (2C), 127.03, 126.52, 122.73, 122.53, 113.84 (2C), 112.56,

110.66, 106.83 67.43, 61.57, 55.41, 43.73, 43.29, 40.58, 36.89, 32.74, 32.21, 26.96; LRMS (EI+): *m/z* = 403.12 (100.0%) [M+] calculated for $C_{25}H_{29}N_3O_2$ 403.23 [M^+]; HPLC Purity: 99% (t_r = 12.13 min).

12. **4-trifluoromethyl-N-((4,7-dimethyl-4,6,6a,7,8,9,10,10a-octahydroindolo[4,3-fg]quinolin-9-yl)methyl)benzamide (FRM 012)**

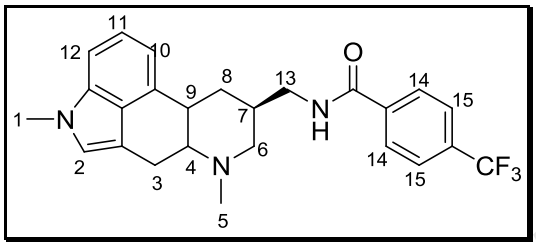

Off-white powder (69.7mg, 43%); m.p 228 – 230°C; δ_H(400 MHz, $CDCl_3$): 7.93 (2H, d, *J* = 8.1 Hz, H-14), 7.75 (2H, d, *J* = 8.7 Hz, H-15), 7.26 – 7.17 (1H, m, H-11), 7.15 (1H, d, *J* = 8.9 Hz, H-10), 6.92 (1H, d, *J* = 8.1 Hz, H-12), 6.76 (1H, d, *J* = 1.4 Hz, H-2), 6.36 (1H, t, *J* = 6.0 Hz, NH), 3.79 (3H, s, H-1), 3.54 (2H, t, *J* = 6.4 Hz), 3.42 (1H, dd, *J* = 14.7, 4.3 Hz), 3.13 (1H, ddd, *J* = 11.2, 3.6, 2.0 Hz), 3.03 (1H, td, *J* = 12.2, 3.6 Hz), 2.74 (2H, dddd, *J* = 16.3, 12.7, 8.4, 2.6 Hz), 2.51 (3H, s, H-5), 2.37 – 2.26 (1H, m), 2.25 – 2.17 (1H, m), 2.10 (1H, t, *J* = 11.3 Hz), 1.28 (1H, q, *J* = 12.3 Hz); δ_C(100 MHz, $CDCl_3$): 166.47, 137.99, 134.46, 133.07, 127.40 (4C), 126.51, 125.71, 125.68, 122.72, 122.59, 112.49, 110.59, 106.91, 67.41, 61.53, 43.99, 43.30, 40.56, 36.78, 32.74, 32.20, 26.97; LRMS (EI+): *m/z* = 440.94 (100.0%) [M+] calculated for $C_{25}H_{26}F_3N_3O$ 441.20 [M^+]; HPLC Purity: 99% (t_r = 13.54 min).

13. **4-acetyl-N-((4,7-dimethyl-4,6,6a,7,8,9,10,10a-octahydroindolo[4,3-fg]quinolin-9-yl)methyl)benzamide (FRM 013)**

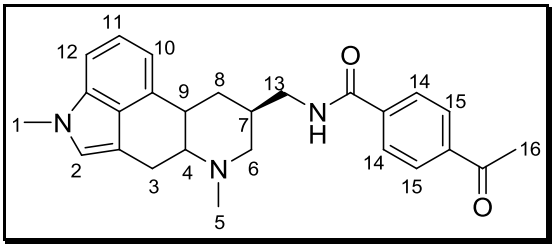

Light brown powder (62.6mg,40.7%); m.p 198 – 200°C; δ_H(400 MHz, $CDCl_3$): 8.01 (2H, d, *J* = 8.2 Hz, H-14), 7.91 (2H, d, *J* = 8.3 Hz, H-15), 7.21 – 7.14 (1H, m, H-11), 7.11 (1H, d, *J* = 8.2 Hz, H-10), 6.88 (1H, d, *J* = 7.0 Hz, H-12), 6.73 (1H, s, H-2), 6.58 (1H, s, NH), 3.75 (3H, s, H-1), 3.48 (3H, q, *J* =

7.0 Hz), 3.39 (1H, dd, *J* = 14.7, 4.2 Hz), 3.21 (1H, d, *J* = 8.7 Hz), 3.11 – 3.01 (1H, m), 2.78 – 2.69 (1H, m), 2.62 (3H, s, H-16), 2.52 (3H, s, H-5), 2.40 – 2.32 (1H, m), 2.32 – 2.22 (1H, m), 2.12 (1H, t, *J* = 11.3 Hz), 1.37 – 1.13 (1H, m); δ_C(100 MHz, $CDCl_3$): 197.40, 166.82, 139.23, 138.51, 134.45, 132.67, 128.54 (2C), 127.34 (2C), 126.42, 122.76, 122.66, 112.58, 110.17, 107.02, 67.39, 65.82, 61.31, 43.86, 42.99, 40.32, 36.37, 32.76, 32.04, 26.76; LRMS (EI+): *m/z* = 414.79 (100.0%) [M+] calculated for $C_{26}H_{29}N_3O_2$ 415.23 [M^+]; HPLC Purity: 99% (t_r = 11.64 min).

14. **4-fluoro-N-((4,7-dimethyl-4,6,6a,7,8,9,10,10a-octahydroindolo[4,3-fg]quinolin-9-yl)methyl)benzamide (FRM 014)**

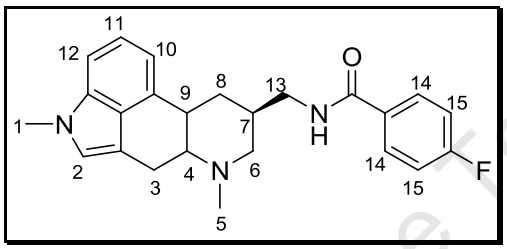

Off-white powder (40.6mg,28.0%); m.p 212 – 214^{o}C; δ_H(400 MHz, $CDCl_3$): 7.83 – 7.77 (2H, m, H-14), 7.21 – 7.15 (1H, m, H-11), 7.12 (3H, t, *J* = 8.5 Hz, H-10, H-15), 6.89 (1H, d, *J* = 7.1 Hz, H-12), 6.73 (1H, d, *J* = 1.3 Hz, H-2), 6.27 – 6.19 (1H, m, NH), 3.75 (3H, s, H-1), 3.52 – 3.45 (2H, m), 3.39 (1H, dd, *J* = 14.7, 4.4 Hz), 3.13 – 3.06 (1H, m), 3.05 – 2.93 (1H, m), 2.77 – 2.63 (2H, m), 2.47 (3H, s, H-5), 2.31 – 2.20 (1H, m), 2.22 – 2.13 (1H, m), 2.06 (1H, t, *J* = 11.3 Hz), 1.30 – 1.18 (1H, m); δ_C(100 MHz, $CDCl_3$): 166.69, 166.00, 134.47, 133.17, 130.92, 129.27, 129.18, 126.54, 122.74, 122.58, 115.78, 115.56 112.54, 110.66, 106.89, 67.44, 61.58, 43.91, 43.34, 40.60, 36.86, 32.76, 32.23, 27.00; LRMS (EI+): *m/z* = 391.18 (100.0%) [M+] calculated for $C_{24}H_{26}FN_3O$ 391.21 [M^+]; HPLC Purity: 99% (t_r = 12.33 min).

15. **N-((4,7-dimethyl-4,6,6a,7,8,9,10,10a-octahydroindolo[4,3-fg]quinolin-9-yl)methyl)benzamide (FRM 015)**

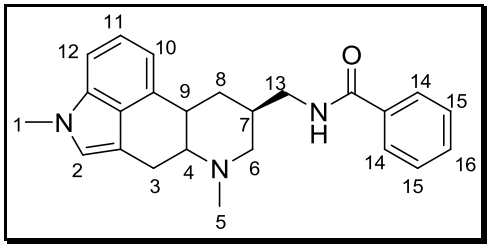

Off-white powder (37.8mg,27.4%); m.p 205 – 207^{o}C; δ_H(400 MHz, $CDCl_3$): 7.86 – 7.80 (2H, m, H-14), 7.54 – 7.42 (3H, m, H-15, H-16), 7.22 – 7.14 (1H, m, H-11), 7.12 (1H, d, *J* = 8.2 Hz, H-10), 6.90 (1H, d, *J* = 7.1 Hz, H-12), 6.74 (1H, s, H-2), 6.44 (1H, s, NH), 3.76 (3H, s, H-1), 3.54 – 3.48 (2H, m), 3.41 (1H, dd, *J* = 14.7, 4.3 Hz), 3.26 (1H, d, *J* = 12.1 Hz), 3.15 – 3.06 (1H, m), 2.84 – 2.70 (2H, m), 2.54 (3H, s, H-5), 2.30 (1H, td, *J* = 10.8, 4.7 Hz), 2.14 (1H, t, *J* = 11.4 Hz), 1.34 – 1.19 (2H, m); δ_C(100 MHz, $CDCl_3$): 167.77, 134.65, 132.75, 131.46, 128.61 (2C), 127.94, 126.98 (2C), 126.43, 122.78, 122.63, 112.63, 110.21, 106.98, 67.41, 61.27, 43.71, 42.92, 40.27, 36.34, 32.77, 32.04, 26.59; LRMS (EI+): *m/z* = 373.13 (100.0%) [M+] calculated for $C_{24}H_{27}N_3O$ 373.22 [M^+]; HPLC Purity: 99% (t_r = 11.95 min).

16. **4-trifluoromethoxy-N-((4,7-dimethyl-4,6,6a,7,8,9,10,10a-octahydroindolo[4,3-fg]quinolin-9-yl)methyl)benzamide (FRM 016)**

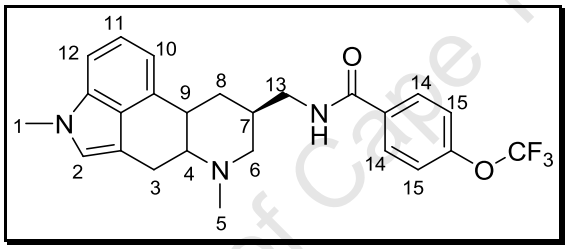

Brown powder (38.8mg,22.9%); m.p 182 – 184^{o}C; δ_H(400 MHz, $CDCl_3$): 7.84 (2H, d, *J* = 8.9 Hz, H-14), 7.29 (2H, d, *J* = 8.9 Hz, H-15), 7.21 – 7.15 (1H, m, H-11), 7.11 (1H, d, *J* = 8.2 Hz, H-10), 6.89 (1H, d, *J* = 6.2 Hz, H-12), 6.73 (1H, d, *J* = 1.4 Hz, H-2), 6.27 – 6.19 (1H, m, NH), 3.75 (3H, s, H-1), 3.49 (2H, t, *J* = 6.4 Hz), 3.39 (1H, dd, *J* = 14.6, 4.4 Hz), 3.13 – 3.07 (1H, m), 3.03 – 2.95 (1H, m), 2.77 – 2.65 (2H, m), 2.48 (3H, s, H-5), 2.27 (1H, dd, *J* = 12.0, 7.0 Hz), 2.23 – 2.14 (1H, m), 2.07 (1H, t, *J* = 11.3 Hz), 1.25 (1H, q, *J* = 12.4 Hz); δ_C(100 MHz, $CDCl_3$): 166.40, 151.49, 134.45, 133.13, 128.77 (2C), 126.50, 122.64, 120.72 (2C), 112.50, 110.59, 106.89, 67.42, 61.53, 43.93, 43.29, 40.56, 36.80, 32.75, 32.19, 26.96; LRMS (EI+): *m/z* = 457.15 (100.0%) [M+] calculated for $C_{25}H_{26}F_3N_3O_2$ 457.20 [M^+]; HPLC Purity: 99% (t_r = 13.84 min).

5.7. Synthesis of the N-(4-chlorobenzyl)-1-(4,7-dimethyl-4,6,6a,7,8,9,10,10a-octahydroindolo [4,3-fg]quinolin-9-yl)methanamine (FRM 017)

A mixture of the amine **FRM000** (1.0 mmol) and 4-chloro benzaldehyde (1.0 mmol) in 5 ml of DCM was left to stir for 2 hr at room temperature to generate the imine *in situ*; the mixture was

then cooled to 0°C using ice and sodium borohydride (2.0 mmol) added. The mixture was then warmed to room temperature and left to stir for 24 hr. The reaction was then quenched with water and extracted with DCM. The DCM layer was the concentrated *in vacuo* to give the crude product that was purified by column silica gel chromatography (MeOH/DCM, 5:95) to yield the desired product.

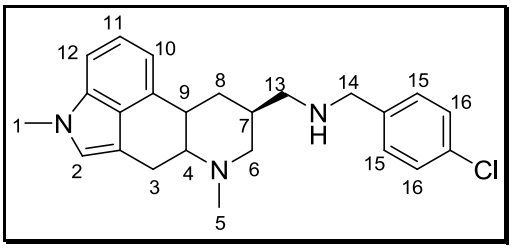

Brown powder (51.5mg,35%); m.p 56 – 58°C; δ_H(400 MHz, $CDCl_3$): 7.37 – 7.31 (4H, m, H-15, H-16), 7.22 (1H, dd, *J* = 8.2, 7.1 Hz, H-11), 7.14 (1H, d, *J* = 8.2 Hz, H-10), 6.94 (1H, d, *J* = 6.8 Hz, H-12), 6.76 (1H, d, *J* = 1.5 Hz, H-2), 3.84 (2H, d, *J* = 3.1 Hz, H-14), 3.78 (3H, s, H-1), 3.42 (1H, dd, *J* = 14.7, 4.3 Hz), 3.20 (1H, ddd, *J* = 11.1, 3.6, 1.8 Hz), 3.03 (1H, td, *J* = 12.3, 3.9 Hz), 2.82 – 2.70 (2H, m), 2.70 – 2.56 (2H, m), 2.52 (3H, s, H-5), 2.28 – 2.11 (2H, m), 1.99 (1H, t, *J* = 11.3 Hz), 1.81 (1H, s, NH), 1.15 (1H, q, *J* = 12.2 Hz); δ_C(100 MHz, $CDCl_3$): 133.54, 132.59, 129.39 (2C), 128.50 (2C), 122.70, 122.46, 112.57, 110.76, 106.72, 67.65, 62.28, 53.55, 53.28, 43.28, 40.59, 36.14, 32.77, 26.97; LRMS (EI+): *m/z* = 392.95 (100.0%) [M+] calculated for $C_{24}H_{28}Cl_3N_3$ 393.20 [M^+]; HPLC Purity: 99% (t_r = 12.42 min).

5.8 Testing protocols

5.8.1 Antimycobacterial Testing protocol

The MIC_{99} was determined using a standard broth microdilution method,[82,83] where a 10 ml culture of *Mycobacterium tuberculosis,*[84] *H37Rv* strain was grown to an OD_{600} of 0.6 – 0.7. The culture was then diluted 1:500 in liquid 7H9 medium, and 50 µl of 7H9 medium was added. The compounds to be tested were added in duplicate, at a final concentration of 640 µM (stocks were made up to a concentration of 12.8 mM in DMSO, and diluted to 640 µM in 7H9 medium). A two-fold serial dilution was prepared; finally, 50 µl of the 1:500 diluted *M. tuberculosis* culture was added. Controls used were media only, 5 % DMSO, Rifampicin and Kanamycin. The microtitre plate was sealed in a ziplock bag and incubated at 37 °C with humidifier to prevent

evaporation of liquid. The lowest concentration of drug that inhibits growth of more than 99 % of the bacterial population was considered to be the MIC_{99}. MIC_{99} values were scored visually at days 7 and 14 post inoculation, and digital images captured and stored.

5.8.2 Antiplasmodial Testing Protocol

The compounds were tested in triplicate against chloroquine sensitive (CQS) strain of *Plasmodium falciparum* (NF54). Continuous *in vitro* cultures of asexual erythrocyte stages of *P. falciparum* were maintained using a modified method of Trager and Jensen.[85] Quantitative assessment of *in vitro* antiplasmodial activity was determined via a modified parasite lactate dehydrogenase assay as described by Malker.[86] The test samples were prepared as a 20 mg/ml stock solution in 100% DMSO and sonicated to enhance solubility. Stock solutions were stored at -20ºC and further dilution were prepared on the day of the experiment. Samples were tested as a suspension if not completely dissolved. Chloroquine (CQ) was used as the reference drug in all experiments. A full dose-response was performed for all compounds to determine the IC_{50} value which is the concentration inhibiting 50% of parasite growth. Test samples were tested at a starting concentration of 10 µg/ml, which was then serially diluted 2-fold in complete medium to give 10 concentrations; with the lowest concentration being 0.02 µg/ml. The IC_{50}-values were obtained using a nonlinear dose-response curve fitting analysis via Graph Pad Prism v.4.0 software.

5.8.3 Cytotoxicity Testing Protocol

The compounds were tested for *in vitro* cytotoxicity against a mammalian cell-line, Chinese Hamster Ovarian (CHO), using the 3-(4,5-dimethylthiazol-2-yl)-2,5-diphenyltetrazoliumbromide (MTT)-assay. The MTT-assay is used as a colorimetric assay for cellular growth and survival.[87,88] The tetrazolium salt MTT was used to measure all growth and chemosensitivity. The test samples were tested in triplicate on one occasion. The test samples were prepared to a 2mg/ml stock solution in 10% methanol or 10% DMSO and were tested as a suspension if not properly dissolved. Test compounds were stored at -20ºC until use. Emetine was used as the reference drug in all experiments. The initial concentration of emetine was 100 µg/ml, which was serially diluted in complete medium with 10-fold dilutions to give 6 concentrations, the lowest being

0.001µg/ml. The same dilution technique was applied to the all test samples. The 50% inhibitory concentration (IC_{50}) values were obtained from full dose-response curves using a non-linear dose-response curve fitting analysis via GraphPad Prism v.4 software.

5.8.4 Turbidimetric Solubility Assay protocol

0.01M pH 7.4 Phosphate Buffered Saline (PBS) was prepared by dissolving 1 intact PBS buffer tablet in sufficient distilled water to make 1000 ml of a solution comprising 0.14M NaCl, 0.003M KCl and 0.01M phosphate buffer. This solution was filtered through a 0.22 µM nylon filter to remove any particulate contaminants and the pH ascertained using a pH meter. 10mM stock solutions of the test samples were prepared by accurately weighing and dissolving each compound in sufficient DMSO to approximately 1000 µl final volume. For each stock solution pre-dilutions of the compounds in DMSO were prepared in triplicate to yield concentrations from 0 to 10mM. From each pre-dilution solution, secondary dilutions of the compounds in both DMSO and 0.01M pH 7.4 PBS were prepared in a 96-well plate, in triplicate. The final volume of solvent in each assay plate well was 200 µl, prepared by pipetting 4 µl each of solution from the pre-dilution plate to the corresponding well into both DMSO and PBS (both 196 µl). This ensured that the final concentration of DMSO in the PBS aqueous buffer did not exceed 2 % v/v. The different concentrations in DMSO were prepared to serve as controls to determine potential false turbimetric absorbance readings arising from the compounds in solution absorbing incident radiation at the analysis wavelength. The plate was then covered and left to equilibrate for 2 hours at ambient room temperature. UV-Vis absorbance readings from the plate were then measured at 620 nm. Corrected absorbance readings at different concentrations of test compounds were calculated by subtracting absorbance of the blank (i.e. DMSO and 1 % DMSO in PBS) from each subsequent concentration's absorbance.[89–93]

5.8.5 Microsomal Metabolic Stability Protocol

0.40 mg protein/ml microsomes (pooled human mixed gender, male rat IGS, male mouse BALB/c) from XenoTech were incubated with 1 µM test compound at 37^{o}C. Metabolic reactions were initiated by the addition of the co-factor NADPH and incubated for 30 minutes. The reactions were quenched with triple the volume of acetonitrile containing carbamazepine as

internal standard. The centrifuged and filtered samples were analysed by HPLC-MS/MS to determine the remaining concentrations of the test compounds. Control standards (midazolam and propranolol) were included in the assay to provide quality control and an indication of the metabolic capacity of the microsomes used. Data analysis was performed as described by Di *et al*.[94]

REFERENCES

(1) Rivers, E. C.; Mancera, R. L. New anti-tuberculosis drugs in clinical trials with novel mechanisms of action. *Drug Discov. Today* **2008**, *13*, 1090–8.

(2) Barnes, D. *The making of a social disease:Tuberculosis in nineteenth-century France*; University of California press: London,England, **1995**.

(3) WHO *Global Tuberculosis Report 2012*; World Health Organisation: Geneva,Switzerland, **2012**.

(4) Dover, L. G.; Coxon, G. D. Current status and research strategies in tuberculosis drug development. *J. Med. Chem.* **2011**, *54*, 6157–65.

(5) Desmond, E.; Ahmed, A. T.; Probert, W. S.; Ely, J.; Jang, Y.; Sanders, C. A.; Lin, S.; Flood, J. Mycobacterium africanum cases, California. *Emerg Infect Dis* **2004**, *10*, 921–3.

(6) Jones, G. *Captain of all these men of death:The History Of Tuberculosis in Nineteenth and Twentieth Century Ireland*; Editions Rodopi B. V.Amsterdam-New York, **2001**.

(7) Kolyva, A. S.; Karakousis, P. C. *Old and New TB Drugs : Mechanisms of Action and Resistance*; InTech, **2009**.

(8) Koul, A.; Arnoult, E.; Lounis, N.; Guillemont, J.; Andries, K. The challenge of new drug discovery for tuberculosis. *Nature* **2011**, *469*, 483–490.

(9) WHO *Gender and Tuberculosis*; World Health Organisation:Department Of Gender and women's Health, **2002**.

(10) WHO *Global tuberculosis control WHO report 2011*; World Health Organisation: Geneva,Switzerland, **2011**.

(11) Corbett, E. L.; Watt, C. J.; Walker, N.; Maher, D.; Williams, B. G.; Raviglione, M. C.; Dye, C. The growing burden of tuberculosis: global trends and interactions with the HIV epidemic. *Arch Intern Med* **2003**, *163*, 1009–21.

(12) Sonnenberg, P.; Murray, J.; Glynn, J. R.; Shearer, S.; Kambashi, B.; Godfrey-Faussett, P. HIV-1 and recurrence, relapse, and reinfection of tuberculosis after cure: a cohort study in South African mineworkers. *Lancet* **2001**, *358*, 1687–93.

(13) Lienhardt, C.; Vernon, A.; Raviglione, M. C. New drugs and new regimens for the treatment of tuberculosis: review of the drug development pipeline and implications for national programmes. *Curr. Opin. Pulm. Med.* **2010**, *16*, 186–193.

(14) Marriner, G. A.; Nayyar, A.; Uh, E.; Wong, S. Y.; Mukherjee, T.; Via, L. E.; Carroll, M.; Edwards, R. L.; Gruber, T. D.; Choi, I.; Lee, J.; Arora, K.; England, K. D.; Boshoff, H. I. M.; Barry III, C. E. The Medicinal Chemistry of Tuberculosis Chemotherapy. *Top Med Chem* **2011**, *7*, 47–124.

(15) DTBE. *Core Curriculum on Tuberculosis : What the Clinician Should Know*; 5TH ed.; CDC, **2011**.

(16) Lewis, K. Platforms for antibiotic discovery. *Nat. Rev. Drug Discov.* **2013**, *12*, 371–387.

(17) Scientific blueprint for tuberculosis drug development. *Tuberculosis (Edinb)* **2001**, *81*, 1–52.

(18) Van den Boogaard, J.; Kibiki, G. S.; Kisanga, E. R.; Boeree, M. J.; Aarnoutse, R. E. New drugs against tuberculosis: problems, progress, and evaluation of agents in clinical development. *Antimicrob Agents Chemother (Bethesda)* **2009**, *53*, 849–62.

(19) Turan-Zitouni, G.; Kaplancikli, Z. A.; Ozdemir, A. Synthesis and antituberculosis activity of some N-pyridyl-N'-thiazolylhydrazine derivatives. *Eur J Med Chem* **2010**, *45*, 2085–2088.

(20) WHO *Treatment of Tuberculosis guidelines*; 4TH ed.; World Health Organisation, **2010**.

(21) Zumla, A.; Nahid, P.; Cole, S. T. Advances in the development of new tuberculosis drugs and treatment regimens. *Nat. Rev. Drug Discov.* **2013**, *12*, 388–404.

(22) Iseman, M. D. Treatment of multidrug-resistant tuberculosis. *N Engl J Med* **1993**, *329*, 784–91.

(23) Janin, Y. L. Antituberculosis drugs: ten years of research. *Bioorg Med Chem* **2007**, *15*, 2479–513.

(24) Roy, K. K.; Singh, S.; Sharma, S. K.; Srivastava, R.; Chaturvedi, V.; Saxena, A. K. Synthesis and biological evaluation of substituted 4-arylthiazol-2-amino derivatives as potent growth inhibitors of replicating Mycobacterium tuberculosis H37Rv. *Bioorg Med Chem Lett* **2011**, *21*, 5589–93.

(25) Nzila, A.; Ma, Z.; Chibale, K. Drug repositioning in the treatment of malaria and TB. *Future Med Chem* **2011**, *3*, 1413–26.

(26) Palomino, J. C.; Martin, A. Is repositioning of drugs a viable alternative in the treatment of tuberculosis? *J Antimicrob. Chemother* **2013**, *68*, 275–83.

(27) Lougheed, K. E. a; Taylor, D. L.; Osborne, S. a; Bryans, J. S.; Buxton, R. S. New anti-tuberculosis agents amongst known drugs. *Tuberculosis (Edinb)* **2009**, *89*, 364–70.

(28) Kar, S.; Kar, S. Control of malaria. *Nat. Rev. Drug Discov.* **2010**, *9*, 511–2.

(29) NIAID *Understanding Malaria*; National Institute of Allergy and Infectioes Diseases, **2007**.

(30) WHO *world malaria report 2012*; World Health Organisation: Geneva,Switzerland, **2012**.

(31) Cox, F. E. History of the discovery of the malaria parasites and their vectors. *Parasit Vectors* **2010**, *3*, 5.

(32) Carter, R.; Mendis, K. N. Evolutionary and Historical Aspects of the Burden of Malaria Evolutionary and Historical Aspects of the Burden of Malaria. **2002**, *15*.

(33) Paquet, T.; Gordon, R.; Waterson, D.; Witty, M. J.; Chibale, K. Antimalarial aminothiazoles and aminopyridines from phenotypic whole-cell screening of a SoftFocus(®) library. *Future Med Chem* **2012**, *4*, 2265–77.

(34) WHO *Guidelines for the treatment of malaria*; second.; World Health Organisation, **2010**.

(35) Aguiar, A. C. C.; Rocha, E. M. M. Da; Souza, N. B. De; França, T. C. C.; Krettli, A. U. New approaches in antimalarial drug discovery and development: a review. *Memórias do Instituto Oswaldo Cruz* **2012**, *107*, 831–45.

(36) Ashley, E.; McGready, R.; Proux, S.; Nosten, F. Malaria. *Travel Med Infect Dis* **2006**, *4*, 159–73.

(37) Peters, W. Antimalarial drugs and their actions. *Postgrad Med J* **1973**, *49*, 573–83.

(38) González Cabrera, D.; Douelle, F.; Feng, T.-S.; Nchinda, A. T.; Younis, Y.; White, K. L.; Wu, Q.; Ryan, E.; Burrows, J. N.; Waterson, D.; Witty, M. J.; Wittlin, S.; Charman, S. A.; Chibale, K. Novel orally active antimalarial thiazoles. *J. Med. Chem.* **2011**, *54*, 7713–9.

(39) Younis, Y.; Douelle, F.; Feng, T.-S.; González Cabrera, D.; Le Manach, C.; Nchinda, A. T.; Duffy, S.; White, K. L.; Shackleford, D. M.; Morizzi, J.; Mannila, J.; Katneni, K.; Bhamidipati, R.; Zabiulla, K. M.; Joseph, J. T.; Bashyam, S.; Waterson, D.; Witty, M. J.; Hardick, D.; Wittlin, S.; Avery, V.; Charman, S. A.; Chibale, K. 3,5-Diaryl-2-aminopyridines as a novel class of orally active antimalarials demonstrating single dose cure in mice and clinical candidate potential. *J. Med. Chem.* **2012**, *55*, 3479–87.

(40) Cohen, A.; Verhaeghe, P.; Crozet, M. D.; Hutter, S.; Rathelot, P.; Vanelle, P.; Azas, N. Tandem synthesis and in vitro antiplasmodial evaluation of new naphtho[2,1-d]thiazole derivatives. *Eur J Med Chem* **2012**, *55*, 315–24.

(41) Barnes, K. I.; White, N. J. Population biology and antimalarial resistance: The transmission of antimalarial drug resistance in Plasmodium falciparum. *Acta Trop* **2005**, *94*, 230–40.

(42) Kokwaro, G. Ongoing challenges in the management of malaria. *Malar. J.* **2009**, *8 Suppl 1*, S2.

(43) Schlitzer, M. Antimalarial drugs - what is in use and what is in the pipeline. *Arch Pharm* **2008**, *341*, 149–63.

(44) Hobbs, C.; Duffy, P. Drugs for malaria: something old, something new, something borrowed. *F1000 Biol Rep* **2011**, *3*, 24.

(45) CDC Malaria-Biology http://www.cdc.gov/malaria/about/biology/ (accessed May 29, 2013).

(46) Kaur, K.; Jain, M.; Kaur, T.; Jain, R. Antimalarials from nature. *Bioorg Med Chem* **2009**, *17*, 3229–56.

(47) Saifi, M. A.; Beg, T.; Harrath, A. H.; Suleman, F.; Altayalan, H.; Quraishy, S. Al Antimalarial drugs : Mode of action and status of resistance. **2013**, *7*, 148–156.

(48) Fidock, D. A.; Rosenthal, P. J.; Croft, S. L.; Brun, R.; Nwaka, S. Antimalarial drug discovery: efficacy models for compound screening. *Nat. Rev. Drug Discov.* **2004**, *3*, 509–20.

(49) Müller, I. B.; Hyde, J. E. Antimalarial drugs: modes of action and mechanisms of parasite resistance. *Future Microbiol* **2010**, *5*, 1857–73.

(50) Gelb, M. H. Drug discovery for malaria: a very challenging and timely endeavor. *Curr Opin Chem Biol* **2007**, *11*, 440–5.

(51) Mutabingwa, T. K. Artemisinin-based combination therapies (ACTs): best hope for malaria treatment but inaccessible to the needy! *Acta Trop* **2005**, *95*, 305–15.

(52) Rosenthal, P. J. Antimalarial drug discovery: old and new approaches. *J. Exp. Biol.* **2003**, *206*, 3735–3744.

(53) MMV - Research and Development portfolio http://www.mmv.org/research-development/rd-portfolio (accessed May 9, 2013).

(54) Ananthan, S.; Faaleolea, E. R.; Goldman, R. C.; Hobrath, J. V; Kwong, C. D.; Laughon, B. E.; Maddry, J. a; Mehta, A.; Rasmussen, L.; Reynolds, R. C.; Secrist, J. a; Shindo, N.; Showe, D. N.; Sosa, M. I.; Suling, W. J.; White, E. L. High-throughput screening for inhibitors of Mycobacterium tuberculosis H37Rv. *Tuberculosis (Edinb)* **2009**, *89*, 334–53.

(55) Kashyap, S. J.; Garg, V. K.; Sharma, P. K.; Kumar, N.; Dudhe, R.; Gupta, J. K. Thiazoles: having diverse biological activities. *Med. Chem. Res.* **2011**, *21*, 2123–2132.

(56) De Souza, M. V. N. Synthesis and biological activity of natural thiazoles: An important class of heterocyclic compounds. *Journal of Sulfur Chemistry* **2005**, *26*, 429–449.

(57) Siddiqui, N.; Arshad, M. F.; Ahsan, W.; Alam, M. S. Thiazoles : A Valuable Insight into the Recent Advances and Biological Activities. *IJPSDR* **2009**, *1*, 136–143.

(58) Siddiqui, N.; Kumar, S.; Ahsan, W.; Azad, B. Diverse biological activities of Thiazoles : A Retrospect. *Int. J. Drug Dev. & Res.* **2011**, *3*, 55–67.

(59) Patrick, G. L. An Introduction to Medicinal Chemistry. **1995**.

(60) Erian, A. W.; Sherif, S. M.; Gaber, H. M. The Chemistry of α-Haloketones and Their Utility in Heterocyclic Synthesis. *Molecules* **2003**, *8*, 793–865.

(61) Zagade, A. A.; P., S. G. Thiazole: A Valuable insight into recent advances,synthesis and biological activities. *der pharma chemica* **2011**, *3*, 523–537.

(62) Joullié, M. M.; Lassen, K. M. Evolution of amide bond formation. **2010**, *2010*, 189–250.

(63) Mojarradi, H. Coupling of substances containing a primary amine to hyaluronan via carbodiimide-mediated amidation. **2011**.

(64) Hay, M. P.; Turcotte, S.; Flanagan, J. U.; Bonnet, M.; Chan, D. A.; Sutphin, P. D.; Nguyen, P.; Giaccia, A. J.; Denny, W. A. 4-Pyridylanilinothiazoles that selectively target von Hippel-Lindau deficient renal cell carcinoma cells by inducing autophagic cell death. *J. Med. Chem.* **2010**, *53*, 787–97.

(65) Kröhnke, F.; Gross, K. F. Beispiele zur King-Reaktion. *Chem Ber* **1959**, *92*, 22–36.

(66) Guo, Y.; Shen, H. *pKa, Solubility, and Lipophilicity*; pp. 1–17.

(67) Lipinski, C. A. Drug-like properties and the causes of poor solubility and poor permeability. *J Pharmacol Toxicol Methods* **2001**, *44*, 235–49.

(68) Turner, E. H.; Schwartz, P. J.; Lowe, C. H.; Nawab, S. S.; Feldman-Naim, S.; Drake, C. L.; Myers, F. S.; Barnett, R. L.; Rosenthal, N. E. Double-blind, placebo-controlled study of single-dose metergoline in depressed patients with seasonal affective disorder. *J Clin Psychopharmacol* **2002**, *22*, 216–20.

(69) Tfelt-Hansen, P.; Saxena, P. R.; Dahlöf, C.; Pascual, J.; Láinez, M.; Henry, P.; Diener, H.; Schoenen, J.; Ferrari, M. D.; Goadsby, P. J. Ergotamine in the acute treatment of migraine: a review and European consensus. *Brain* **2000**, *123 (Pt 1*, 9–18.

(70) Grimes, J. D.; Hassan, M. N. Bromocriptine in the long-term management of advanced Parkinson's disease. *Can J Neurol Sci* **1983**, *10*, 86–90.

(71) De Groot, A. N. Prevention of postpartum haemorrhage. *Bailliere Clin Ob Gy* **1995**, *9*, 619–31.

(72) Kang, K.; Wong, K.-S.; Seneviratne, C. J.; Samaranayake, L. P.; Fong, W.-P.; Tsang, P. W.-K. In vitro synergistic effects of metergoline and antifungal agents against Candida krusei. *Mycoses* **2010**, *53*, 495–9.

(73) Kang, K.; Wong, K.-S.; Fong, W.-P.; Tsang, P. W.-K. Metergoline-induced cell death in Candida krusei. *Fungal Biol* **2011**, *115*, 302–9.

(74) Gurguis, G. N.; Turkka, J.; Linnoila, M. Effects of serotonin and metergoline on 125[I]-iodocyanopindolol binding parameters to beta-adrenergic receptors in rat brain. *Eur Neuropsychopharmacol* **1998**, *8*, 131–40.

(75) Meiri, G.; Ben-Zion, I. Z.; Greenberg, B. D.; Murphy, D. L.; Benjamin, J. Influence of the serotonin antagonist, metergoline, on the anxiogenic effects of carbon dioxide, and on heart rate and neuroendocrine measures, in healthy volunteers. *Hum Psychopharmacol* **2001**, *16*, 237–245.

(76) Roca, C. A.; Schmidt, P. J.; Smith, M. J.; Danaceau, M. A.; Murphy, D. L.; Rubinow, D. R. Effects of metergoline on symptoms in women with premenstrual dysphoric disorder. *Am J Psychiatry* **2002**, *159*, 1876–81.

(77) AID 1332 - PubChem BioAssay Summary http://pubchem.ncbi.nlm.nih.gov/assay/assay.cgi?aid=1332&loc=ea_ras#aDescription (accessed Apr 29, 2013).

(78) NIH Quantitative high throughput screen for delayed death inhibitors of the malarial parasite plastid, 48 hour incubation - BioAssay Summary http://pubchem.ncbi.nlm.nih.gov/assay/assay.cgi?aid=488752 (accessed May 14, 2013).

(79) Hooker, J. M.; Kim, S. W.; Reibel, A. T.; Alexoff, D.; Xu, Y.; Shea, C. Evaluation of [(11)C]metergoline as a PET radiotracer for 5HTR in nonhuman primates. *Bioorg Med Chem* **2010**, *18*, 7739–45.

(80) Coleman, M. D. *Human Drug Metabolism: An Introduction*; John Wiley & Sons, Ltd: West Sussex, England, **2005**.

(81) Nassar, A. F.; Kamel, A. M.; Clarimont, C. Improving the decision-making process in the structural modification of drug candidates: enhancing metabolic stability. *Drug Discov. Today* **2004**, *9*, 1020–8.

(82) Collins, L.; Franzblau, S. G. Microplate alamar blue assay versus BACTEC 460 system for high-throughput screening of compounds against Mycobacterium tuberculosis and Mycobacterium avium. *Antimicrob Agents Chemother (Bethesda)* **1997**, *41*, 1004–9.

(83) Collins, L. A.; Torrero, M. N.; Franzblau, S. G. Green fluorescent protein reporter microplate assay for high-throughput screening of compounds against Mycobacterium tuberculosis. *Antimicrob Agents Chemother (Bethesda)* **1998**, *42*, 344–7.

(84) Ioerger, T. R.; Feng, Y.; Ganesula, K.; Chen, X.; Dobos, K. M.; Fortune, S.; Jacobs, W. R.; Mizrahi, V.; Parish, T.; Rubin, E.; Sassetti, C.; Sacchettini, J. C. Variation among genome sequences of H37Rv strains of Mycobacterium tuberculosis from multiple laboratories. *J Bacteriol* **2010**, *192*, 3645–53.

(85) Trager, W.; Jensen, J. B. Human malaria parasites in continuous culture. *Science* **1976**, *193*, 673–5.

(86) Makler, M. T.; Ries, J. M.; Williams, J. A.; Bancroft, J. E.; Piper, R. C.; Gibbins, B. L.; Hinrichs, D. J. Parasite lactate dehydrogenase as an assay for Plasmodium falciparum drug sensitivity. *Am J Trop Med Hyg* **1993**, *48*, 739–41.

(87) Mosmann, T. Rapid colorimetric assay for cellular growth and survival: application to proliferation and cytotoxicity assays. *J Immunol Methods* **1983**, *65*, 55–63.

(88) Rubinstein, L. V; Shoemaker, R. H.; Paull, K. D.; Simon, R. M.; Tosini, S.; Skehan, P.; Scudiero, D. A.; Monks, A.; Boyd, M. R. Comparison of in vitro anticancer-drug-screening data generated with a tetrazolium assay versus a protein assay against a diverse panel of human tumor cell lines. *J Natl Cancer Inst* **1990**, *82*, 1113–8.

(89) Lipinski, C. A.; Lombardo, F.; Dominy, B. W.; Feeney, P. J. Experimental and computational approaches to estimate solubility and permeability in drug discovery and development settings. *Adv Drug Deliv Rev* **2001**, *46*, 3–26.

(90) Kerns, E. .; Di, L. *Drug-like properties: Concepts, structure design and methods: from ADME to toxicity optimization*; Academic Press: San Diego, **2008**; pp. 56–82.

(91) Bevan, C. D.; Lloyd, R. S. A high-throughput screening method for the determination of aqueous drug solubility using laser nephelometry in microtiter plates. *Anal Chem* **2000**, *72*, 1781–7.

(92) Pan, L.; Ho, Q.; Tsutsui, K.; Takahashi, L. Comparison of chromatographic and spectroscopic methods used to rank compounds for aqueous solubility. *J Pharm Sci* **2001**, *90*, 521–9.

(93) Alsenz, J.; Kansy, M. High throughput solubility measurement in drug discovery and development. *Adv Drug Deliv Rev* **2007**, *59*, 546–67.

(94) Di, L.; Kerns, E. H.; Gao, N.; Li, S. Q.; Huang, Y.; Bourassa, J. L.; Huryn, D. M. Experimental design on single-time-point high-throughput microsomal stability assay. *J Pharm Sci* **2004**, *93*, 1537–44.